A Study of the Interaction Between MAPKAP Kinase 5 / MK5 and DNAJB1

By Kari J. Lægreid

A Master Thesis in Medical Biology
May 2011

Host-Microbe Interactions Research Group
Department of Medical Biology
University of Tromsø

Acknowledgments

This study was performed at the Host-Microbe Interactions Research group, Department of Medical Biology at the University of Tromsø from February 2010 to March 2011.

First of all, I would like to thank my supervisors, Prof. Ugo Moens and Dr. Sergiy Kostenko for their knowledge and guidance and for always having time.

I would also like to thank Gianina for patiently taking time in her busy schedule to teach and explain some of the basic protocols to someone very green. A thanks also goes to Mari and Dr. Mona Johannessen for answering any questions I might have, big or small, stupid or relevant.

Thanks to my fellow students for pep-talks and sharing of mishaps in the lab. Pallavi and Sophie, thank you for being such nice office-mates!

Finally I would like to thank my family and friends for giving me the thumbs up when I was feeling down, and my Remi for invaluable IT-support and for putting up with me on the moody days.

Abstract

The mitogen activated protein kinases (MAPK) are a large and diverse family of protein kinases, contributing to the cells ability to respond to external stimuli by relaying messages in a well orchestrated way until they reach their final destinations. This is achieved through successive phosphorylation events. One member of this large family is mitogen activated protein kinase activated protein kinase 5 (MAPKAPK5/MK5), which is activated by the upstream atypical MAPKs extracellular signal-regulated kinases 3 and 4 (ERK3 and ERK4), and possibly also the conventional MAPK $p38^{MAPK}$. MK5 has been shown to be implicated in F-actin rearrangement through phosphorylation of heat shock protein 27 (HSP27), tumor suppression through at least two different pathways and cell cycle arrest in response to energy depletion. There has been done relatively little research on this protein, and few bona fide substrates for MK5 are known, although knowledge is emerging. One possible interaction partner for MK5 is DNAJB1, which has been shown to be phosphorylated by MK5 *in vitro*. DNAJB1 is a member of the heat shock protein 40 (HSP40) family/DNAJ family, which is a subunit of the much larger heat shock protein superfamily. Heat shock proteins mostly function as chaperones and co-chaperones in the cell, assisting in the maintenance of protein homeostasis, by refolding or degrading misfolded proteins. Conditions of stress in the cell can lead to increased levels of misfolded proteins, which in turn are thought to initiate the increased transcription of heat shock proteins observed in stressed cells. DNAJB1 mainly serves as a co-chaperone for heat shock protein 70, and has been implicated to play a role in various types of cancer and neurodegenerative disorders.

In this study we demonstrated that MK5 phosphorylates DNAJB1 *in vitro*, and that Tyrosine residue 6 and Serine residues 149, 151 and 171 in DNAJB1 are *in vitro* phosphorylation sites for MK5. Our results also indicate that other phosphorylation sites may be present. Further experiments are needed to elucidate the *in vivo* potential of these phosphoacceptor sites. We also found that MK5 and DNAJB1 exist in complexes. This interaction proved hard to reproduce, indicating that it might be of a transient nature, or perhaps a product of non-physiological conditions. We also showed that both proteins localize mainly to the nucleus in resting cells, when ectopically expressed, and that DNAJB1 seems to downregulate the level or the transcriptional activity of MK5 when both proteins are ectopically expressed in the cell.

Abbreviations

Ala, A	Alanine
BSA	Bovine Serum Albumine
Cat #	Catalog number
Co-ip	Co-immunoprecipitation
DMBA	Dimethylbenzanthracene
ds	Double stranded
EGFP	Enhanced green fluorescent protein
ERK	Extracellular signal-regulated kinase
FBS	Fetal bovine serum
G/F	Glycine/Phenylalanine
GFP	Green fluorescent protein
HSF1	Heat shock factor 1
HSP	Heat shock protein
IVK	In vitro kinase
MAP2K	Mitogen activated protein kinase kinase
MAP3K	Mitogen activated protein kinase kinase kinase
MAPK	Mitogen activated protein kinase
MAPKAP	MAPK activated protein kinase
MK5	Mitogen activated protein kinase activated protein kinase 5
MS	Mass spectrometry
mTORC1	Mammalian target of Rapamycin Complex 1
NES	Nuclear export signal
NLS	Nuclear localisation signal
o.n.	Over night
ORF	Open reading frame
PCR	Polymerase chain reaction
Poly-Q	Polyglutamine
Rheb	Ras homolog enriched in brain
Rpm	Rounds per minute
SCA3	Spinocerebellar ataxia type 3
Ser, S	Serine
Thr, T	Threonine
Tyr, Y	Tyrosine
WB	Western blot

Table of contents

Index of Tables

1 Introduction

1.1 Protein kinases and signal transduction

Living cells are subject to a variety of chemical and physical stimuli from their immediate environment. In order for a cell to survive and function normally, it needs to respond to these stimuli in an appropriate manner. To achieve this, the extracellular signals need to reach their intracellular destinations. Such conversion from an extracellular signal to an intracellular response is referred to as signal transduction, and is often mediated by reversible phosphorylation of target proteins by protein kinases and protein phosphatases through a signaling cascade (Figure 1).

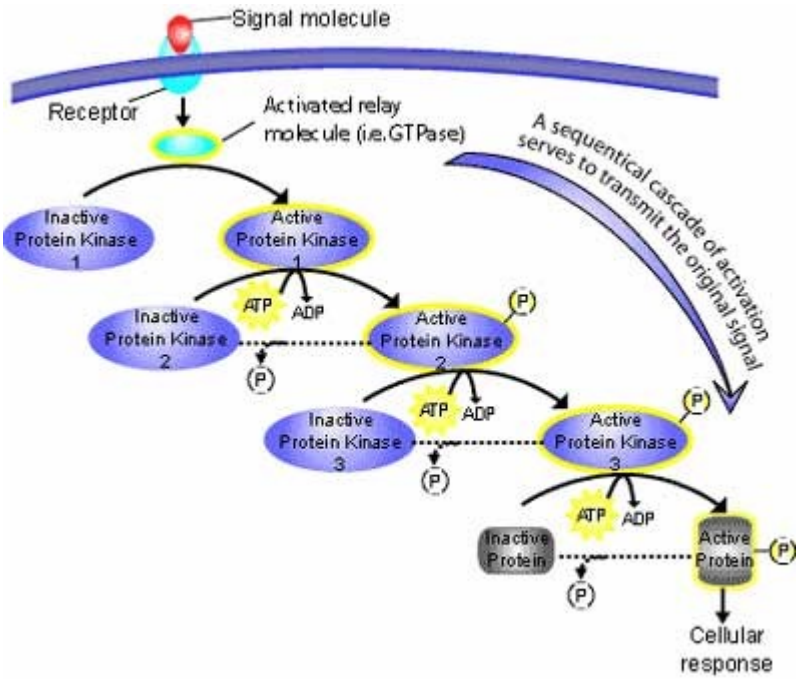

Figure 1: Schematic illustration of signal transduction relayed by protein kinases. The figure is adapted from [1]

Protein kinases are responsible for most of the signal transduction in eukaryotic cells, and are among the largest of protein superfamilies, comprising 1.5–2.5% of all genes. They control several cellular processes, such as metabolism, transcription, cell cycle progression, cytoskeletal rearrangement and cell movement, apoptosis and differentiation [2].

1.1.1 The MAPK signaling pathway

The MAPK signaling pathway consists of individual components called MAP kinases (mitogen activated protein kinases). These kinases constitute a large family of Serine/Threonine kinases that regulate a myriad of cellular processes.

As their name implies, the first group of signals that was identified as stimulators of the MAPK pathway, were mitogens. Others soon followed, like UV-irradiation and cytokines [3]. MAPKs are among the most ancient signal transduction pathways, and are widely conserved throughout evolution in a wide range of physiological processes. Their importance in cellular processes is underscored by the fact that all eukaryotic cells possess multiple MAPK pathways [4].

1.1.1.1 The MAPK family members

So far, 14 MAPKs have been characterized in mammals. These are divided into seven groups, four of which comprise the so-called conventional MAPKs and three that constitute the atypical MAPKs [4]

The conventional mammalian MAPK pathway is a three-tiered cascade composed of a MAPK kinase kinase (MAP3K), a MAPK kinase (MAP2K) and a MAPK (Figure 2). MAPK members of this group are; extracellular signal-regulated kinases 1/2 (ERK1/2), c-Jun amino (N)-terminal kinases 1/2/3 (JNK1/2/3), $p38^{MAPK}$ isoforms (α, β, γ, δ) and the big MAPK (BMK1/ERK5).

The atypical MAPKs, which are not organized in the conventional tripartite module, comprise ERK3/4, ERK7 and Nemo-like kinase (NLK) [5].

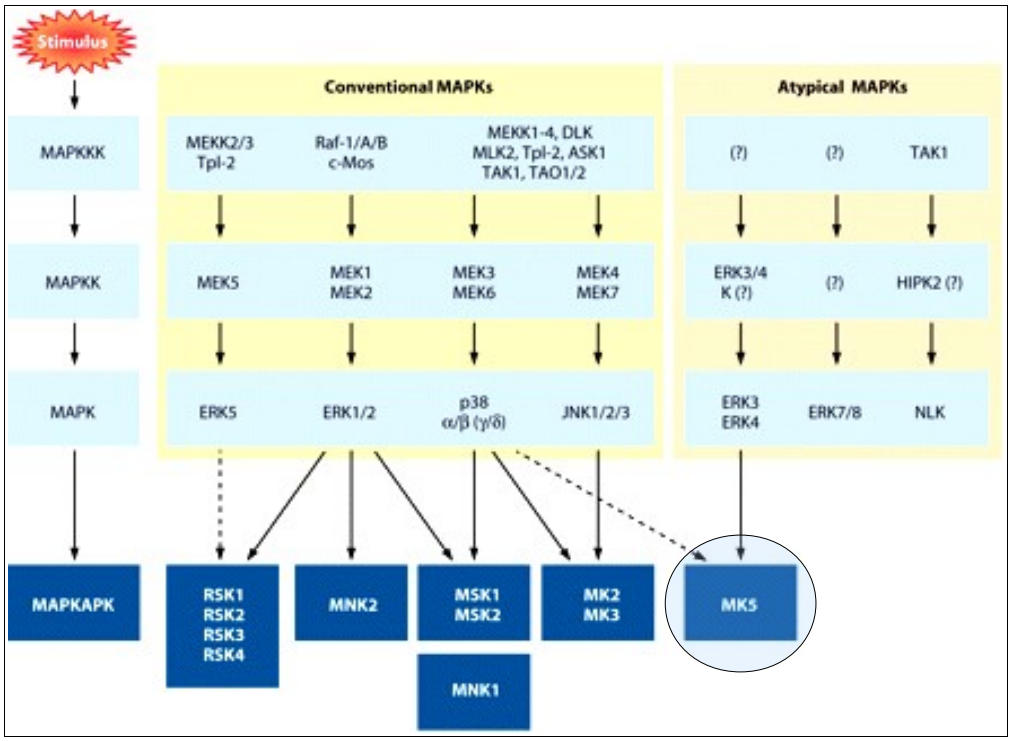

Figure 2: MAPK signaling cascades and subsequent activation of MAPKAPKs. Dotted lines indicate that substrate regulation by the respective kinase remains to be thoroughly demonstrated. MK5, the MAPKAPK investigated in this study, is circled. The figure is adapted from [4].

1.1.1.2 MAPK structure

The MAPKs have an N-terminal and a C-terminal lobe, which are connected by a hinge-region. The gap between the N- and C-terminal lobes forms the catalytic site, which, in unphosphorylated MAPKs, is blocked by an a-helix. Upon phosphorylation by an upstream kinase, the gap opens, exposing the catalytic site, and thus activating the kinase [3].

1.1.2 MAPK-activated protein kinases

Both conventional and atypical MAPKs can phosphorylate not only non-protein kinase substrates, but also another family of protein kinases, referred to as MAPK-activated protein kinases (MAPKAPs). So far, 11 human MAPKAPs have been identified, and divided into five subfamilies consisting of several members (Figure 3). These families comprise the p90 ribosomal-S6-kinases (RSK1/4), the MAPK-interacting kinases (MNK1 and 2), the mitogen- and stress-activated kinases (MSK 1 and 2), the MK2/MK3 subgroup and MK5 [5].

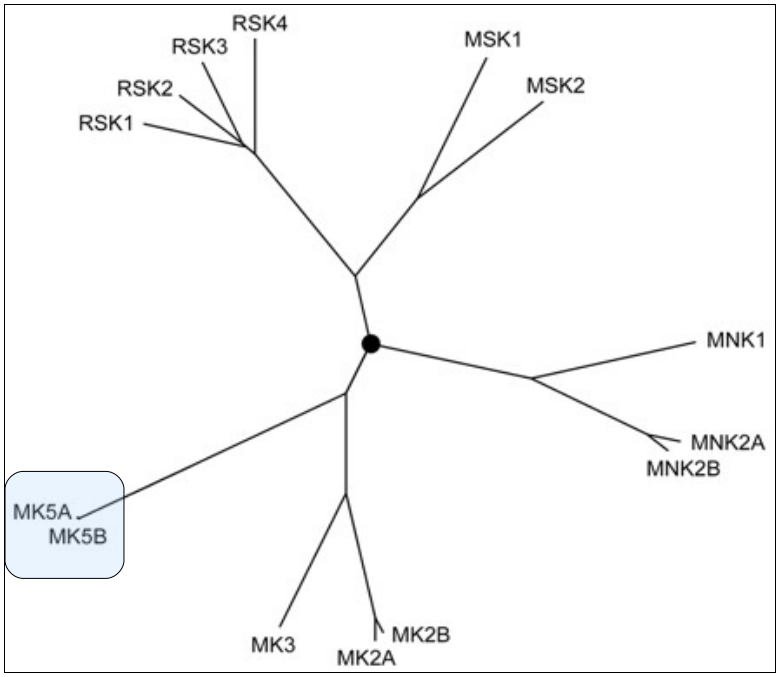

Figure 3: Phylogenetic tree of the human MAPKAPKs based on alignment generated by the CLUSTAL X program. MK5 isoforms A and B are circled. The figure is adapted from [6]

1.1.2.1 MK5/PRAK

The MAPKAP5, or MK5, is the main focus of this thesis. This kinase was originally discovered in 1998 as a mouse expressed sequence tag by searching a database for sequences with a high degree of homology to MK2 [7]. Later

that same year, an independent research group reported the isolation of a p38^{MAPK} regulated and activated kinase, PRAK, which turned out to be the human homologue of MK5 [8].

MK5 is extremely well conserved within the animal kingdom, and present in all vertebrates examined, including mammals, birds, reptiles and fish. This means that both ectothermic and endothermic animals possess an MK5 protein with high sequence homology, suggesting that this protein may possess catalytic activity over a wide range of temperatures [5].

Humans express two isoforms of MK5, as a result of differential splicing. The two isoforms differ by only two additional amino acids in the C-terminal of the larger variant, and are designated MK5A (473 amino acids) and MK5B (471 amino acids). It is not known whether these two isoforms exert different functions in the cell [5].

1.1.2.1.1 Sequence and motifs

MK5 shares approximately 45% and 46% sequence identity with MK2 and MK3 respectively. In contrast, MK2 and MK3 share approximately 75% sequence identity with each other. This contrast in homology is probably due to the unique 100 amino acid C-terminal tail of MK5 [3] (Figure 4). MK2, MK3 and MK5 all contain the conserved regulatory phosphorylation motif LXTP in the activation loop between kinase subdomain VII and VIII [2]. This is represented by T182 in MK5. MK2 and MK3 both contain additional regulatory sites between the catalytic domain and the C-terminal regulatory domain. This is not the case for MK5. Nor does MK5 contain the N-terminal Proline-rich region which is present in both MK2 and MK3 [9]. However, all three proteins contain nuclear localization signals (NLS) and nuclear export signals (NES) in their C-terminal domain, and, interestingly, in MK5 these signals overlap [10]. The NLS of MK5 also overlaps with the p38^{MAPK} docking site, and consequently, binding of p38^{MAPK} prevents nuclear localization of MK5 [3]. The 100 amino acid C-terminal extension previously mentioned is thought to play an auto-inhibitory role, and is, at least, required for interaction with ERK3 and ERK4 [10].

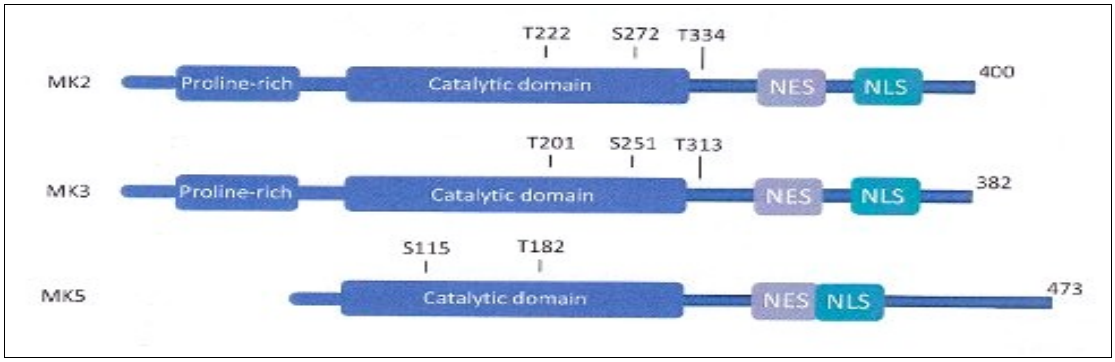

Figure 4: Schematic illustration of the primary structure of MK2, MK3 and MK5. The figure is adapted from [11]

1.1.2.1.2 Regulation of subcellular localization

Subcellular localization of MK5 is regulated by several factors, including NLS/NES, docking interactions and phosphorylation. Several studies have shown that both endogenous and ectopically expressed MK5 reside predominantly in the nucleus of resting cells, but seem to be able to shuttle between the cytoplasm and the nucleus [5].

Stimulation of the $p38^{MAPK}$ pathway has been shown to cause nuclear exclusion of MK5, and $p38^{MAPK}$ is known to phosphorylate MK5 *in vitro.* Recent results suggest that different isoforms of $p38^{MAPK}$ direct MK5 to different subcellular localizations. MK5-p38α complexes are exclusively found in the nucleus, whilst MK5-p38β complexes reside in the cytoplasm [12]. However, the role of $p38^{MAPK}$ in MK5 regulation is still disputed. Endogenous MK5 could only be regulated by ectopic expression of $p38^{MAPK}$, and binding of endogenous $p38^{MAPK}$ and exogenous MK5 is weaker compared to $p38^{MAPK}$ interaction with other substrates. In addition, the activity of MK5 is not significantly increased upon stimulation of the $p38^{MAPK}$ pathway, and no interaction between endogenous MK5 and $p38^{MAPK}$ has ever been detected [2].

Co-expression of MK5 with both ERK3 and ERK4 leads to nuclear export of MK5, and kinase activity of neither MK5 nor ERK3/4 seems to be important for the subcellular relocalization, indicating that interaction rather than kinase activity of either protein is responsible for the subcellular redistribution of MK5 [5].

Kostenko et al. showed that activation of cAMP/PKA (protein kinase A) pathway by Forskolin led to transient nuclear export of endogenous and EGFP-tagged MK5. No such redistribution was observed in PKA-deficient cells. NLS-tagged PKA remained in the nucleus, while MK5 was still exported, indicating that PKA and MK5 do not leave the nucleus in a complex. Serine 115 in MK5 was identified as PKA phosphoacceptor site. Substitution of Serine 115 to Alanine led to an MK5 mutant that no longer translocated upon cAMP/PKA activation, while a phosphomimicking S115D mutant was distributed in both nucleus and cytoplasm even in the absence of activated PKA [13].

1.1.2.1.3 Activation

MK5 has proven to be phosphorylated and activated by $p38^{MAPK}$ α and β *in vitro,* but an *in vivo* connection has not yet been established. *In vivo* activation by ERK3 and ERK4 on the other hand is undisputed, but the physiological implications so far remain unknown. Recent studies indicate that p21 activated protein kinases, PAK1 and PAK2 could act as upstream activators of ERK4, and thereby as indirect activators of MK5. Phosphorylation of Serine 115 by PKA leads to activation and nucleocytoplasmic redistribution of MK5 and subsequent phosphorylation of heat shock protein 27 [5].

1.1.2.1.4 Substrates and physiological roles

As previously mentioned, MK5 has been shown to phosphorylate HSP27 both *in vivo* and *in vitro*. Kostenko et al. showed that depletion of HSP27 or over-expression of a non-phosphorylatable HSP27 mutant ablated PKA/MK5 triggered F-actin remodeling, as established by Gerits et al. [14], suggesting that MK5 is involved in HSP27-controlled F-actin dynamics in response to activation of the cAMP-dependent protein kinase pathway [15].

Recently, MK5 has been shown to phosphorylate and thereby activate the transcription factor FoxO3a. Upon phosphorylation, FoxO3a binds to and activates the promoter that controls expression of the precursor RNA of miR-34b and miR-34c, which target the three prime untranslated region (3' UTR) of Myc, thereby repressing translation. The Myc oncoprotein is a central regulator that stimulates cell growth and proliferation in response to extracellular signals. Downregulation of Myc is essential to ensure cell cycle arrest and survival of cells in response to DNA damaging agents. MK5 and Myc are engaged in a negative feed-back loop, with Myc binding to the MK5 promoter, thereby enhancing expression of MK5 [16]. Aberrant Myc expression plays a central role in oncogenesis. MK5 was observed to be downregulated in colorectal tumor cells compared to normal cells, whilst for Myc, the situation was the opposite, indicating a role for MK5 as a tumor suppressor through downregulation of Myc.

MK5 has also been shown to function as a tumor suppressor *in vivo* by mediating senescence upon activation by $p38^{MAPK}$ in response to oncogenic ras. MK5 deficiency in mice displayed enhanced dimethylbenzanthracene (DMBA) induced skin carcinogenesis. This coincided with compromised senescence induction [17]. DMBA is a well-characterized mutagen that causes skin tumors that are 90% positive for ras-mutations [4]. The results of the study suggest that MK5-mediated senescence likely suppresses skin carcinogenesis at the tumor promotion stage by preventing proliferation of genetically altered cells, such as those containing the activating ras-mutations. The authors suggest that the tumor-suppressing effect of MK5 is likely due to its ability to modulate p53 activity through direct phosphorylation of Serine37. They propose that phosphorylation of p53 by MK5 in response to activation of $p38^{MAPK}$ by ras plays an important role in ras-induced senescence and tumor suppression [17].

Another way in which MK5 may mediate cell growth arrest, is by phosphorylation of ras homolog enriched in brain (Rheb). This is a small G protein, which is one of the key regulators of mammalian target of Rapamycin Complex 1 (mTORC1). mTORC1 regulates cell growth in response to different signals. The group of Han recently discovered that certain forms of energy starvation caused activation of $p38\beta^{MAPK}$ and phosphorylation of T182 and thereby activation of MK5. MK5 can bind and phosphorylate Rheb at Serine130 *in vivo*. This phosphorylation severely impairs Rhebs ability to bind and retain GTP, which again inhibits mTORC1 [5].

Both ERK3 and ERK4 are known *iv vivo* substrates of MK5, but the exact physiological consequences of MK5/ERK3 and MK5/ERK4 complex formation are still not known [5]. Certain observations suggest that ERK3 may play some roles in tumor suppression, and there is the possibility that MK5 may be an important ERK3 effector protein mediating these effects [4].

1.2 Heat Shock Proteins

Heat shock proteins (HSPs) were originally identified as stress-responsive proteins required to deal with proteotoxic stress, i.e. they are upregulated upon, and protective against situations that increase the fraction of proteins that are in a fully or partially unfolded state. Such misfolded proteins increase the risk of protein aggregates, harmful to cellular processes. It is however not only conditions of stress that challenge the cellular protein homeostasis, but also numerous normal cellular processes, such as translation and transport over membranes [18]. Thus, HSPs are also present at lower concentrations in the cell under perfectly normal conditions, ”monitoring” the cell.

The HSPs make up a group of structurally unrelated proteins broadly classified into six major families based on their relative molecular mass in kiloDaltons: HSP110/HSPH, HSP90/HSPC, HSP70/HSPA, HSP60/HSPD, HSP40/DNAJ and small heat shock proteins sHSP/HSPB. Each family consists of several members. These all play a prime role in protein homeostasis by binding to substrates at risk, keeping them in a conformation either competent for refolding or degradation. As such, they belong to a much larger superfamily of chaperones [18].

Increase in expression of HSPs is transcriptionally regulated, and is usually induced by heat shock factor (HSF) as shown in Figure 5.

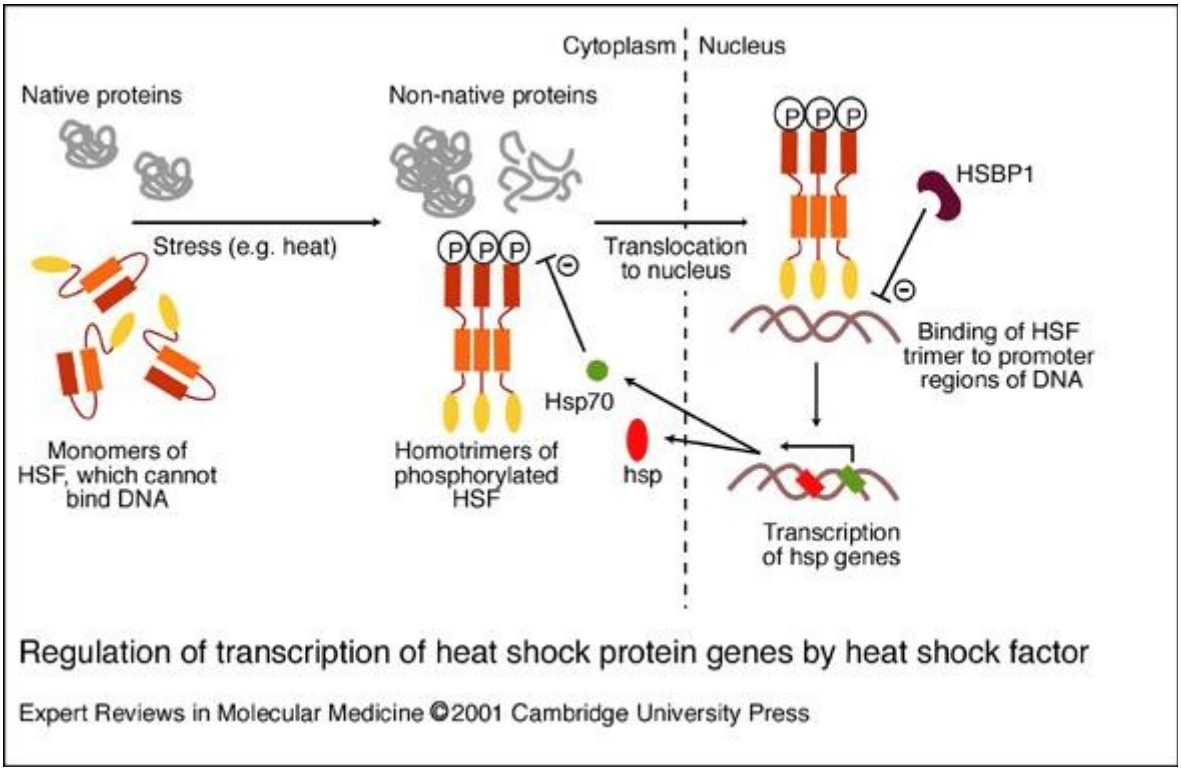

Figure 5: Schematic illustration of the HSF-regulated transcription of heat shock proteins.

Various diseases challenge the normal function of the cell, and induce a variety of stress-responses. Protein conformational diseases, acute and chronic renal diseases, heart diseases and various aspects and types of cancers show involvement of different types of HSPs. For instance, HSPs are over-expressed in a wide range of human cancers, conferring resistance to cytotoxic therapies [19].

1.2.1 The HSP40/DNAJ family

All eukaryotic cells contain DNAJ proteins, and the human genome encodes at least 41 members of the DNAJ family [20]. The common domain that defines this family is the J-domain. This is a 70 amino acid sequence which consists of four helices in addition to a loop region between helix II and III that contains a highly conserved tripeptide of Histidine, Proline and Aspartic acid (HPD). 34 of the members in the DNAJ family contain the typical J-domains, while 7 bear only partially conserved J-like domains, but are still suggested to function as DNAJ proteins [20]. They are localized in different intracellular compartments and organelles, such as mitochondria, cytosol, endoplasmic reticulum, nuclei, endosomes and ribosomes [19].

The DNAJ family of heat shock proteins is known to stimulate the ATPase domain of HSP70/HSPA chaperones through their J-domains, and, as such, function as co-chaperones. HSPAs bind selectively to unfolded hydrophobic

regions of substrate polypeptides, and their activity is controlled by the cycle of ATP binding, hydrolysis and nucleotide exchange [20]. In its ATP-bound configuration, HSPA is in an open state with high association and dissociation rates for substrates, meaning low substrate specificity. Upon binding to a substrate, ATP is hydrolyzed, stabilizing HSPAs affinity for its substrate. This reaction is regulated by co-factors like DNAJs and CHIP. Subsequently, nucleotide exchange is stimulated (BAG-1, HSPB1 and HSPH), resulting in an ATP bound HSPA complex, followed by substrate release [18].

The DNAJ family can be further divided into three subfamilies based on their domain similarity to the *E. coli* DNAJ protein: type I HSP40/DNAJA, type II HSP40/DNAJB and type III HSP40/DNAJC. Each of these subfamilies contain several members.

1.2.1.1 DNAJA

The subfamily A DNAJ proteins are the closest human orthologues of the *E. coli* DNAJ protein. They contain a conserved N-terminal J-domain and a variable C-terminal peptide-binding fragment [21]. Adjacent to the J-domain, a Glycine/Phenylalanine (G/F) rich region is believed to function as a flexible spacer that separates the N-terminal J-domain from the rest of the molecule. In the center of the molecule, there are four conserved Cysteine-rich repeats that fold around two zinc atoms, constituting two Zinc-finger motifs [18].

DNAJA proteins have proven to be able to bind non-native polypeptides by themselves, without the assistance of HSPA proteins, and suppress protein aggregation in the cell [19].

1.2.1.2 DNAJB

The subfamily B DNAJ proteins, similar to DNAJA, also contain the conserved N-terminal J-domain, the variable C-terminal domain, and the G/F rich spacer. They do not however harbor the Cysteine rich repeats with the Zinc-finger motifs.

DNAJB proteins can also bind to polypeptides by themselves, but can not prevent protein aggregation without the interaction of HSPA proteins [19].

1.2.1.3 DNAJC

The subfamily C DNAJ proteins also contain the conserved J-domain, but unlike DNAJA and DNAJB, it can be located at any position within the protein. The other conserved domains found in the DNAJA and DNAJB subfamilies are absent in DNAJC.

1.2.2 DNAJ proteins and their implication in disease

The DNAJB subfamily, and DNAJB1 (also named HSP40, Hdj1 or HSPF1) in particular, has been the most extensively studied mammalian DNAJ member. It has been shown to interact with both HSPA1A and HSPA8 in Luciferase-folding *in vitro* and *in vivo* [18].

Recently Zijlstra et al. found that levels of DNAJB members, in particular DNAJB1, correlate with the age onset of disease in patients with spinocerebellar ataxia type 3 (SCA3). Ataxia is a polyglutamine (Poly-Q) expansion disorder. These disorders are dominantly inherited adult-onset neurodegenerative diseases, and the disease corresponding Poly-Q proteins are aggregate-prone. The length of the expanded CAG (Q) repeat shows a strong inverse correlation with age onset, yet up to 50 % of the variation in age onset is determined by other additional factors. On the basis of the fact that several HSPs can modulate protein aggregate formation, Zijlstra and colleagues tested whether inter-individual differences in HSP expression could be related to CAG-independent variations in the age onset of SCA3. They found that DNAJ members exclusively, and DNAJB1 in particular, showed a correlation to age onset. DNAJB1 levels were lowest in the patient group with the earliest age onset, and highest in the patients with the latest age onset. Furthermore, they found that aggregation of Ataxin 3 with a Poly-Q expansion was largely reduced by co-expression of DNAJB1. These findings indicate that DNAJ members might be contributors to the variation in age of onset of SCA3, and also highlights a possible use for DNAJB proteins as therapeutic targets [22].

DNAJ proteins have also been implicated in various types and aspects of cancer. To date, two DNAJA members, three DNAJB members and three DNAJC members of the HSP40 family have been reported to play certain roles in cancer biology. Some seem to act as tumor suppressors, such as DNAJB4 and DNAJA3. DNAJB4 expression has been shown to correlate inversely with cancer cell invasion ability, and inhibits several attributes of aggressiveness of lung adenocarcinoma, such as proliferation, tumorigenesis, motility and invasion. DNAJA3 has been shown to negatively regulate the migratory potential of cancer cells in skin cancer, colon cancer and glioblastomas. In addition, DNAJB6 has been found to be one of the most frequently under-expressed genes in ductal carcinoma when compared to normal breast epithelium. However, many HSP40 proteins are overexpressed in many types of cancerous tissues, conferring resistance to cytotoxic therapies. One such protein is DNAJA1, which has been reported to contribute to radiotherapy resistance in glioblastomas [19]. It seems DNAJ proteins play diverse roles in cancer biology, acting as both promoters and repressors of tumors and metastasis. Research in this field is emerging, but many questions remain to be answered in order to understand the mechanisms behind the involvement of DNAJ proteins in cancer biology.

1.3 HSF1

The cellular response to diverse forms of of environmental and physiological stress involves the rapid transcriptional induction of target genes whose activity is regulated by different stress-specific trans-activators. The genes encoding heat shock proteins are such genes, and their transactivators are principally heat shock factors (HSFs). The heat shock factors are ubiquitously expressed and maintained in an inert, non-DNA binding state in unstressed cells. Upon exposure to stress conditions, the heat shock factors become activated to DNA-binding, transcriptionally active trimers, which promote transcription of heat shock genes (see Figure 5). The transcription of heat shock genes is rapid, yet transient, and, as Shi and colleagues proved, autoregulated by heat shock proteins. In their study they showed that overexpression of both HSP70 and the DNAJ family member Hdj1/DNAJB1 resulted in negative regulation of HSF1 transcriptional activity. Both proteins interacted directly with the HSF1 transactivation domain with little effect on the DNA-binding or inducibly phosphorylated state of HSF1, indicating a function as repressors of transcriptional activity of the heat shock-specific transactivator [23].

2 Aims of the study

1. Investigate whether DNAJB1 and MK5 interact physically with each other.

2. Map putative *in vitro* phosphoacceptor sites for MK5 in DNAJB1.

3. Investigate possible physical implications of the interaction between MK5 and DNAJB1.

3 Materials and methods

3.1 Materials

Table 1: Buffers and solutions used in this study

Buffer	Contents/manufacturer	Purpose
PBS	8 g NaCl, 0.2 g KCL, 1.44 g Na_2HPO and 0.24 g KH_2PO dissolved in 800 ml distilled H_2O. Hcl to pH 7.4, distilled H_2O to 1 liter. [Sambrook, vol 3, appendix B]	Mammalian cell culture, western blotting, immunofluoroscence staining
PBST	PBS with 0.1% Tween 20	Western Blotting
PBT	PBS with 1% Triton X-100	GST purification
TE buffer, pH	10 mM Tris·HCl (pH), 1 mM EDTA (pH 8.0)	Plasmid DNA purification, Gateway® cloning
Clear Page 20 x running buffer	C.B.S. Scientific, working dilution: 1:20	SDS-PAGE
Nu Page 20 x running buffer	Invitrogen, working dilution: 1:20	SDS-PAGE
Blotting buffer	800 ml distilled H_2O, 200 ml Methanol, 29 g Glycin, 5.8 g Tris base	Western Blotting
Blocking buffer	150 ml PBS, 7.5 g non-fat dry milk powder, 150 µl Tween 20	Western Blotting
10 x Washing buffer	100mM Tris HCl pH 9.5, 100 mM NaCl, 10 mM $MgCl_2$, distilled H_2O. Working dilution: 1:10	Western Blotting
CDP Star Buffer	5 ml DEA in 420 ml double distilled H_2O, pH 9.5. Add 1 g $MgCl_2$, then double distilled H_2O to 500 ml.	Western Blotting
CDP-Star®		
50 x TAE buffer	242 g Tris base, 57.1 ml glacial acetic acid, 100 ml 0.5 M EDTA (pH 8.0), distilled H_2O to 1 liter.	Agarose gel electrophoresis
6 x loading buffer	0.25% bromophenol blue and 40% sucrose	Agarose gel electrophoresis
LDS sample buffer	20 µl 4X NuPAge LDS buffer (Invitrogen), 52 µl H_2O, 8 µl reducing agent (Invitrogen)	SDS-PAGE

Coomassie Blue solution	0.25 g Coomassie brilliant blue R-250, 250 ml Methanol, 50 ml Acetic acid, 200 ml distilled H_2O	Coomassie blue staining
Fixation solution	400 ml distilled H_2O, 500 ml Methanol, 200 ml Acetic acid	Coomassie blue staining
Destaining solution	880 ml distilled H_2O, 50 ml Methanol, 70 ml Acetic acid	Coomassie blue staining
Lysis buffer	50 mM Tris Hcl pH8, 150 mM NaCl, 1 mM EDTA, 1mM DTT, 200 µl protease inhibitor cocktail	Co-immunoprecipitation
Tropix® lysis buffer	Applied Biosystems	Luciferase assay
PFA 0.8 %	0.8 g Paraformaldehyde dissolved in 9 ml distilled H_2O. 1M NaOH added dropwise unitl Paraformaldehyde dissolved, 1 ml 10x PBS	Fixation of cells
TBD buffer	10 mM Tris Hcl pH 7.5, 0.1mg/ml BSA, 1 mM DTT, distilled H_2O	In vitro kinase assay
Kinase buffer	250 mM Tris Hcl pH 7.5, 100mM $MgCl_2$, distilled H_2O	In vitro kinase asay
Big Dye® Terminator v3.1 5 x sequencing buffer	Applied Biosystems. Cat# 4336697	DNA sequencing PCR
Neb buffer 1	Bio Labs, Cat# B7001S	Restriction cloning
Neb buffer 2	Bio Labs, Cat# B7002S	Restriction cloning
Neb buffer 3	Bio Labs, Cat# B7003S	Restriction cloning
10 x cloned PFU reaction buffer	Stratagene, Cat# 600153-82	Site directed mutagenesis
10 x TA buffer	330 mM Tris-acetate (pH 7.8), 660 mM potassium acetate, 100 mM magnesium acetate and 5 mM Dithiothreitol (DTT)	Restriction cloning
10 x T4 DNA ligase buffer with 10 mM ATP	Bio Labs, Cat# B0202S	Restriction cloning
Luciferase substrate	Promega, Luciferase 1000 Assay System Cat# E4550	Luciferase assay

Table 2: Growth media used in this study

Growth medium	Contents	Purpose
LB medium	950 ml deionized H_2O, 10 g bacto-tryptone, 5 g yeast extract, 10 g NaCl, 5 N NaOH to pH 7.0 (~0.2 ml), deionized water to 1 liter	Growth of bacterial cultures for plasmid purification and GST protein purification
LB agar plate	LB medium + 15 g bacto-agar per liter	Transformation of bacterial cells
NZCYM	950 ml deionized water, 10 g NZ amine, 5 g NaCl, 5 g bacto-yeast extract, 1 g casaminoacids, 2 g $MgSO_4 \cdot 7H_2O$, 5 N NaOH to pH 7 (~0.2 ml), deionized water to 1 liter.	GST protein purification
SOC	950 ml deionized water, 20 g bacto-tryptone, 5 g bacto-yeast extract, 0.5 g NaCl, 20 mM glucose 10 ml 250 mM KCL, 5 N NaOH to pH 7.0 (~0.2 ml)	Transformation of bacterial cells
Normal growth medium	Standard Dulbecco's Modified Eagles medium (DME), 10% Fetal Bovine Serum (filtered), Penicillin (100U/ml), Streptomycin(100µl/ml)	Mammalian cell culture
FBS	Heat inactivated Fetal Bovine Serum, Gibco	Mammalian cell culture
Opti-MEM®	A modification of Eagle's Minimum Essential Media, buffered with HEPES and sodium bicarbonate and supplemented with hypoxanthine, thymidine, sodium pyruvate, L-glutamine, trace elements and growth factors. Gibco, Invitrogen.	Transient transfection
Trypsin/EDTA	0.05% Trypsin in EDTA	Mammalian cell culture

Table 3: Plasmids used in this study

Plasmid	Comment	Reference/source	Purpose
pG_5E1b-luc	Luciferase reporter plasmid with five binding sites for the yeast transcription factor Gal4 cloned upstream of a minimal promoter, an Adenovirus E1b TATA-box driving a Luciferase gene	A gift from Prof. Roger Davis [24]	Luciferase assays
pGAL4-HSF1	DNA binding domain of GAL4 (amino acid 1-147)		Luciferase assays
pM-MK5	Encodes a fusion protein containing the DNA binding domain of GAL4 and MK5.	Clontech	Luciferase assays
pcDNA3	A vector for constitutive expression in a variety of mammalian cell lines. Contains (CMV) enhancer-promoter.	Invitrogen	Control vector Luciferase assays
pENTR™1A dual selection vector	Entry vector in the Gateway® system	Invitrogen	Gateway® cloning
pENTR™3C dual selection vector	Entry vector in the Gateway® system	Invitrogen	Gateway® cloning
pDest15	Destination vector in the Gateway® system, containing a GST fusion	Invitrogen	Gateway® cloning
pDestHA	Destination vector in the Gateway® system, containing a HA-tag	Invitrogen	Gateway® cloning
pDest3xFLAG	Destination vector in the Gateway® system, containing 3 x FLAG-tags	Invitrogen	Gateway® cloning

pDest-EYFP	Destination vector containing EYFP	A gift from Prof. Terje Johansens group, Department of Biochemistry, University of Tromsø	Gateway® cloning
pDest-ECFP	Destination vector containing ECFP	A gift from Prof. Terje Johansens group, Department of Biochemistry, University of Tromsø	Gateway® cloning
pDest-Cherry	Destination vector containing Cherry (dsRED mutant, excitation around 590nm, emission 610nm)	A gift from Prof. Terje Johansens group, Department of Biochemistry, University of Tromsø	Gateway® cloning
pcDNA3-CREB	CREB cloned into pcDNA3	Invitrogen	Restriction cloning
pDest3xFLAG-HSP40	DNAJB1 cloned into pDest3xFLAG by Gateway® system	This study	Co-ip, Luciferase assays
pDestHA-MK5	MK5 cloned into pDestHA by Gateway® system	This study	Co-ip
pEGFP-MK5-L337A-NES	Constitutively active MK5 wih additional NES-sequence	This group	Confocal studies
pEGFP-HSF1	cDNA fragment encoding the mouse HSF1 ORF cloned between *XhoI* and *EcorI* into the pEGFP-N1 vector	[25]	Restriction cloning
pENTR1A-HSF1	HSF1 cloned into pENTR1A between EcorI and SalI	This study. For details see appendix D.	Gateway® cloning
pENTR3C-CREB	CREB-fragment cloned into pENTR3C between *KpnI* and *NotI*	This study. For details see appendix C.	Gateway® cloning
pENTR1A-DNAJB1-J-domain	Amino acid 1-70 of DNAJB1 cloned into pENTR1A	Kostenko, unpublished results.	Gateway® cloning
pENTR3C-DNAJB1-G/F-rich domain	Amino acid 71-105 of DNAJB1 cloned into p Entr3C	Kostenko, unpublished results.	Gateway® cloning

pENTR3C-DNAJB1-C-term1	Amino acid 106-175 of DNAJB1 cloned into pENTR3C.	Kostenko, unpublished results.	Gateway® cloning
pENTR3C-DNAJB1-C-term2	Amino acid 176-245 of DNAJB1 cloned into pENTR3C.	Kostenko, unpublished results.	Gateway® cloning
pENTR3C-DNAJB1-C-term3	Amino acid 139-341 of DNAJB1 cloned into pENTR3C.	Kostenko, unpublished results.	Gateway® cloning
pENTR3C-DNAJB1Y6A	DNAJB1 with single mutation Y6A	Kostenko, unpublished results.	Gateway® cloning
pENTR3C-DNAJB1S16A	DNAJB1 with single mutation S16A	Kostenko, unpublished results.	Gateway® cloning
pENTR3C-DNAJB1S149A	DNAJB1 with single mutation S149A	Kostenko, unpublished results.	Gateway® cloning
pENTR3C-DNAJB1S151A	DNAJB1 with single mutation S151A	Kostenko, unpublished results.	Gateway® cloning
pENTR3C-DNAJB1S171A	DNAJB1 with single mutation S171A	Kostenko, unpublished results.	Gateway® cloning
pENTR3C-DNAJB1S149A_S151A	DNAJB1 with double mutation S149A_S151A	This study	Gateway® cloning
pENTR3C-DNAJB1S149A_S151A_S171A	DNAJB1 with triple mutation S149A_S151A_S171A	This study	Gateway® cloning
pDest-ECFP-DNAJB1	DNAJB1 cloned into pDest-ECFP by Gateway® technology	Kostenko unpublished results	Confocal studies
pDest-EYFP-MK5	MK5 cloned into pDest-EYFP by Gateway® technology	Kostenko unpublished results	Confocal studies
pDest-EYFP-MK5L337A	MK5L337A cloned into pDest-EYFP by Gateway® technology	Kostenko unpublished results	Confocal studies
pDest-Cherry-HSF1	HSF1 cloned into pDest-Cherry by Gateway® technology	This study	Confocal studies

Table 4: Antibodies used in this study

Antibody	Comment	Reference/manufacturer	Experiment
Anti-FLAG® M2 antibody	Purified IgG Source: Mouse	Stratagene	Co-IP
Anti HSF1	Polyclonal Source: rabbit	Cell Signaling Technology	Co-IP, WB
Anti HA	Mouse monoclonal $IgG_{2b\kappa}$ that recognizes HA peptide sequence [YPYDVPDYA] derived from human influenza Hemagglutinin protein.	Roche	Co-IP
Anti-GFP	Mixture of two monoclonal antibodies against GFP. $IgG_{1\kappa}$ Source: mouse	Roche	Co-IP
Anti HSP40	Polyclonal. Detects endogenous levels of total HSP40 protein. Source: rabbit	Cell signaling technology	Immunofluoroscence staining Co-IP
Anti PRAK (A7) (anti MK5)	Mouse monoclonal IgG_1 raised against amino acids 294-473 mapping at the C-terminus of PRAK (MK5) of human origin	Santa Cruz Biotechnology inc.	Immunofluoroscence staining Co-IP
Alexa Fluor 488	Goat anti rabbit IgG conjugated to Alexa Fluor dye 488	Invitrogen	Immunofluoroscence staining
Alexa Fluor 555	Goat anti mouse IgG conjugated to Alexa Fluor dye 555	Invitrogen	Immunofluoroscence staining
Goat anti rabbit	Alkaline phosphatase conjugated IgG + IgM	Southern Biotech	WB
Rabbit anti mouse	Polyclonal Alkaline phosphatase conjugated immunoglobulins	Dako	WB
Anti β-tubulin isotype III	Monoclonal. Recognizes carboxyl terminal sequence of human β-tubulin isotype III Source: mouse	Sigma Aldrich	Immunofluoroscence staining
Alexa Fluor® 594 Phalloidin	A high-affinity probe for F-actin that is made from a phallotoxin conjugated with Alexa Fluor 594 dye.	Invitrogen	Immunofluoroscence satining
DRAQ5™	Far-red fluorescent DNA dye that stains dsDNA/nuclei of live or fixed cells.	Biostatus limited	Immunofluoroscence satining

Table 5: Enzymes used in this study

Enzyme	Manufacturer /catalog number (Cat #)	Purpose
Big Dye® Terminator v3.1	Applied Biosystems	Sequencing PCR
PFU turbo	Stratagene, Cat # 600252	Site directed mutagenesis
T4 DNA ligase	Bio Labs, Cat # M0202S	DNA ligation
Gateway® LR Clonase® II enzyme mix	Invitrogen, Cat # 11791020	Gateway® cloning
Dpn I	Bio Labs, Cat # R0176S	Site directed mutagenesis
Ecor I	Promega, Cat # R601A	Restriction digestion
Kpn I	Bio Labs, Cat # R0142S	Restriction digestion
Xho I	Bio Labs, Cat # R0146S	Restriction digestion
Xba I	Bio Labs, Cat # R0145S	Restriction digestion

Table 6: Primers used in this study (all primers were purchased from Sigma)

Primer	Sequence	Source	Purpose
5' ENTR	5' CTACAAACTCTTCCTGTTAGTTAG		Sequencing PCR of Entry vectors
DNAJB1 S149A/S151A F	5' GAACTTTGGCCGC**G**CCCGC**G**CTGCCCAAGAG	This thesis	Site directed mutagenesis
DNAJB1 S149A/S151A R	5' CTCTTGGGCAG**C**GCGGG**C**GCGGCCAAAGTTC	This thesis	Site directed mutagenesis
DNAJB1 S171A F	5' CACGACCTTCGAGTC**G**CCCTTGAAGAGATC	This thesis	Site directed mutagenesis
DNAJB1 S171A R	5' GATCTCTTCAAGGG**C**GACTCGAAGGTCGTG	This thesis	Site directed mutagenesis

Table 7: Commercial proteins used in this study

Protein	Description	Manufacturer	Purpose
HSP40/DNAJB1	Recombinant full length human HSP40 expressed in E.coli using an N-terminal GST-tag. >90% purity Approximate MW = 65kDa	SignalChem	In vitro kinase assay
MK5/PRAK	Human recombinant full-length protein Histidine tagged. Expressed in insect cells. Activated in vitro by GST-tagged MAPK14	Invitrogen	In vitro kinase assay

Table 8: Transfection reagents used in this study

Transfection reagent	Manufacturer	Purpose
Lipofectamine™ 2000	Invitrogen, Cat # 11668-019	Transient transfection for subsequent Luciferase assays and confocal studies
Metafectene® Pro	Biontex, Cat # T040-2.0	Transient transfection for subsequent Co-ip
Cell Line Nucleofector® kit V	Lonza, Cat # VCA-1003	Transient transfection of PC12 cells

Table 9: Kits used in this study

Kit	Manufacturer	Purpose
Nucleobond®Xtra Midi kit	Machery Nagel	Plasmid purification, medium quantities
NucleoSpin® Plasmid kit	Machery Nagel	Plasmid purification, small quantities

Table 10: Bacterial strains used in this study

Bacterial strain	Description	Purpose
Escherichia coli DH5α	A recombination-deficient, suppressing, competent *E. coli* strain	Storage and amplification of different plasmid-vectors
Escherichia coli BL21	A protease deficient, competent *E. coli* strain	Storage and expression of GST fusion proteins

Table 11: Mammalian cell lines used in this study

Cell-line	Organism	Organ	ATTC number	Purpose
HEK293	Human	Kidney	CRL-1573	Transient transfection
HeLa	Human	Cervix	CCL-2	Transient transfection, immunofluoroscence staining
PC12	Rat	Adrenal medulla	CRL-1721	Transient transfection, immunofluoroscence staining

3.2 Methods

3.2.1 Purification/extraction of plasmid DNA from bacterial cells

Pure plasmid DNA is essential in many experiments within the field of molecular biology. Genetically manipulated plasmids serve as vectors into which genetic elements of interest can easily be inserted, multiplied and expressed. By transforming such plasmid-vectors into competent bacterial cells, the copy number can easily be multiplied ten-thousand fold. In order to utilize this plasmid DNA in further studies, it needs to be separated from the genomic DNA and other cellular components. There are many commercially available kits that serve this purpose. In this study, two different protocols from Machery Nagel were used to perform extraction of plasmid DNA from bacterial cells. Both protocols are based on Alkaline lysis of the bacterial cells, followed by equilibration and loading onto a column consisting of a special, patented, silica-based anion-exchange resin. The column in the midi kit operates by gravity flow, while the column in the NucleoSpin kit operates by centrifugal forces. Under acidic conditions, the resin in the column has an overall positive charge, which allows high affinity binding of the negatively charged phosphate backbone of DNA. A pH-shift to slightly alkaline conditions

neutralizes the positive charge of the resin, and pure plasmid DNA is eluted [26].

3.2.1.1 Plasmid DNA purification using Nucleobond®Xtra Midi kit from Machery-Nagel for High-copy plasmid purification [26].

1. 100 ml over night culture was prepared by scraping the frozen surface of bacteria stock* containing the desired plasmid with a sterile pipette tip, and adding the tip to a 500 ml flask with 100 ml LB medium supplemented with the appropriate selective antibiotic (Kanamycin or Ampicillin). Alternatively, 100 µl of a small starter culture made from a single colony on a freshly streaked agar plate was added to the culture flask.

2. The culture was then grown overnight at 37°C and on the shaker (220 rpm) for 12 to 16 hours.

3. Bacterial cells were harvested by centrifugation at 6000 x g for 10 minutes at 4°C, and the supernatant was completely discarded by inverting the centrifuge flask.

4. The bacterial pellet was further completely resuspended by adding 8 ml Resuspension Buffer, RES, supplemented with RNaseA and pipetting the cells up and down.

5. Cell lysis was then performed by adding 8 ml Lysis Buffer, LYS, to the suspension, and mixing carefully by inverting the tube 5 times. The mixture was incubated at room temperature for 5 min.

6. In the meantime, a Nucleobond®Xtra column and filter was equilibrated by applying 12 ml Equilibration Buffer, EQU, along the rim of the filter, making sure the entire filter was wet. The column was then allowed to empty by gravity flow.

7. The Lysis-suspension (step 5) was neutralized by adding 8 ml Neutralization Buffer, NEU, and immediately mixing by inverting the tube 10-15 times. No incubation is required.

8. Making sure the suspension was homogenous by inverting the tube 3 times directly before adding it to the equilibrated column filter, the suspension was loaded onto the column, and the column allowed to empty by gravity flow.

9. The filter and column were then washed by applying 5 ml of Equilibration Buffer, EQU, along the rim of the filter, and the column once more allowed to empty by gravity flow.

10. The column filter was then discarded, and the column washed by adding 8 ml Wash Buffer, WASH.

11. Plasmid DNA was then eluted by adding Elution Buffer, ELU, collecting the eluate in a 15 ml centrifuge tube.

12. 5 ml room temperature Isopropanol was next added for precipitation of the eluted plasmid, followed by vigorous pipetting up and down.

13. The mixture was incubated for 2 min at room temperature, and then centrifuged at 15000 x g for 30 min at room temperature The supernatant was carefully discarded by inverting the tube.

14. The plasmid-DNA pellet was washed and dried by adding 2 ml room temperature absolute ethanol and spinned down at 15000 x g for 5 minutes at room temperature.

15. The supernatant was removed by carefully inverting the tube, and the tube was left to dry upside-down for 5-10 min.

16. Finally, the DNA pellet was dissolved in 100 µl of TE buffer.

*Bacteria culture made from a single colony on a freshly streaked agar-plate mixed with glycerol (final concentration 15%) for cryo-protection and kept at -70°C for further use.

3.2.1.2 Miniprep of plasmid DNA using NucleoSpin® Plasmid kit from Machery Nagel

1. A culture in 3 ml LB medium + appropriate selective antibiotic was grown at 37°C and 220 rpm shaking over night (o.n.).

2. The following day, the culture was transferred to a microcentrifuge tube (eppendorf tube) and centrifuged for five minutes at 11000 x g in a standard benchtop microcentrifuge.

3. The supernatant was discarded, and as much liquid as possible removed.

4. 250 µl resuspension buffer (A1) was then added and the cells resuspended completely by vortexing or pipetting up and down. No cell clumps should remain in the suspension.

5. Next 250 µl lysis buffer (A2) was added, and the suspension was mixed gently by inverting the tube 6-8 times, to avoid shearing of genomic DNA, and incubated at room temperature for up to five minutes.

6. Then 300 µl Buffer A3 was added to neutralize the lysis reaction

mixture. The lysate was mixed thoroughly by inverting the tube 6-8 times, and centrifuged at 11 000 x g for five minutes at room temperature. This step was repeated if supernatant was not clear.

7. A NucleoSpin® Plasmid Column was placed in a collection tube and a maximum of 750 µl of the supernatant was pipetted onto the column.

8. The column was then centrifuged for one minute at 11,000 x g, and flow-through discarded.

9. Next 600 µl Buffer A4 supplemented with ethanol was added, and the columns centrifuged for 1 min at 11,000 x g. Flow-through was discarded, and the column placed in the empty collection tube.

10. In order to dry the DNA, the column was centrifuged for 2 min.

11. At the end of the centrifugation, the column was placed in an empty 1.5 ml eppendorf tube, and supplied with 50 µl Elution buffer. This was incubated for 1 minute at room temperature, before centrifugation at 11 000 x g for 1 minute.

12. The resulting suspension in the eppendorf tube now contained the purified plasmid DNA, and was kept at -20 C until evaluation of purity and concentration.

3.2.2 Evaluation of Plasmid DNA concentration and purity

Concentration and purity of plasmid DNA can be evaluated by two general methods; UV-spectrophotometry and Agarose gel electrophoresis. The most comprehensive approach is to use both methods.

In this study, for most DNA-preps, UV-spectrophotometric measurements were used.

3.2.2.1 UV-spectrophotometry

DNA itself, and most of the common contaminants found in DNA preps, have absorbances in the region 230 nm to 320 nm. Measurement of the absorbances in this region thus allows measurement of the DNA concentration and provides information about the contaminant levels.

Guanidium salts and Phenol used in the purification procedure absorb light strongly at 230 nm, Tyrosine and Tryptophan residues in proteins do the same at 280 nm, while DNA absorbs most strongly at 260 nm. High absorbances at 230 nm indicate there might be carry-over from the preparation, and high absorbances at 280 nm indicate protein contamination. A good quality DNA

sample should have a A260/A280 ratio of 1.7-2.0 and an A260/A230 ratio of greater than 1.5 [27].

3.2.2.2 Agarose gel electrophoresis

Agarose gel electrophoresis is a simple and highly effective method for separating, identifying and purifying DNA-fragments in the size-range 0.5 to 25 kb. It also allows determination of the conformation of plasmid DNA. Plasmid DNA can occur in three forms: covalently closed circular (CCC), open covalent circular (OC) and linear. CCC DNA transfects better than OC and linear, so for transfection studies it is important that plasmid DNA is mainly in the CCC configuration.

To do Agarose gel electrophoresis, first, a gel is prepared with an Agarose concentration appropriate for the size of the DNA fragments to be separated. Next, the DNA samples are loaded into the sample wells, and the gel run at a voltage and time-period that ensures optimal separation of the fragments. Finally, the gel is stained, or if Ethidium Bromide has been incorporated into the gel, the DNA-fragments are visualized directly upon UV-illumination [28].

Protocol:

For a small gel (40 ml) of 1% Agarose

1. 0.4 g Agarose was added to 40 ml 1x TAE buffer (table 1) in an erlenmeyer flask, and heated in the microwave at full effect for 90 seconds. The flask was swirled a couple of times, to ensure even mixing.

2. The mixture was cooled down to approximately 50 °C, before 2 µl Ethidium bromide (10 mg/ml) was added.

3. The gel was poured into a gel-mold, with a comb already in place, and any air bubbles were removed with a pipette tip.

4. The gel was left to solidify for at least 15 minutes.

5. The gel was next transferred to a running-chamber filled with 1 x TAE buffer.

6. 2 µl DNA-sample was supplied with 8 µl ddH_2O and 2 µl 6 x loading buffer (table 1).

7. DNA-samples were applied to the sample wells in the gel.

8. 5 µl $1kb^+$ ladder was added to one of the wells, to serve as a reference for the size of the DNA-fragments.

9. The gel was run at 90 V, 400 mA for approximately 45 minutes.

3.2.3 Mammalian cell culture techniques

A number of experiments in the field of molecular biology rely on the use of mammalian cell cultures to mimic/simulate living systems. There are a number of different cell lines to work with, derived from different species and different kinds of tissues. Each cell line displays their own characteristics, and different cell lines may require slightly different culture protocols. Cells can be cultured in a monolayer attached to the plastic surface of a culture vessel, or they can be grown in suspension. For this study, cells were cultured in the former manner.

3.2.3.1 Subculturing (splitting) of cells

When the cells grow confluent, space, oxygen and nutrients become scarce resources. If kept at such conditions, the cells will die, and detach from the surface of the culture vessel. To avoid such a scenario, the cells have to be subcultured regularly. This practice is also referred to as «splitting» the cells. The process involves detaching cells from the surface by Trypsin treatment, followed by reuspension of the cells in a small volume of culture medium, and finally transfer of a small volume of this concentrated cell suspension to a larger volume of fresh growth medium, thereby making the cell suspension «thinner», quite commonly by a order of ten.

Protocol:

Before starting, PBS, normal growth medium and Trypsin were prewarmed to 37 °C.

1. Growth medium was carefully aspirated by water suction.

2. Prewarmed PBS was carefully added, and the flask was swirled gently to cover the entire surface, thereby washing the cells thoroughly. PBS was then removed by water suction.

3. Trypsin in EDTA was added to the flask, and the flask put in the incubator for a few minutes, until cells had rounded up. The flask was then tapped gently against the palm of the hand in order to detach the cells from the surface.

4. The cells were then resuspended in fresh growth medium supplied with 10% FBS and Pen-Strep.

5. 1 ml of this suspension was transferred to a culture flask already containing fresh growth medium.

Amounts of medium, PBS and Trypsin are given in table 12.

Table 12: Cell culture volumes

Reagent	Large culture flask	Medium culture flask
Normal growth medium	30 ml	15 ml
PBS	10 ml	5 ml
Trypsin/EDTA*	1 ml	0.5 ml
Normal growth medium for resuspension	10 ml	5 ml

* May vary according to cell line. Some cells, like HEK 293 detach very easily and do not require more than the volumes given in the table. Other cell lines, such as HeLa or PC12 cells may require larger volumes or higher concentrations to detach properly.

3.2.3.2 Seeding out cells for transient transfection

For different transfection procedures, different amounts of cells are needed. The optimal cell density for transfection is usually provided by the manufacturer of the transfection reagent. To calculate the number of cells in a cell suspension, a small drop was applied to the edge of a Bürker counting chamber, and cells were counted under a light microscope.

3.2.3.3 Harvesting cells

3.2.3.3.1 For Co-immunoprecipitation

Cells were washed twice with prewarmed PBS.

Then, 300 µl lysis buffer was added, and the cells detached from the surface by scraping with a cell scraper.

The resulting suspension was transferred to an eppendorf tube, and spinned down at 13 000 rpm for 10 minutes.

3.2.3.3.2 For Western Blot

Cells were washed twice with prewarmed PBS.

Then, 80 µl LDS sample buffer was added, and the cells detached from the surface by scraping with a cell scraper.

The resulting suspension was transferred to an eppendorf tube, and sonicated 3 x 10 seconds, before denaturation at 70 °C for 10 minutes.

3.2.3.3.3 For Luciferase studies

Cells were washed twice with prewarmed PBS.

Then, 100 µl Tropix lysis buffer supplied with 0.5 mM DTT was added, and the cells harvested by scraping with a cell scraper.

The resulting suspension was transferred to an eppendorf tube and spinned down at 13 000 rpm for 5 minutes.

3.2.4 GST-protein purification

The Glutathione S-Transferases (GSTs) represent a major group of detoxification enzymes. All eukaryotic species possess multiple cytosolic and membrane-bound GST isoenzymes [29]. These enzymes protect cells against toxic substrates by conjugating them to Glutathione, thereby neutralizing their electrophilic sites, and rendering the products more water-soluble. The Glutathione conjugates are metabolized further to Mercapturic acid and then excreted [30]. GSTs bind Glutathione with high affinity and specificity. The strength and selectivity of this interaction enables Glutathione-based affinity resins to effectively purify GST-tagged proteins. Such GST-tagged proteins (GST fusion proteins) are constructed by incorporating a GST gene into an expression vector, followed by cloning of a protein of interest into the vector, directly downstream of the GST gene. To ensure high levels of transcription of the resulting fusion protein, the expression vector usually contains an easily inducible promoter, like the *lac*-promoter from *E. coli*. This promoter can be induced by the compound IPTG (Isopropyl β-D-1-thiogalactopyranoside). This compound is used as a molecular mimic of Allolactose, a lactose metabolite that triggers transcription of the *lac* operon. Induction of the promoter leads to transcription of the fusion protein.

Protocol:

Prior to protein purification, Glutathione Sepharose beads were washed 3 times in PBT, and finally resuspended in PBT to a concentration of 50%. The beads were left at 4 °C for at least 2 hours prior to use.

Protease inhibitor cocktail was prepared by dissolving one tablet of protease inhibitor into 2 ml of distilled H2O.

1. 5 ml LB with Ampicillin was inoculated with protease deficient bacteria (BL21) carrying a plasmid vector containing the desired fusion protein.

2. The culture was grown o.n., and transferred into 50 ml NZCYM with Ampicillin.

3. The culture was then grown until OD_{600} = 0.6

4. When OD600 = 0.6, 50 µl 1M IPTG was added (to make a final concentration of 1 mM), and the culture left to grow for two hours at room temperature.

5. The bacterial culture was then transferred to a 50 ml centrifuge tube, and spinned down at 4000 rpm for 20 min.

6. The supernatant was removed, and the bacterial pellet stored at -20 °C until further use.

7. Before carrying on with the rest of the procedure, the bacterial pellet was transferred to –70 °C overnight.

8. The pellet was then thawed on ice, and resuspended in 1 ml PBT + 200 µl protease inhibitor cocktail + 10 µl 1M DTT (final concentration of 10mM).

9. The suspension was next sonicated 3 x 10 seconds on ice, to disrupt the cell membrane, and release the intracellular contents. The lysate was transferred to an eppendorf tube, and then spinned down at 13 000 rpm for 10 minutes at 4 °C.

10. The supernatant, containing the intracellular proteins, was transferred to a new eppendorf tube, and 100 µl 50% Glutathione beads were added.

11. The tube was placed on a rotator at 4 °C for one hour.

12. The beads were then washed 3 x PBT followed by 3x PBS. After the last wash, as much supernatant as possible was removed.

13. GST-fusion proteins were eluted by adding 250 µl 5 mM Glutathione in 50 mM Tris pH 8.0, and placing the tube on a rotator at room temperature for 15 minutes. Free Glutathione competes with the immobilized Glutathione on the beads for epitopes on the GST-part of the GST-fusion proteins, thus releasing them from the solid phase and into suspension. This step was repeated to obtain two eluates.

3.2.5 Evaluation of GST-protein purification by Coomassie Blue staining

It is important to evaluate the result of GST-protein purification, before moving on to further experiments. One way to do this is by Coomassie Blue staining. Coomassie Brilliant Blue is a dye that binds non-specifically to virtually all proteins. By subjecting the purified GST-fusion proteins to a SDS-PAGE (see section 3.2.6), followed by fixation and staining of the gel by a solution

containing Coomassie Brilliant Blue, all proteins in the sample can be visualized as blue bands appearing in the gel. By including a protein standard in the gel, the size of the individual protein-bands can be estimated, and conclusions drawn as to whether the purification was successful or not. This is, however a purely qualitative measurement of protein concentration. To obtain more accurate measurements of protein concentration, other methods must be applied.

1. Protein samples (eluates) were first subject to SDS-PAGE (see section 3.2.6.1)

2. The gel was transferred to a petri-dish containing Fixation buffer, and put on a shaker for 1 hour at room temperature.

3. The Fixation buffer was removed, and replaced with Coomassie Blue solution for 30 minutes.

4. The gel was then washed once with Fixation buffer, before destaining solution was added, together with a small piece of paper towel (to increase destaining).

5. The destaining solution was changed regularly, and the gel left to destain o.n.

6. The following day a picture was taken, and an assessment made as to whether the desired protein was indeed enriched in the process, and whether it seemed to be present at sufficient concentrations.

3.2.6 SDS-PAGE

SDS-PAGE (Sodium Dodecyl Sulfate PolyAcrylamide Gel Electrophoresis) is a technique that is used to separate proteins based on molecular mass.

The gel is made by polymerized acrylamide, which creates a meshwork that functions as a barrier to the movement of polypeptides. Smaller polypeptides will work their way through this meshwork quicker than larger ones, and so the polypeptides can be separated by size. Some gels have a constant concentration of acrylamide throughout the gel, while others have a graded concentration.

Native proteins harbor secondary, tertiary and sometimes quaternary structures, governed by their composition of differently charged amino acids. In their native conformations, two proteins of approximately the same size could potentially migrate through the gel at significantly different rates. To be able to separate the proteins in a sample based purely on their size, they need to be denatured. That means their secondary, tertiary and quaternary structures need to be eliminated, so that the polypeptide is linearized. This is

achieved by the addition of SDS to the samples. SDS is an anionic detergent which binds to the protein in a constant weight ratio of 1.4 g/g of polypeptide, giving the proteins a net negative charge in the process [31]. This negative charge is also important for the proteins' electrophoretic mobility. The negative charge allows migration from the cathode to the anode, “pulling” the proteins through the gel.

3.2.6.1 Using the Clear Page 10x10 cm SDS Cassette gels, 4-12%

The Clear Page gels were used to evaluate the result of GST-protein purification:

1. The gel was removed from the plastic, and rinsed in deionized water.
2. The wells were rinsed three times with Clear Page running buffer, and the gel mounted in the XCell *SureLock™* Mini-cell.
3. The inner chamber was filled with fresh running buffer, and the outer chamber filled with running buffer that had been used no more than two times before, but need not be fresh.
4. 15 µl of protein sample (eluate) was transferred to an eppendorf tube, and supplied with 5,5 4x NuPage LDS sample buffer and 2 µl 1M DTT.
5. The samples were then denatured at 70 °C for 10 minutes.
6. 18 µl of each sample was applied to the gel. 2 µl SeeBlue® protein standard was also applied to the gel.
7. The gel was run at NuPage gel-program, at 200V for approximately 45 minutes

3.2.6.2 Using the NuPage® Novex® Bis-Tris Mini SDS Gels, 4-12%

These gels were used for SDS-PAGE prior to Western blotting and for IVK.

1. The gel was removed from the plastic, and rinsed in deionized water..
2. The comb was pulled out to access the wells, and the white tape at the bottom part of the gel was removed.
3. The wells were washed three times with fresh 1 x NuPage running buffer, and the gel mounted in the XCell *SureLock*™ Mini-cell.
4. The inner chamber was filled with fresh running buffer, and the outer chamber filled with running buffer that had been used no more than two

times before, but need not be fresh.

5. 18 µl cell lysate for western blotting (see section 3.2.3.3.2) or sepharose G beads from Co-ip (see section 3.2.10) was applied to the gel.

6. 2 µl SeeBlue® protein standard, and 2 µl MagicMark™ protein standard were also applied to the gel.

7. The gel was run at NuPage gel-program, at 200V for approximately 45 minutes.

3.2.7 Western blotting

Western blotting is a method to detect one specific protein/peptide in a complex mixture of proteins. The method depends on separation of proteins by SDS-PAGE prior to blotting. The protein-bands from the SDS-PAGE are transferred onto a solid support, usually a nitrocellulose or nylon membrane by electrophoretic transfer, and subsequently subjected to a an antibody specific to the protein/peptide in question. This antibody can be enzyme-labeled or radio-isotope labeled for visualization. The immunoblotting can also be performed indirectly by detecting antigen-antibody complexes by a secondary labeled antibody with improved sensitivity. Enzymatic catalyzed methods are widely preferred over autoradiography, because it eliminates the need for radioactive isotopes, and offers easy detection by chemiluminescence or chromogen detection [32].

Protocol:

Prior to blotting, a PVDF (Polyvinylidene fluoride) Immobilon® membrane from Millipore® with a pore size of 45 µm had been washed for 3 seconds in methanol, followed by 10 seconds in distilled water, and finally a minimum of 5 minutes in Blocking buffer.

1. The gel was removed from the XCell *SureLock*™ Mini-cell, and the wells and the «ridge» at the bottom cut off.

2. In a blotting unit, was placed in the following order:

   i. 2 blotting pads, soaked in blotting buffer

   ii. 2 filter papers, soaked in blotting buffer

   iii. The gel

   iv. The PVDF-membrane

   v. 2 filter papers, soaked in blotting buffer

vi. 3 or more blotting pads, soaked in blotting buffer (enough to make the seal tight).

3. The blotting unit was then placed in the XCell *SureLock*™ Mini-cell. The inner chamber was filled up with fresh blotting buffer, while the outer chamber was filled with cold, deionized water.

4. The Mini-cell was connected to the power supply, and the blot performed at NuPage blot program, at 30V for 1 hour.

5. After blotting, the membrane was transferred to a beaker containing PBS and washed for 10 minutes on the shaker.

6. Next, the PBS was exchanged for Blocking buffer for 1 hour, still on the shaker.

7. After blocking, the membrane was transferred to a 50 ml centrifuge tube, and 3 ml blocking buffer + primary antibody in the desired dilution was added.

8. The tube was sealed with parafilm, and put on the rotator at slow speed at 4 °C o.n.

9. The following day, the primary antibody-Blocking buffer solution was removed, and the membrane washed 3 x 5 minutes with PBST.

10. Then secondary antibody diluted in 3 ml PBST was added to the membrane, and the tube placed at rotator, slow speed at room temperature for 1 hour.

11. After incubation with secondary antibody, the membrane was washed 2 x 5 minutes with PBST, followed by 2 x 5 minutes wash with Washing buffer.

12. After the last wash, 3 ml CDP Star buffer + 6 µl CDP Star was added to the tube, and the tube placed at the rotator for 5 minutes.

13. The membrane was removed from the tube, and sealed in plastic.

14. After a few minutes in the dark, the membrane was developed on the lumi-Analyst machine.

3.2.8 Transient transfection of Mammalian cells

There are many reasons for artificially introducing DNA into living cells, whether it be mutant, or wild-type genetic elements. It can be done in order to analyze the characteristics of a specific gene, and its effect on cellular growth

and differentiation, or in order to create over-expressing cell lines for purification of the product for biochemical characterization or even large-scale drug-production [33].

There is a variety of strategies available for delivery of genes into eukaryotic cells, all of which fall into one of three categories:

- Transfection by biochemical methods
- Transfection by physical methods
- Virus-mediated transduction

Biochemical methods include calcium-phosphate mediated and diethylaminoethyl (DEAE)-dextran mediated transfection in addition to liposome-mediated transfection. Physical methods include microinjection and electroporation [34]. Virus-mediated transduction is beyond the scope of this study.

Transfection can either be made transient or stable, depending on the needs of the researcher. In transient transfection, recombinant DNA is introduced into a recipient cell-line in order to obtain a temporary, but high level of expression of the target gene. The transfected DNA does not usually get integrated into the chromosome, and will eventually be lost from the cells through mitosis. This is the method of choice when samples are to be analyzed within a short period of time. In stable transfection, the target gene is integrated into the chromosomal DNA, from where it directs the synthesis of moderate amounts of target proteins. This type of transfection is less efficient than transient transfection, typically by one to two orders [34].

In this study, cells were transfected by liposome-mediated transfection and electroporation, depending on the cell-line being transfected.

In liposome-mediated transfection, negatively charged phosphate groups on DNA binds to the positively charged surface of the liposome, and the residual positive charge then presumably mediates binding to negatively charged sialic residues on the cell surface. This is, however, a mechanism which is incompletely understood [33].

In electroporation, brief electrical pulses create transient pores in the plasma membrane, through which DNA can enter the cell [34]. This technique is not dependent upon specific characteristics of the cell, and thus can be applied to virtually any cell line. The optimal parameters for each cell-line will vary however, and need to be optimized in order to obtain efficient transfection[33].

3.2.8.1 Liposome-mediated transient transfection

3.2.8.1.1 By Lipofectamine™2000

1. The day before transfection, cells were seeded out in 6 well trays (for Luciferase assay) or cover-slips (for confocal studies), 250 000 and 15 000 cells per well respectively.

2. Lipofectamine was combined with OptiMem, and left at room temperature for 5 minutes.

Table 13: Reaction volumes for Lipofectamine™2000 transfection

Reagent	Luciferase assay	Confocal studies
Culturing vessel	6 well plate	8 well cover-slip
Lipofectamine™2000	10 µl	1 µl
Lipofectamine Diluting medium (OptiMem)	250µl	25 µl
DNA	2 µg	0.4 µg
DNA-diluting medium (OptiMem)	250 µl	25 µl

3. In the mean time, DNA was diluted in the same amount of OptiMem as the Lipofectamine™2000 .

4. The two solutions were combined, and incubated at room temperature for 20 minutes.

5. The medium was removed from the cells by water-suction, and each well was supplied with 500 µl or 50 µl OptiMem respectively for 6 well plates and 8 well cover-slips.

6. Next, the Lipofectamine™2000 /DNA solution was added to the wells.

7. The cells were put back into the incubator at 37 °C and 5% CO_2.

8. After 4 hours, the medium was aspirated off the cells by water-suction, and exchanged for fresh, normal growth medium (2 ml and 200 µl respectively for 6 well plates and 8 well cover-slips).

9. The cells were out back into the incubator until the following day.

3.2.8.1.2 By Metafectene®Pro

1. 1.5 x 10^6 HEK293 cells were seeded out in 10 cm plates.

2. The following day, 1 ml Optimem was mixed with 10 µl Metafectene®Pro and 2 µg plasmid DNA, in that particular order of events, and incubated at room temperature for 20 minutes.

3. The mixture was added to the plates, and the plates swirled carefully to distribute the transfection mixture evenly.

4. The plates were then put back into the incubator until the next day.

5. Cells were harvested according to protocol in section 3.2.3.3.1

3.2.8.2 Transient transfection by electroporation

This technique was applied to transfections of PC12 cells. This is a cell line which is hard to transfect by other methods.

1. 2x 10^6 PC12 cells were transferred to 15 ml centrifuge tubes, and spinned down at 200 rpm for 10 minutes.

2. The medium was carefully removed by water-suction.

3. The cells were then resuspended in 82 µl Nucleofector® solution + 18 µl supplement from the Cell Line Nucleofector® kit V + 2 µg plasmid DNA or 300 nM siRNA.

4. The resulting suspension was next transferred to a Nucleofector® cuvette, and electroporated in the Nucleofector® II machine at program U 029.

5. 10 µl of the suspension was transferred to each well in an 8 well cover-slip coated with collagen.

6. The cells were then put back into the incubator until the next day (DNA-transfection) or for 48 hours (siRNA transfection).

3.2.9 Luciferase assay

Transcriptional activator proteins bind to specific enhancer elements in eukaryotic promoters, and stimulate transcription of nearby genes. Separable, functional domains of activator proteins confer specific DNA-binding properties. These functional domains are remarkably flexible, and readily tolerate fusion to heterologous proteins. A popular technique for studying activating and regulatory elements of transcriptional activators in mammalian systems involves fusion to the DNA-binding domain of the yeast GAL4 protein [35]. By co-transfection of such fusion-proteins with a Luciferase-reporter plasmid, containing upstream GAL4 activating sequences it is possible to monitor the

effect of the (suspected) transcriptional activator protein, without any confounding factors, as only fusion proteins containing the yeast GAL4 DNA-binding domain can bind to the yeast-derived activating sequence. However, it is difficult to say whether this protein interacts with the promoter directly, or through interaction partners in a pre-initiation complex.

1. From the supernatant of the harvested cells (see section 3.2.3.3.3), 20 µl of each sample was transferred to a well in a white 96 well plate. Two wells were supplied with lysis buffer alone, to serve as reference measurements.

2. 100 µl Luciferase buffer was added to each well (reference samples included), and the plate covered with aluminum foil to protect the samples from exposure to light.

3. Luciferase activity was measured by a luminometer.

3.2.10 Co-immunoprecipitation

Coprecipitation of proteins from whole-cell extracts is a valuable approach to test for physical interactions between proteins of interest. When a precipitating antibody is used, the method is referred to as co-immunoprecipitation. Coprecipitation techniques can be used to study interactions between known proteins, or to identify members of a complex [36].

Before starting, it is important to generate reagents that detect the two proteins in the co-precipitate under non-denaturating conditions. If specific antibodies for the proteins in question are hard to come by/obtain, the proteins can alternatively be tagged with a short peptide or epitope that is recognized by commercially available high-affinity monoclonal antibodies. Examples of such epitopes are influenza Hemagglutinin protein (HA), human c-Myc and FLAG (an epitope specifically designed for use as a tag) [36].

After incubation of the cell extract with the antibody specific for the protein to be precipitated (pulled down) or its tag, the cell extract is supplied with Sepharose beads conjugated to Protein G or Protein A. These are bacterial proteins from Group G Streptococci and *Staphylococcus aureus*, respectively, and both have high affinity for the Fc region of IgG from a variety of species.

The precipitated protein is in this way immobilized on a solid matrix, along with any proteins that might be part of a complex with this protein. Through several washing steps, other cellular contaminants are removed, and finally the precipitated proteins are separated by SDS-PAGE.

By subsequent western blotting with the appropriate antibody, interacting proteins may be detected (Figure 6).

For confirmation of the presence of the precipitated protein, it is advisable to strip the WB membrane and re-probe with the antibody directed against this protein.

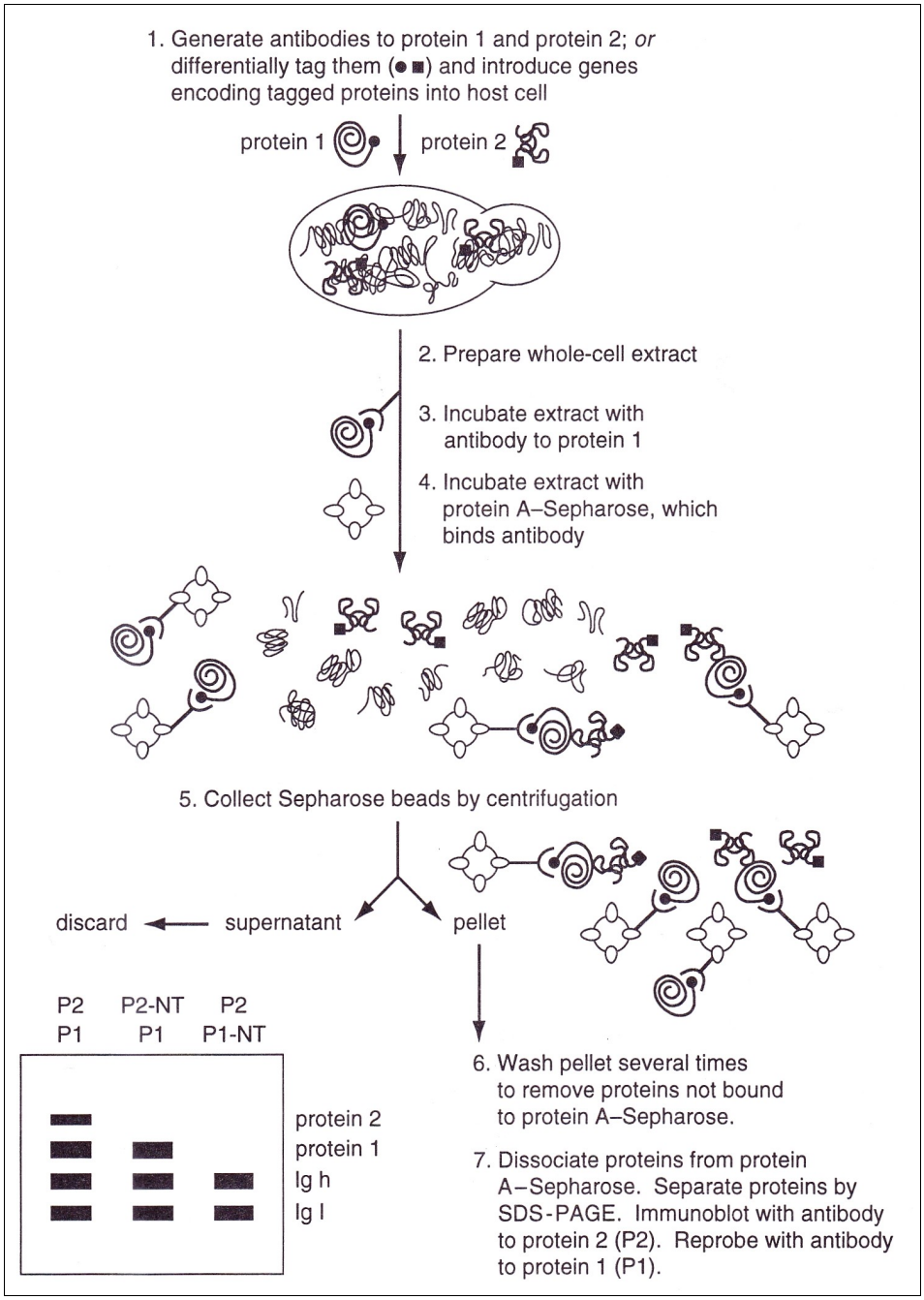

Figure 6: Flow-chart of co-immunoprecipitation. Ig h and Ig l = Immunoglobulin heavy and light chains, NT = no tag. The figure is adapted from [36].

Before starting, Sepharose G beads were washed three times in lysis buffer. After the last wash, lysis buffer was added to make a 50% Sepharose G solution.

1. The supernatant from the harvested cells (see section 3.2.3.3.1) was transferred into new eppendorf tubes.

2. 30 µl of each supernatant was transferred to a new eppendorf tube to serve as input control. 8 µl 4x NuPage LDS sample buffer and 2 µl 1M DTT was added, and the samples denatured at 70 °C for 10 minutes.

3. To the rest of the supernatant, the appropriate antibody was added in the desired dilution, and the tube placed at a rotator, slow speed, at 4 °C for 1 hour or o.n.

4. 80 µl 50% Sepharose G beads were added, and the tube returned to the rotator for 1 hour.

5. The beads were washed 5 times in 1 ml cold lysis buffer. After the last washing step, as much buffer as possible was removed.

6. To the beads, 10 µl 4x NuPage LDS Sample buffer, 2 µl 1M DTT and 8 µl distilled H_2O was added.

7. The tubes were incubated at 70 °C for 10 minutes, and stored at -20 °C until further processing by SDS-PAGE and Western blot (see section 3.2.6.2 and 3.2.7).

3.2.11 In vitro kinase assay

MAP kinases activate their substrates by transferring a γ-phosphate from ATP to a phosphoaccepting residue in the substrate, typically a Serine, Threonine or Tyrosine. To investigate potential *in vitro* substrates for MAP kinases, the two proteins are brought together in the presence of radioactively labeled ATP under favorable conditions. The samples are subsequently separated by SDS-PAGE, and visualized on a radiographic plate (IP) containing photostimulable storage phosphors. The imaging plate is run through a special laser scanner, or CR reader, that reads and digitizes the image. The digital image can then be viewed and enhanced using software [37].

Protocol:

1. TBD buffer and kinase buffer (table 1) were prepared fresh for each experiment.

2. 20 µl of each protein to be investigated was added to two eppendorf tubes. Half of these were to be supplied with premix not containing MK5, and the other half with premix supplied with MK5.

3. Premix was prepared for as many samples as needed:

Table 14: Premix for in vitro kinase assay (per sample)

Reagent	Amount
Kinase buffer	4 µl
800 µM ATP	2.5 µl
100 mM DTT	0.8 µl
^{32}p-γ-ATP*	0.3 µl

* ^{32}p-γ-ATP was added in the HOT-lab

4. To half of the premix, 3 µl active MK5 (0.45 µg/ µl) per sample was added.

5. The samples were supplied with TBD buffer and premix to reach a total volume of 35 µl:

Table 15: Preparation of samples for in vitro kinase assay

Sample	Protein	TBD buffer	Premix
Without MK5	20 µl	7,4 µl	7,6 µl
With MK5	20 µl	5,1 µl	9,9 µl
MK5 only	-	25,1 µl	9,9 µl

6. All samples were incubated in a heating block at 30 °C for 1 hour.

7. The reaction was terminated by adding 12 µl 4 x LDS sample buffer + 1.4 µl 1M DTT to each sample, followed by incubation at 70 °C for 10 minutes.

8. The samples were run on a NuPage® Novex® Bis-Tris Mini SDS Gel, 4-12% (SDS-PAGE) for 45 minutes. SeeBlue® protein standard was included.

9. After SDS-PAGE, the gel was wrapped in cling-film, and dried in a gel-drier at 80 °C for 1 hour.

10. The dry gel was placed in a photo-cassette and covered with an Image Plate that had been wiped clean by exposure to fluorescent light. The plate was left to develop o.n.

11. The following day, the plate was scanned in a FUJI-BAS5000 CR-scanner, and the picture developed with Image Reader software.

3.2.12 Immunofluorescent labeling of cells

Immunocytochemistry is a common laboratory technique that uses antibodies to target peptides or proteins in the cell via their specific antigens.

Such studies are easily performed on cultured cells that are grown as monolayers. The cells are briefly fixed in low concentrations of Paraformaldehyde. What happens next depends on whether the antigen of interest is considered to be present at the cell surface or in the cytoplasm. If the antigen is present in the cytoplasm, the cells need to be permeabilized. This can be done by subjecting them to Triton X-100 or Methanol. Both methods work well, but permeabilization by Triton frequently gives a better final morphology. After incubation with primary antibody, followed by washing steps, a secondary antibody conjugated to a fluorochrome is added. When examined under the microscope and exited by a laser of the appropriate wavelength, the fluorochrome emits light, and thus reports the location of the protein.

1. The cells were fixed by adding 150 µl ice-cold PFA 0.8% to each well in a 8 well cover-slip, without removing the growth medium first, followed by incubation on ice for 10 minutes.

2. The medium/PFA was removed, and the cells washed carefully with ice-cold PBS twice.

3. PBS was removed from the cells, and replaced with 150 µl ice-cold 0.1 % Triton® x-100 in PBS for permeabilization.

4. The cells were incubated on ice for 10 minutes, followed by careful washing in ice-cold PBS twice.

5. The PBS was removed, and replaced with 200 µl PBS with 3% goat serum, for blocking, for 1 hour at room temperature, with shaking.

6. Primary antibody was added in the appropriate dilution, and the cells put on the shaker at room temperature for 1 hour.

7. The cells were washed twice with ice-cold PBS.

8. PBS was removed, and secondary antibody conjugated to a fluorophore added in the appropriate dilution.

9. The cells were incubated once more at room temperature, with shaking for 1 hour.

10. The cells were washed 4 x 5 minutes with PBS.

11. To the cells, DraQ5 nuclear stain was added in a 1:1000 dilution, and incubated at room temperature for 5 minutes, followed by two times wash with PBS.

12. Finally the cover-slip was covered in aluminum foil to protect the fluorophores from exposure to light, and kept at 4 °C until investigation by confocal microscope.

3.2.13 Site-directed mutagenesis mediated by oligonucleotides

Oligonucleotide-directed mutagenesis is used to add, delete or substitute nucleotides in a segment of DNA whose sequence is known. In contrast to most other methods of mutagenesis, which typically spawn mixed populations of variants, oligonucleotide-mediated mutagenesis specifically generates mutations designed by the experimenter. This is achieved by designing and synthesizing an oligonucleotide whose sequence contains the desired mutation, hybridizing it to a template containing the wild-type sequence, and extending the primer with a DNA polymerase harboring proof-reading activity in a Polymerase Chain Reaction (PCR) [38].

PCR is a widely used, and highly effective method for *in vitro* amplification of DNA. Through several cycles of rising and lowering temperatures, a heat stable DNA polymerase from a thermophilic organism synthesizes new DNA from a parental template. The reaction is primed by two artificially made oligonucleotides, referred to as primers, and also requires the presence of free nucleotides in the reaction mixture. At the beginning of each PCR-cycle, the temperature is raised to a level where the double-helix denaturates (the strands separate from each other). Then the temperature is slightly decreased to a level where the primers anneal to the template. Finally the temperature is once more slightly raised to a level where the DNA-polymerase most efficiently synthesizes a new DNA strand. Then the cycle is repeated several times, creating an exponentially growing number of DNA-strands.

Table 16: Premix for site-directed mutagenesis (per sample)

Reagent	Amount (µl)
dH_2O	39.6
10 x Pfu buffer	5
Primer 1 (100 ng / µl)	1.3
Primer 2 (100 ng / µl)	1.3
12.5 mM dNTP	0.8
Pfu Turbo enzyme	1
Total:	49

The premix was transferred into an eppendorf tube, and 1 µl plasmid DNA (25 ng/µl) was added.

In this experiment, a graded PCR was used, to investigate the optimal annealing temperature of the primers

Table 17: PCR conditions for site-directed mutagenesis

95 °C	30 seconds
Gradient 50 °C – 70 °C	30 seconds
68 °C	7 minutes
Cycles	14

After the PCR reaction 1 µl *Dpn*I was added to each sample, and the samples incubated at 37 °C for 1 hour. This was done in order to remove the template which was not mutated, but methylated. The DNA generated during PCR will contain the mutation, but is not methylated. *Dpn*I cuts the sequence GATC when A is methylated. In this way, unmutated DNA is destroyed.

3.2.14 Cloning using restriction endonucleases

Restriction endonucleases recognize short DNA sequences and cleave double-stranded DNA at specific sites within or adjacent to these recognition sites [28]. Most plasmid vectors contain several restriction sites for easy cloning of genetic elements. These restriction sites are often contained within a geographically constricted part of the vector called a multiple cloning site or polylinker. Before cloning a genetic element from one vector into another, it is necessary to investigate the polylinkers of each vector, to decide whether they contain compatible restriction sites. If not, restriction sites may be introduced by site directed mutagenesis. After cutting with restriction endonucleases, the fragmets are separated on an Agarose gel. The desired fragments are cut out of the gel, and the DNA retrieved by centrifugation of the gel through a column. Finally, the fragments are joined together by DNA-ligase. The ligated fragments are then transformed into competent bacteria, which produce large amounts of the clone. The cloned DNA can then be purified and sequenced to verify that the desired fragment has been cloned into the recipient vector in the correct reading-frame and orientation.

Protocol:

1. All reagents were mixed, and the samples incubated at 37 °C for 2 hours or overnight. In this study, the recipient vectors were pENTR1A and pENTR3C (table 3).

Table 18: Reaction set-up for cutting of dsDNA with restriction endonucleases

Sample	1	2
Buffer*	2 µl	2 µl
Donor vector	1 µg	
Recipient vector		1 µg
Restriction endonuclease 1	1 µl	1 µl
Restriction endonuclease 2	1 µl	1 µl
BSA	0.7 µl	0.7 µl
ddH_2O	To 20 µl	To 20 µl

2. The resulting fragments were next run on a 1% Agarose gel, and the desired fragments cut out of the gel.

3. The DNA was retrieved by spinning the gel-fragment through a custom-made column, consisting of eppendorf tubes and filter papers.

4. The two DNA-fragments were then joined together by DNA-ligase in the following reaction:

Table 19: Ligation reaction

Reagent	Amount
T4 ligation buffer	2 µl
T4 DNA ligase	1 µl
Donor fragment	X µl*
Recipient fragment	1-2 µl
ddH_2O	To 20 µl

* Several samples were made for each reaction, each with different amounts of donor fragment (in the range 7- 16 µl)

5. The samples were incubated at 16 °C o.n. before transformation into competent DH5 cells, followed by sequencing.

3.2.15 Gateway® cloning

The Gateway® system for easy cloning is developed by Invitrogen. In principle, the system is based on cloning the DNA sequence of interest into the multiple cloning site of an ENTRY vector, using restriction endonucleases and DNA ligase, thereby creating an ENTRY clone. The ENTRY vector contains attL1 and attL2 sites for specific recombination with a Gateway destination vector, so that the ENTRY clone can easily be cloned into a variety of destination vectors, displaying different features, thereby creating different expression clones. The

destination vectors also contain dual selection markers, to ensure that only bacteria carrying clones in which the DNA sequence has been inserted correctly, will propagate. This eliminates the need for subsequent sequencing reactions, and ensures consistent results throughout the experiment. The recombination between ENTRY clones and destination vectors is achieved by using pre-made enzyme mixes, containing buffers and enzymes, and is performed in a one hour, room temperature reaction.[29]

Protocol:

1. The following components were added to an eppendorf tube:

Table 20: Reaction set-up for Gateway® cloning

Reagent	Amount
ENTRY clone (50-150 ng)	1-7 µl
Destination vector (150 ng/µl)	1 µl
TE buffer, pH 8.0	To 8 µl

2. The LR clonase® II enzyme mix was thawed on ice, and vortexed briefly x 2.

3. To each sample, 1 µl* LR clonase® II enzyme mix was added, and the contents mixed well by vortexing briefly x 2.

4. The samples were incubated at 25 °C for two hours.

5. Then, 1 µl Proteinase K solution was added to each sample to terminate the reaction. The samples were vortexed briefly, and incubated at 37 °C for 10 minutes.

6. The cloned DNA was further transformed into competent DH5α cells by the procedure in section 3.2.16.

   * The original protocol from Invitrogen states 2 µl, but in order to reduce costs, it was decided upon using only half the amount LR clonase® II enzyme mix, and double the incubation time from one to two hours.

3.2.16 Transformation of competent bacteria

Bacteria that are able to take up naked DNA directly from their environment, are said to be competent. Some bacteria are naturally competent, and those that are not, can be made competent artificially, either by treatment with Ca Cl_2 or by electroporation.

The process of introducing DNA into competent cells is called transformation. In $CaCl_2$ treated cells this is achieved by briefly heat-shocking a mixture of cells and DNA, and for cells made competent by electroporation, the transformation is executed by mixing DNA with the bacterial cells as they are elctroporated. Electroporation creates transient pores in the cell membrane, through which The DNA can enter the cells.

In this study, $CaCl_2$ treated competent cells were used for transformation.

Protocol:

1. Competent cells were collected from the nitrogen tank, and thawed on ice.

2. To 200 µl competent cells, approximately 20 ng* plasmid DNA was added.

3. The mixture of cells and DNA was incubated on ice for 30 minutes.

4. The cells were then heat-shocked at 42 °C for 90 seconds, followed by incubation on ice for another 90 seconds.

5. 800 µl SOC medium was added, and the cells put in the incubator at 37 °C with horizontal shaking for 45 minutes.

6. The cells were plated out on LB-plates containing the appropriate selective antibiotic, as specified by the plasmid in question.

7. The plates were incubated at 37 °C overnight.

* For transformation of ligation-products (section 3.2.14) the amount was variable.

3.2.17 DNA sequencing

When clones have been made and purified, they need to be verified by sequencing of the DNA. To achieve this, the DNA is combined with a mixture containing a *Taq*-polymerase, unlabeled dNTPs and ddNTPs that are labeled with fluorescent dyes, one specific color for each ddNTP (A, T, G, C). The ratio of dNTPs vs ddNTPs is approximately 100:1. One such mixture is Big Dye 3.1. Specific primers for the DNA are also included. The samples are next subjected to a PCR reaction, and the DNA amplified much the same way as described earlier. The ddNTPs lack a 3' hydroxyl end to which the next nucleotide can attach. Thus, each time a ddNTP is incorporated into the growing strand, the reaction terminates, resulting in a myriad of DNA fragments of different lengths, each ending with a specific ddNTP as ordinated by the DNA template. When the run has ended, the fragments are separated on a gel, and the fluorescent dyes that are attached to the ddNTPs exited by a UV laser [30]. An

automatic scanner then"reads" the gel, shortest fragment first, followed by the one which is one nucleotide longer and so on, ascribing A, T, G or C as directed by the color of the dye.

Protocol:

1. The following premix was made:

Table 21: Premix for DNA sequencing

Reagent	Amount
5 x sequencing buffer	3 µl
Big Dye 3.1	0.5 µl
pENTR 5' primer	1 µl

2. To the premix, 500 ng plasmid DNA was added.

3. The samples were run at the following program:

Table 22: PCR conditions for sequencing PCR

96 °C	10 seconds
50 °C	5 seconds
60 °C	4 minutes
Cycles:	30

4. The samples were delivered to the sequencing lab/facility at Universitetssykehuset i Nord-Norge (UNN) where the electrophoresis and scan was performed on a 3130*xl* Genetic Analyzer from Applied biosystems/HITACHI.

3.2.18 FRET-studies

Förster resonance energy transfer, also called fluorescence resonance energy transfer or FRET for short, is a technique that allows establishment of molecular interactions that would otherwise be beyond the resolution of a light microscope. FRET occurs when two fluorochromes, which are closely associated with each other, can interact such that the light used to excite one will be transferred as internal energy to the other fluorochrome, and then emitted as longer wavelength light characteristic of the second fluorochrome. For FRET to occur, the fluorescence emission from the first fluorophore, the donor, must overlap with excitation spectrum of the second fluorophore, the acceptor, and the molecules must be within a distance of 2-6 nm of each other [31].

Protocol:

1. 15 000 HeLa cells were seeded out in a cover-slip, and transfected by Lipofectamine according to the procedure in section 3.2.8.1.1

2. The following day, the cells were fixed by adding 150 µl ice-cold 0.8% PFA and incubating on ice for 10 minutes.

3. The cells were washed twice with ice-cold PBS.

4 Results

Studies by our group had shown that HSP27 is a bona fide substrate for MK5 [15]. This prompted us to examine whether other heat shock proteins could be targets for MK5. Sergiy Kostenko in our group showed that the HSP40 member DNAJB1 could also be phosphorylated by MK5 in vitro (Figure 7).

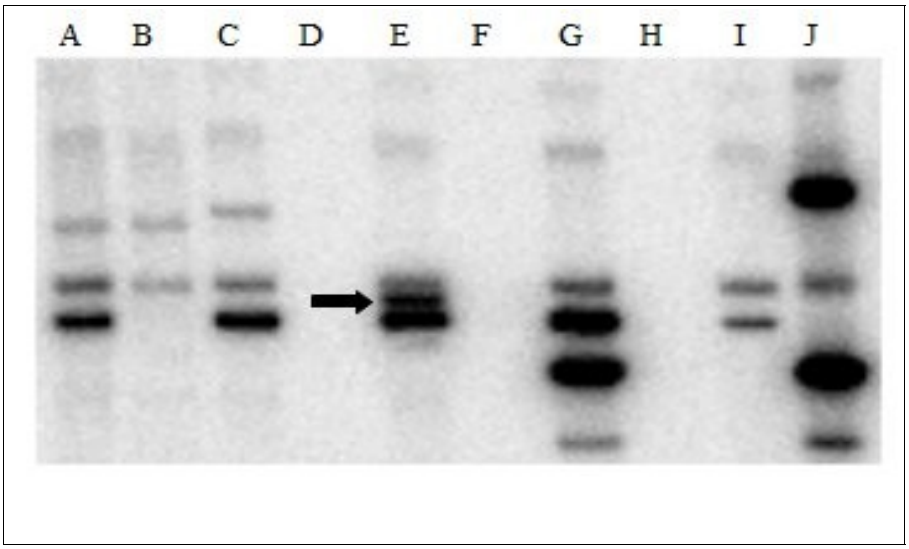

Figure 7: In vitro kinase performed on various heat shock proteins in the presence of active MK5. Lane A: HSP90 + MK5. Lane B: HSP90. Lane C: HSP70 + MK5. Lane D: HSP70. Lane E: HSP40/DNAJB1 + MK5. Lane F. HSP40/DNAJB1. Lane G: HSP27 + MK5. Lane H: HSP27. Lane I: MK5. Lane J: HSP27 + PKD (included as a positive control for phosphorylation of HSP27). Phosphorylation of DNAJB1 is indicated by an arrow. [Kostenko unpublished results].

To investigate DNAJB1 as a possible substrate of MK5, the two proteins were included in further in vitro kinase assays, co-localization studies and interaction studies (Co-ip and FRET).

4.1 MK5 and DNAJB1 co-localize in the cell

The original finding that MK5 could phosphorylate HSP40 suggests that there is a physical interaction between these two proteins. To test this, we first set out to study the subcellular localization of both proteins. Fluorescently tagged MK5 and DNAJB1 proteins were ectopically expressed in HeLa and PC12 cells and their localization was visualized by confocal microscopy studies. As shown in Figure 8, 9 and 10, both proteins localize mainly to the nucleus in both cell lines. HSF1 was also included in some of these studies, and it seems that this protein is also localized mainly within the nucleus (Figure 8 and 11).

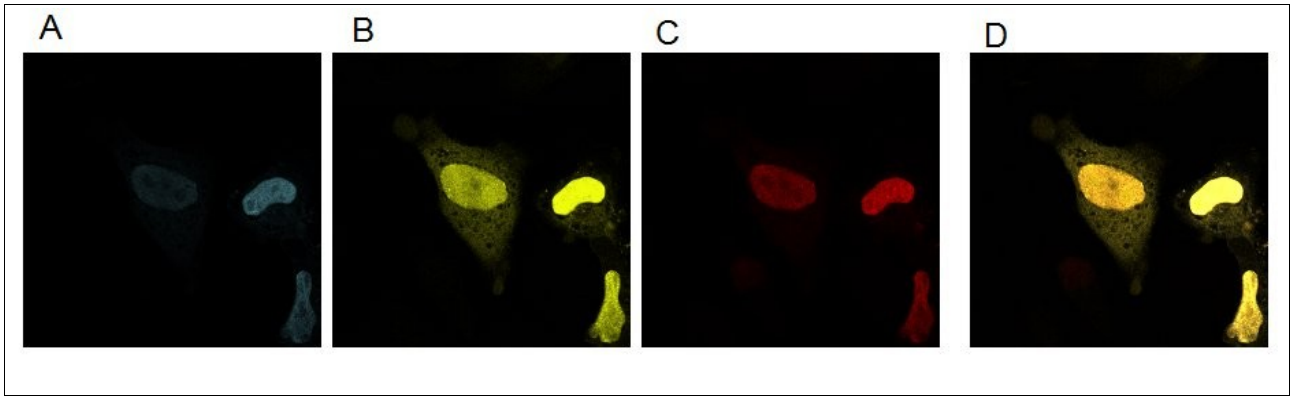

Figure 8: HeLa cells co-transfected with ECFP-DNAJB1, EYFP-MK5 and Cherry-HSF1. A: only ECFP-DNAJB1 shown. B: only EYFP-MK5 shown. C: only Cherry-HSF1 shown. D: Pictures A-C merged.

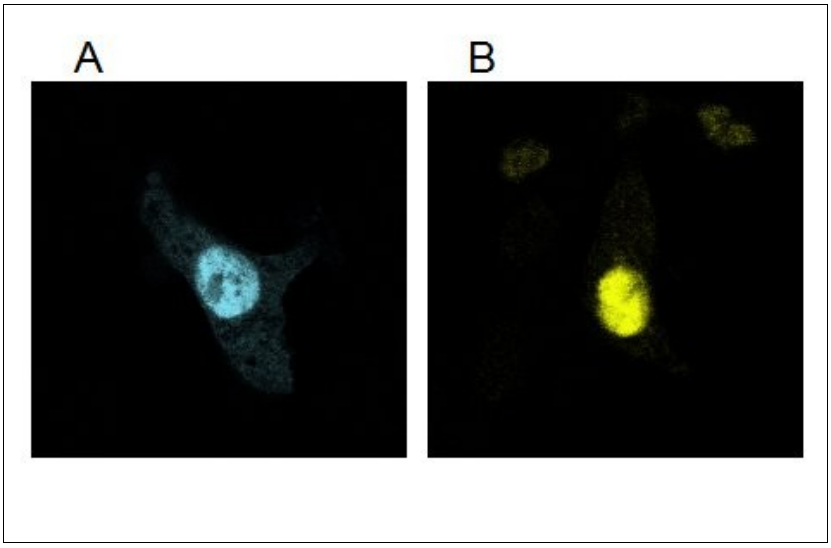

Figure 9: PC12 cells. A: transfected with ECFP-DNAJB1. B: Transfected with EYFP-MK5.

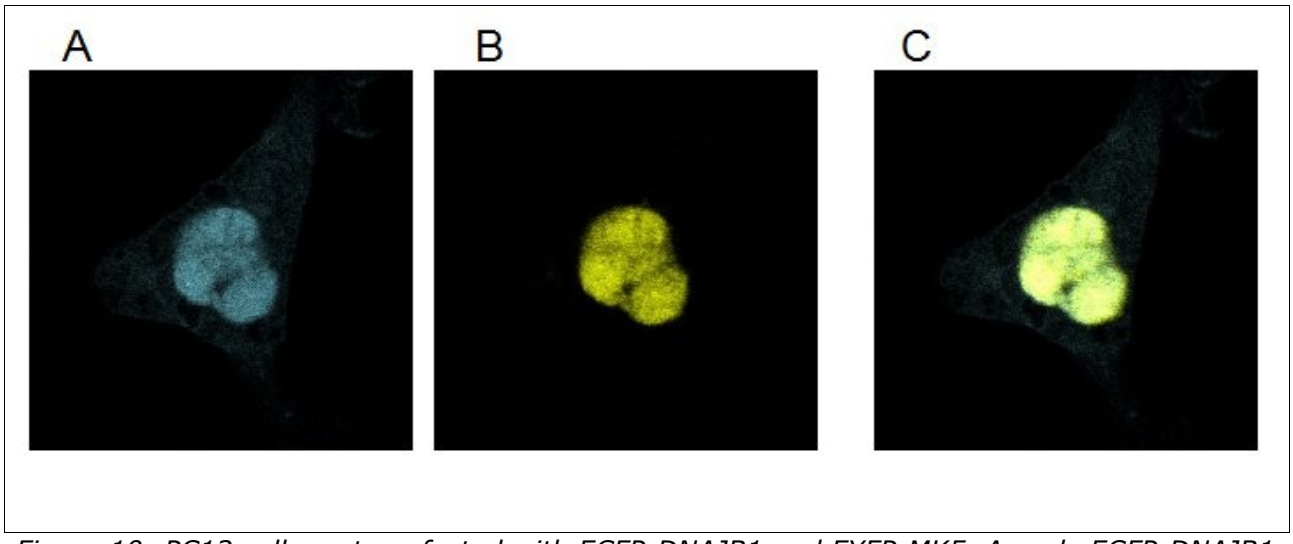

Figure 10: PC12 cells co-transfected with ECFP-DNAJB1 and EYFP-MK5. A: only ECFP-DNAJB1 shown. B: only EYFP-MK5 shown. C: Pictures A and B merged.

As seen in Figure 11, Co-transfection of DNAJB1 and HSF1 with the constitutively active MK5L337A did not seem to alter the pattern of subcellular localization of either protein.

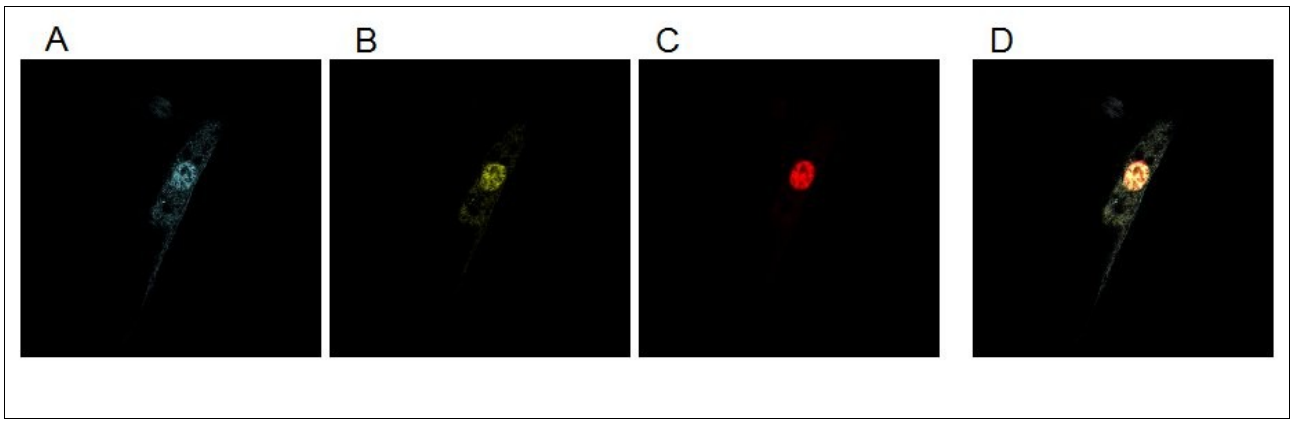

Figure 11: HeLa cells co-transfected with ECFP-DNAJB1, EYFP-MK5L337A and Cherry-HSF1. A: only ECFP-DNAJB1 shown. B: only EYFP-MK5L337A shown. C. only Cherry-HSF1 shown. D: Pictures A-C merged.

Forskolin treatment of MK5 led to nucleocytoplasmic redistribution, as expected [13][14], while it did not seem to alter the subcellular distribution of DNAJB1 (Figure 12). Forskolin is a diterpene that raises the level of cAMP in the cell, thus activating the cAMP/PKA pathway. These results therefore indicate that activation of MK5 by the cAMP/PKA pathway does not influence subcellular distribution of DNAJB1.

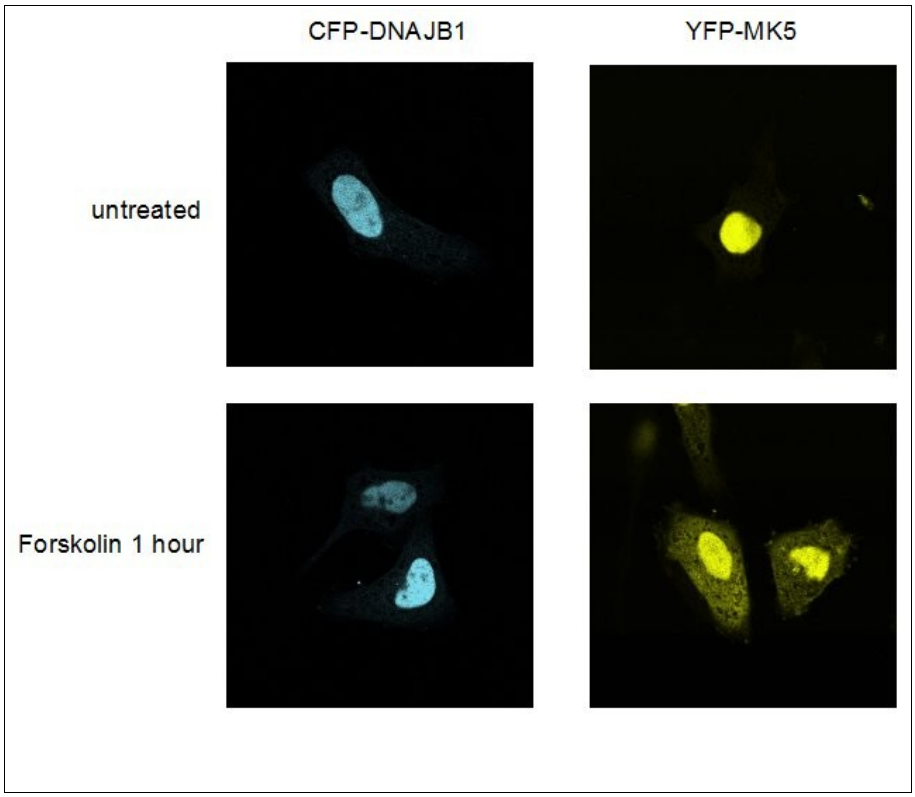

Figure 12: HeLa cells transfected with ECFP-DNAJB1 and EYFP-MK5. With and without Forskolin treatment.

Co-expression of ECFP-DNAJB1 and EYFP-MK5 did not seem to alter the localization of either protein upon Forskolin treatment (Figure 13). One would normally expect EYFP-MK5 to re-localize to the nucleus, and could, as such, speculate that interaction with ectopically expressed DNAJB1 retained the protein in the nucleus. Previous experience with MK5 in HeLa cells, however, has shown that MK5 does not always relocate to the cytoplasm upon forskolin treatment [Kostenko unpublished results], and, based on this experience it would be unwise to conclude that the lack of nucleocytoplasmic redistribution of MK5 is due to the presence of DNAJB1.

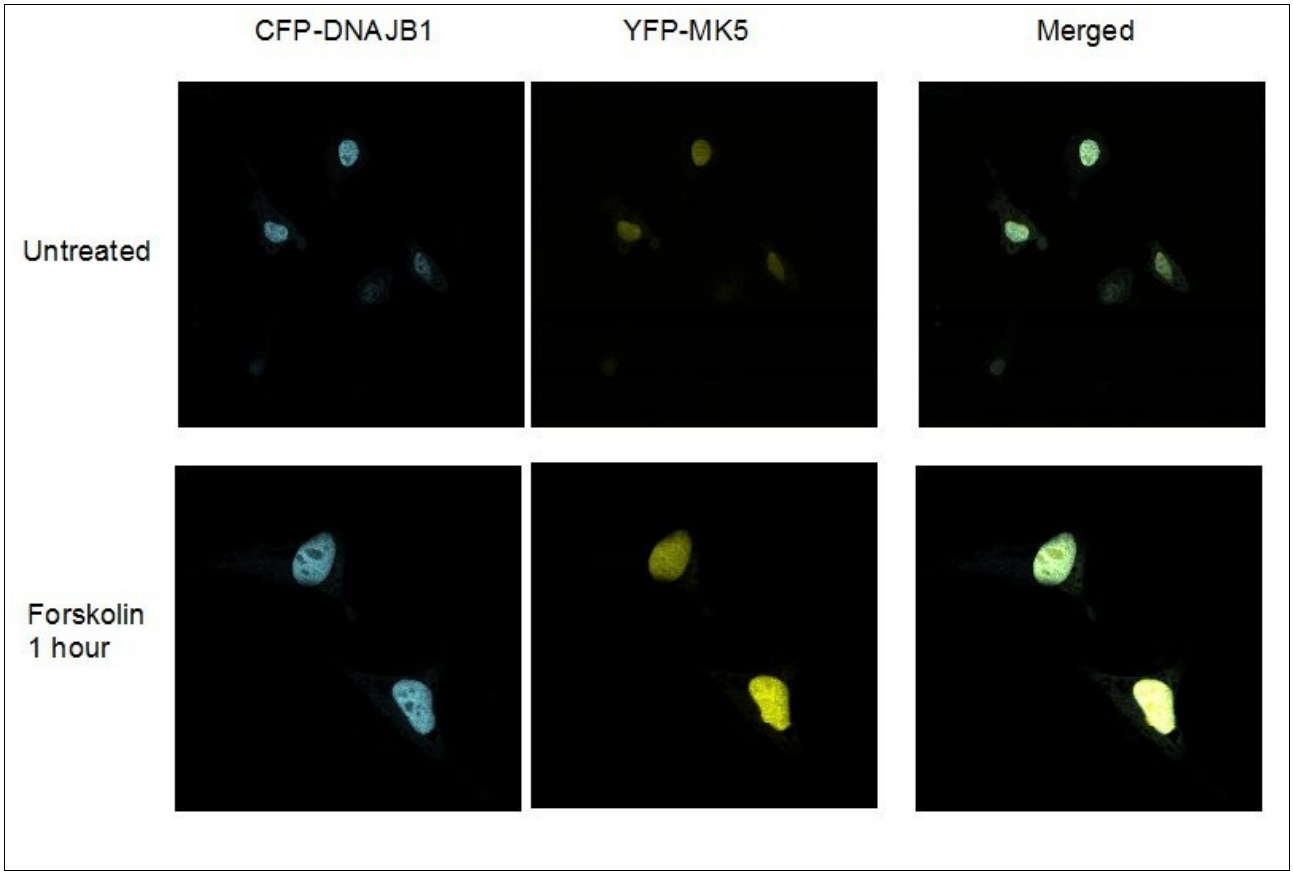

Figure 13: HeLa cells co-transfected with ECFP-DNAJB1 and EYFP-MK5. With and without Forskolin treatment.

4.2 MK5 and DNAJB1 exist in complexes.

If DNAJB1 is indeed a substrate for MK5, the two proteins must at some point engage in physical interaction. This interaction, if existent, can be transient as an enzyme-substrate complex, and, as such, difficult to capture. In an attempt to monitor such interaction, FRET-studies and co-immunoprecipitation of MK5 and DNAJB1 were performed.

4.2.1 FRET-analysis indicates physical interaction between MK5 and DNAJB1.

HeLa cells were co-transfected with pDest-ECFP-MK5 and pDest-EYFP-DNAJB1 or pDest-EYFP-CREB. CREB has previously proven to have no interaction with MK5 [14], and as such functioned as a negative control. Details on the construction of the pENTR3C-CREB vector that was used to make EYFP-CREB are supplied in appendix C. The cells were analyzed by confocal microscope.

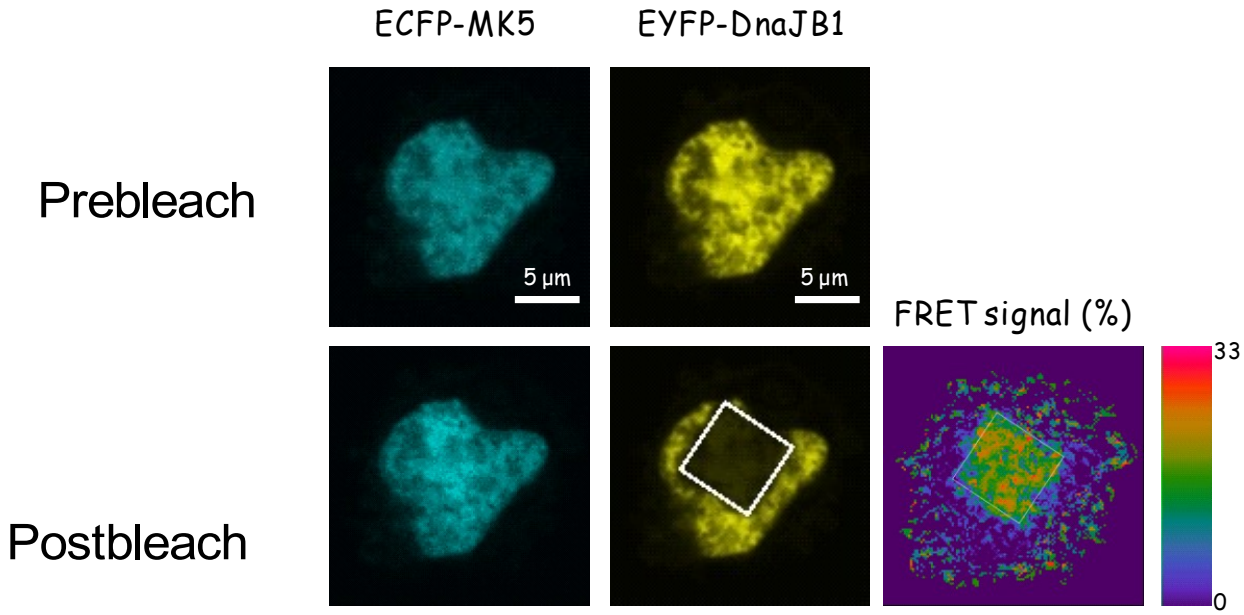

Figure 14: Result of FRET study. CFP and YFP emission signals were captured before and after 50% photobleaching of YFP. FRET is indicated as the relative increase in CFP emission following YFP photobleaching.

The data from the FRET-study indicate that FRET occurs between CFP-MK5 and YFP-DNAJB1, corresponding to a physical proximity of the two fluorophores between 2 and 6 nm, indicating a molecular interaction (Figure 14). Between pDestECFP-MK5 and the negative control pDestEYFP-CREB, no energy transfer was observed after photobleaching (results not shown).

4.2.2 Co-immunoprecipitation

To further establish evidence of an interaction between MK5 and DNAJB1, co-immunoprecipitation was applied. In the first attempt, EGFP-tagged MK5 and 3xFLAG-tagged DNAJB1 were co-transfected into HEK293 cells. Several repetitions were made to optimize dilution of the antibodies.

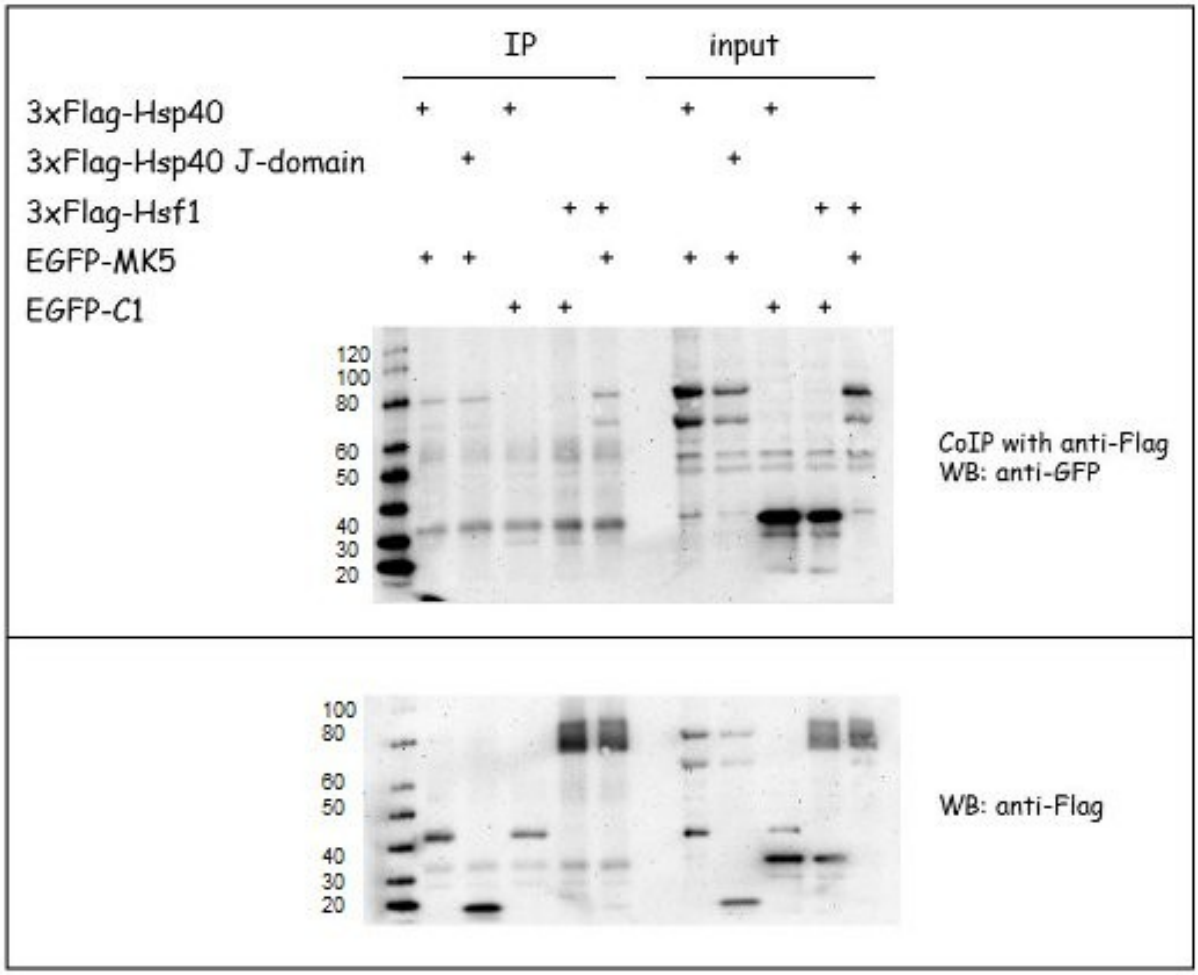

Figure 15: Upper panel: Co-ip performed in HEK293 cells co-transfected with DNAJB1 and MK5, DNAJB1 J-domain and MK5 and HSF1 and MK5. EGFP-C1 served as empty control. Lower panel: The membrane in the upper panel stripped and re-probed with anti FLAG in WB.

EGFP-MK5 is a fusion protein of approximately 81 kDa (27+54). As seen in Figure 15, it appears EGFP-MK5 is present in immunoprecipitates of full length DNAJB1 (HSP40) and DNAJB1 J-domain, but absent in immunoprecipitates of the empty control vector, indicating interaction between both MK5 and full length DNAJB1 and MK5 and DNAJB1 J-domain. HSF1 was also included in this experiment, and similar to DNAJB1, there seemed to be an interaction with MK5.

Because of the fact that the light chain of the antibody has a molecular mass of approximately 25 kDa, and GFP has a molecular mass of approximately 27 kDa, questions can be raised as to whether the band seen in the samples containing the empty EGFP vector is antibody light chain or GFP. This further leads to the speculation that the immunoprecipitation of EGFP-MK5 might be due to interactions between DNAJB1 and the GFP-part of the fusion protein rather than between DNAJB1 and MK5.

To avoid the possible confusion of GFP with the light chains of the antibody, EGFP-tag was substituted with HA-tag. This approach soon presented us with a problem. The signals reported by the antibody from the co-immunoprecipitates were a lot stronger than the signals reported from the input controls (Figure 16). By idea, the amount of HA-MK5 should be higher in the input controls than in the co-immunoprecipitates, and as such, should report a stronger signal when probed with the anti HA antibody. In addition, the band corresponding to the size of HA-MK5 seemed to be present in both immunoprecipitates containing DNAJB1 and not containing DNAJB1; indicating that if there was indeed an interaction, it most probably was between HA-MK5 and the FLAG-tag. However, the size of HA-MK5 (~55 kDa) is quite close to the size of the heavy chain of the antibody (~50 kDa) and therefore the bands appearing close to 50 kDa might also be the IgG heavy chain. Several attempts, and dilutions of the anti HA antibody, did not change the outcome of the co-ip. Finally it was decided to substitute anti HA for anti MK5 in the WB.

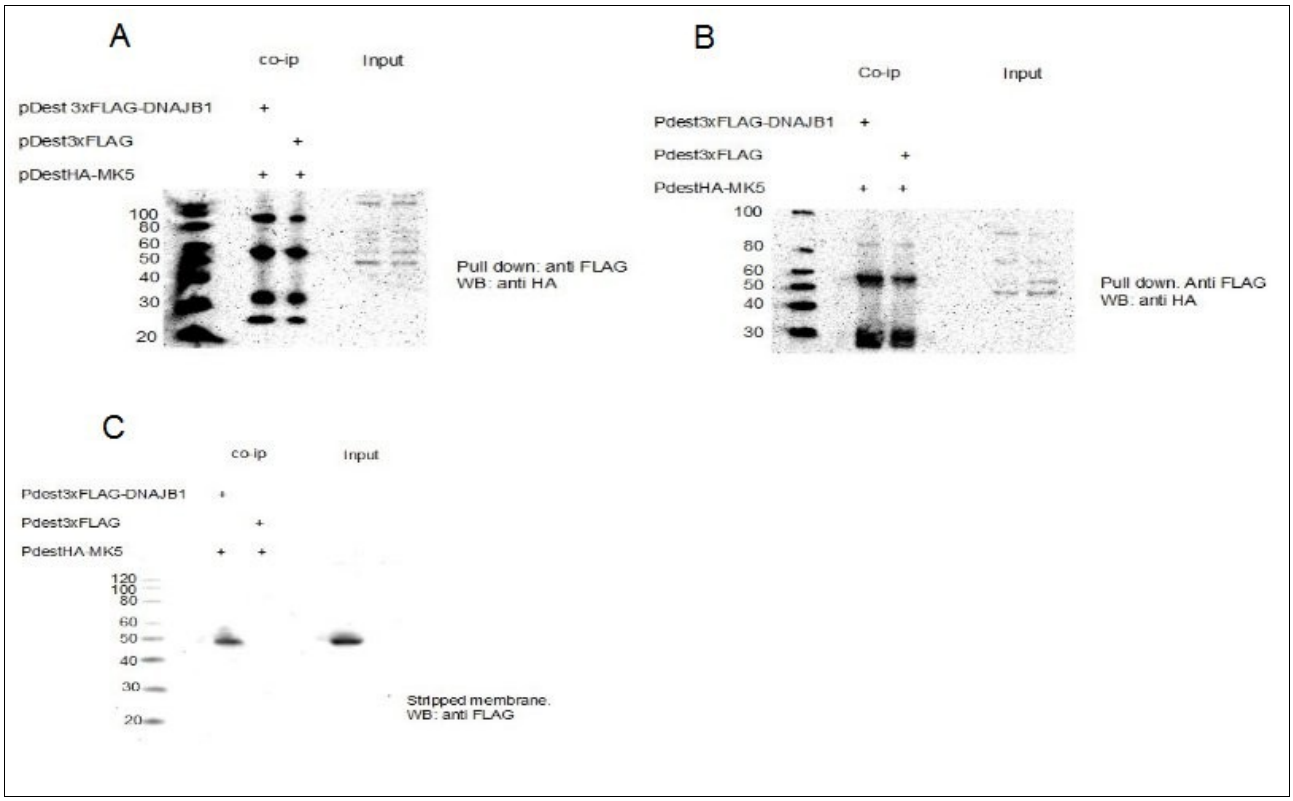

Figure 16: Co-immunoprecipitation of DNAJB1 and MK5 performed in HEK293 cells. A: Co-ip and input controls. Immunoprecipitation performed with anti FLAG, WB performed with anti HA. B: Same Co-ip as A, performed on another blot. C: Membrane A stripped and re-probed with anti FLAG. FLAG alone is too small to be visualized on the blot.

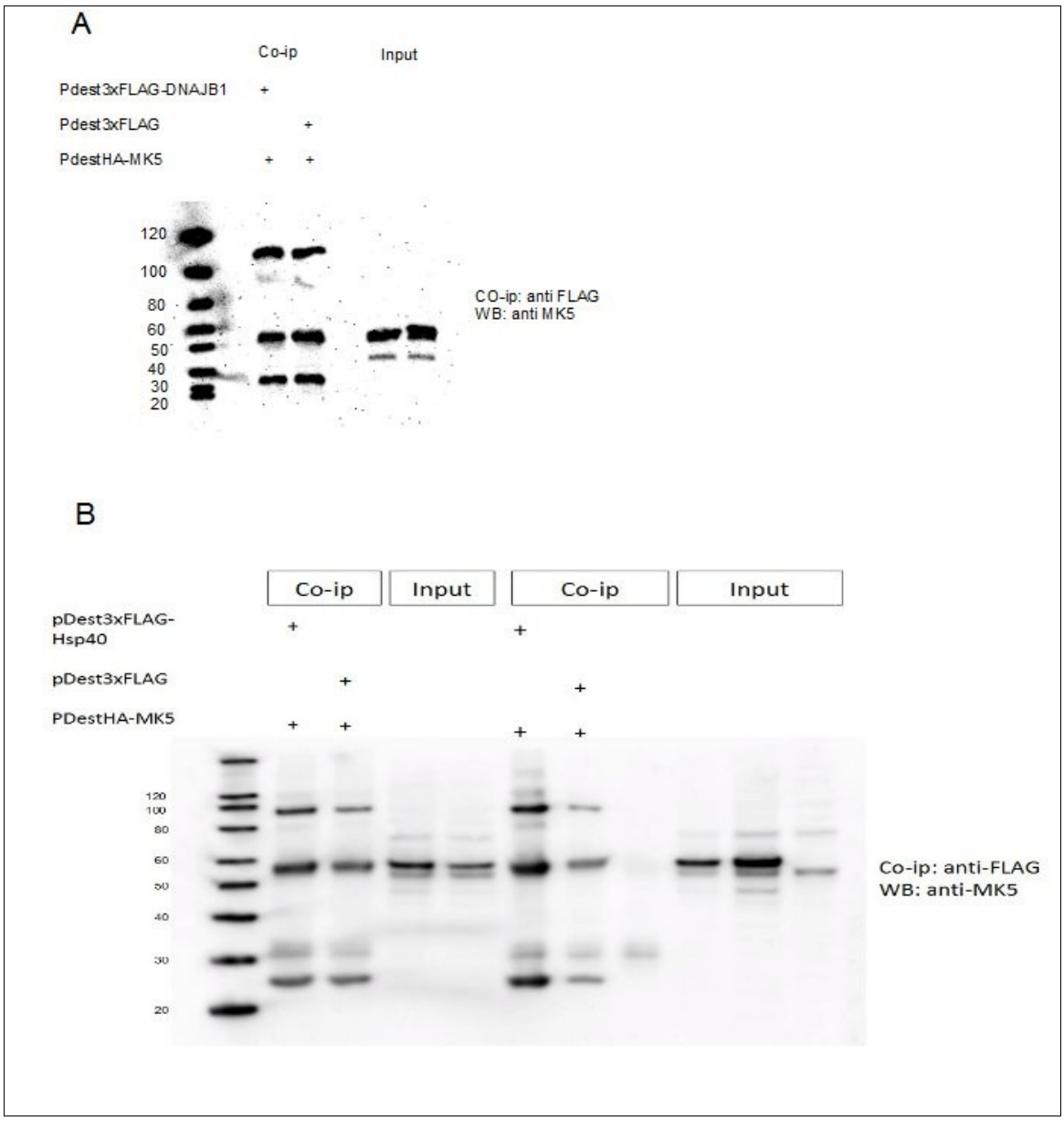

Figure 17: Three different Co-ip performed in HEK293 cells. A: Co-ip and input controls. Immunoprecipitation performed with anti FLAG and Western blotting with anti MK5. B: Two different Co-ip performed on the same blot. Same procedure as in A. In the Co-ip to the right, the empty lane is endogenous cell suspension, immunoprecipitation was performed with anti HSP40.

As seen in Figure 17, substitution of anti HA with anti MK5 in the western blotting did not lead to any dramatic changes in the outcome of the co-ip, apart from the fact that signals from the input controls now appeared to be of equal strength as the signals reported from the immunoprecipitates. Still, a band close to 50 kDa appeared in both immunoprecipitates containing DNAJB1 and not containing DNAJB1, indicating, once more, that there might be interaction between HA-MK5 and the FLAG-tag, or that it is actually the heavy chain of the antibody that is detected. Additionally, endogenous co-ip turned out negative, suggesting that there is no interaction between MK5 and DNAJB1. Based on the co-ip experiments, it remains inconclusive whether MK5 and DNAJB1 interact directly with one another in a stable complex.

4.3 MK5 phosphorylates DNAJB1 *in vitro.*

Previous findings showed that MK5 can phosphorylate DNAJB1 *in vitro*. We wanted to identify possible phosphoacceptor sites. To narrow down the search, the protein was separated into its individual domains [Kostenko unpublished results]. For details on the construction of these domains, see appendix A.

Figure 18: Schematic illustration of full length DNAJB1 protein, individual domains and three single mutations in the proximal part of the C-terminal domain as constructed by Sergiy Kostenko [Kostenko unpublished results].

All domains were included in an in vitro kinase assay. Prior to the kinase assay, all recombinant proteins/protein-domains needed to be purified. This was achieved by cloning their coding sequence from the ENTRY vector in which they resided into the pDEST™15 vector (table 3) by the Gateway® technology. The pDEST™15 vector contains a GST-tag for the construction of GST-fusion proteins, and an IPTG-inducible promoter for high expression levels of the fusion protein [39]. The approximate molecular mass of each fusion-protein is given in table 23.

Table 23: Approximate molecular mass of DNAJB1 fusion proteins

Fusion-protein	Approximate molecular mass (kDa)
GST-DNAJB1, full length	64
GST-DNAJB1 J-domain	34
GST-DNAJB1 G/F-rich domain	30
GST-DNAJB1 Proximal part of C-terminal domain (aa 106-175)	34
GST-DNAJB1 Central part of C-terminal domain (aa 176-245)	34
GST-DNAJB1 Distal part of C-terminal domain (aa 239-341)	37

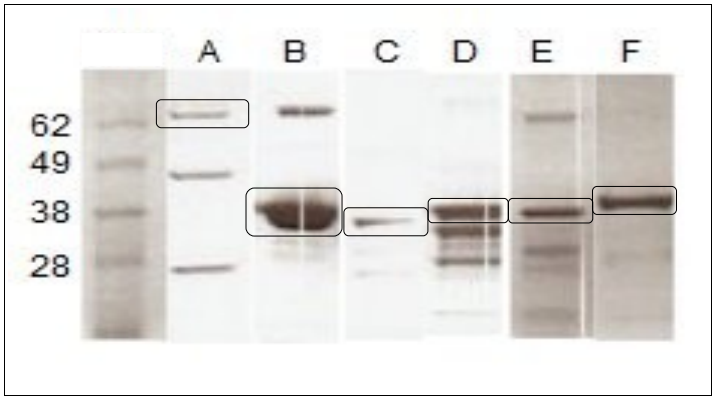

Figure 19: Result of GST-fusion protein purification using Thrombin as eluting agent. Protein standard in the far left lane is SeeBlue®. Lane A: Full length DNAJB1. Lane B: J-domain. Lane C: G/F-rich domain. Lane D: Proximal part of C-terminal. Lane E: Central part of C-terminal. Lane F: Distal part of C-terminal. The band corresponding to the protein of interest is circled in each lane. The proteins were stained by Coomassie Brilliant Blue.

The first in vitro kinase assay indicated phosphorylation of J-domain and the proximal part of C-terminal domain (see Figure 20 below).

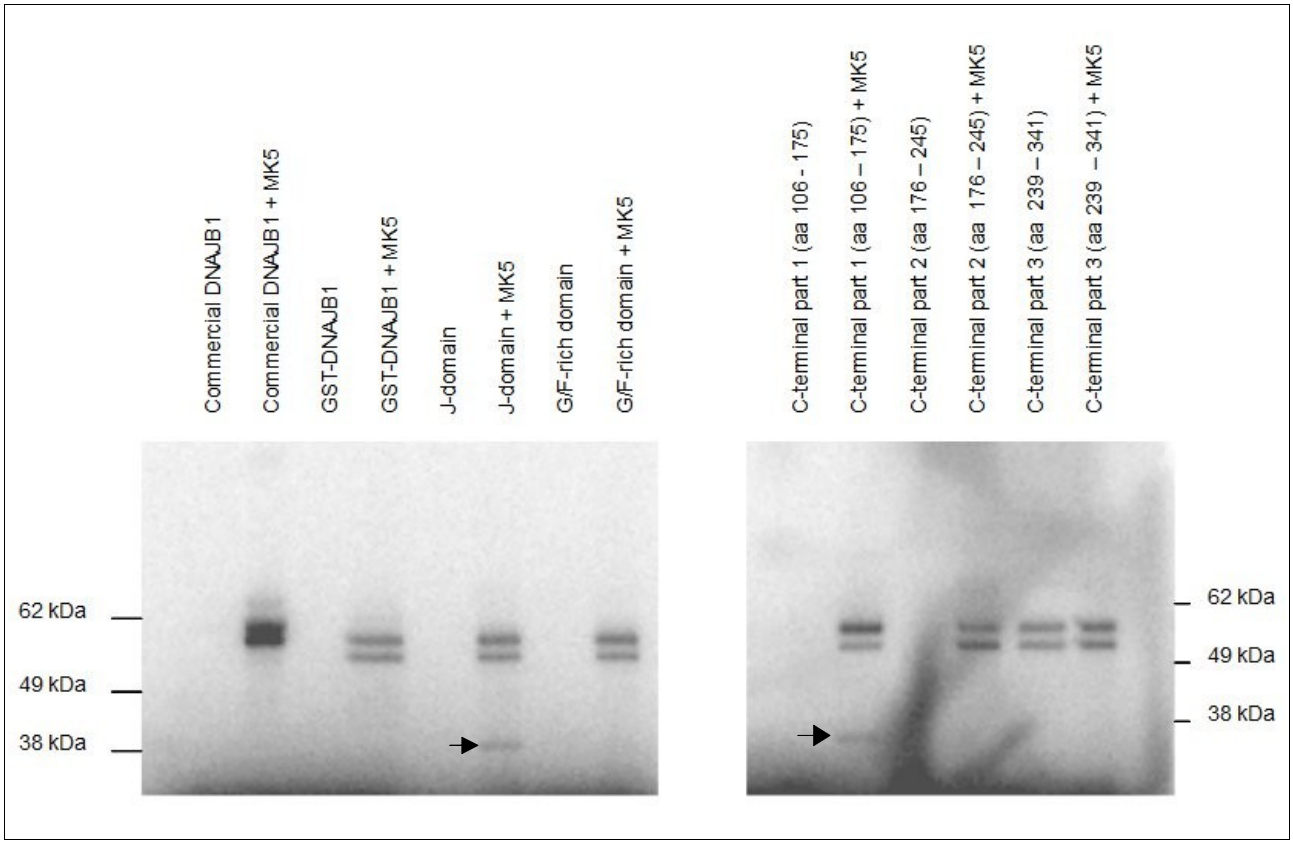

Figure 20: In vitro kinase assay performed on full length DNAJB1 and its individual domains in the presence of active MK5. Phosphorylation of J-domain and proximal part of C-terminal is indicated by arrows.

Based on these results, the sequences of the two domains were investigated for possible phosphoacceptor sites using an online phosphorylation prediction algorithm, NetPhos 2.0 [40]. Two putative phosphoacceptor sites were predicted for the J-domain, and three for the proximal part of the C-terminal domain (Figure 21).

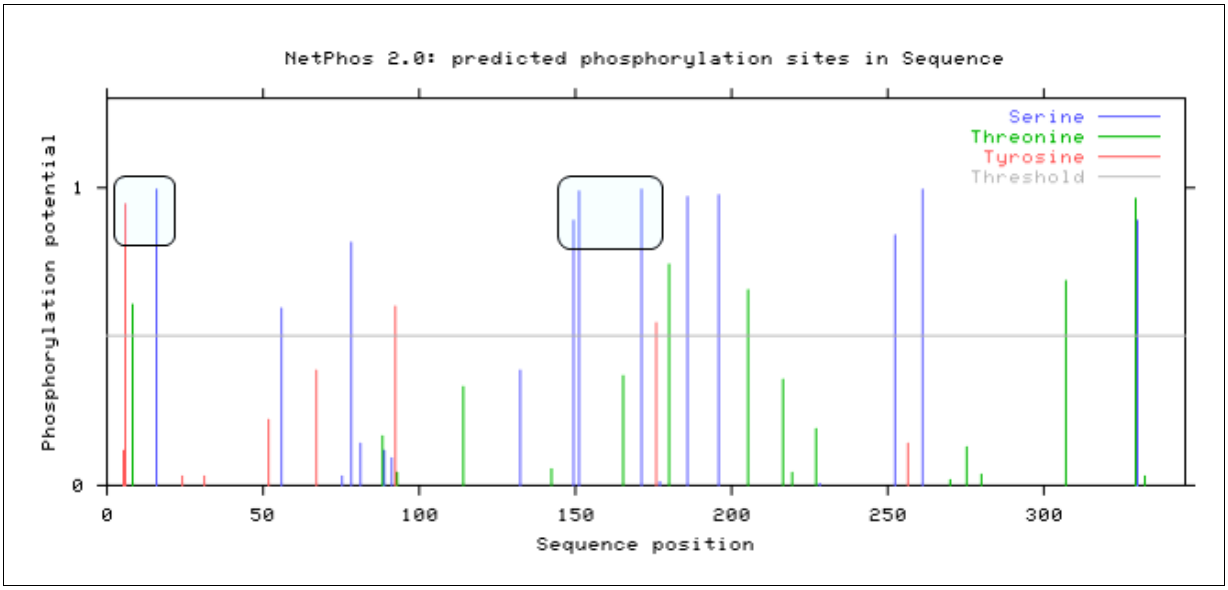

Figure 21: Result of phosphorylation site prediction in DNAJB1 using the NetPhos 2.0 phosphorylation prediction algorithm. Two putative phosphosites within the J-domain are circled to the far left in the diagram, and three putative phosphosites within proximal part of C-terminal domain (aa 106-175) are circled in the middle of the diagram. The circled peaks represent the phosphosites that were chosen to be investigated further by site directed mutagenesis and IVK .

As seen in the figure, there were two other possible phosphosites within the J-domain that reported signals above the threshold (one Threonine and one Serine), but compared to the other two sites, the signals reported were relatively low. We therefore decided to first concentrate on investigating the phosphoacceptor potential of the other two. Detailed information about the results of the phosphosite prediction is given in appendix E.

According to the results of the phosphorylation site prediction, primers were designed to create mutations that would leave the putative phosphosites inert to phosphorylation by kinases. This was achieved by substituting a Serine (S) or a Tyrosine (Y) with an unphosphorylatable Alanine (A) by site-directed mutagenesis. The following mutants were generated: in the J-domain: Y6A and S16A, and in the proximal part of C-terminal (amino acid 106-175): S149A, S151A and S171A [Kostenko, unpublished results] For further details on construction of the mutants, see appendix B.

In vitro kinase assay was performed with the three mutants of the proximal part of the C-terminal domain of DNAJB1.

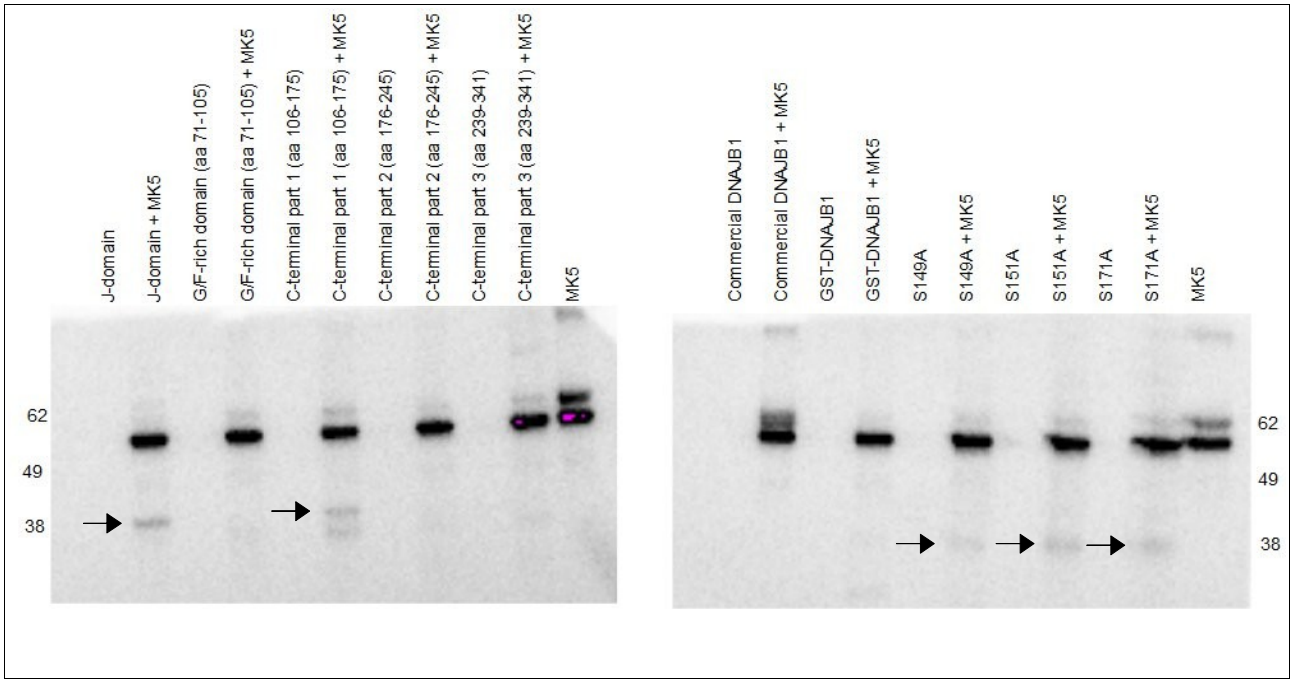

Figure 22: In vitro kinase assay on full length DNAJB1, individual domains and single mutants in the proximal part of C-terminal domain in the presence of active MK5. Phosphorylation of J-domain, proximal part of C-terminal and single mutants is indicated by arrows.

As seen in Figure 22, all three mutants in the proximal part of the C-terminal domain still became phosphorylated, though signals of lower intensity were detected for each of them than for the wild-type domain. The observed residual phosphorylation of the single mutants was possibly due to phosphorylation of the two other phosphosites that were still present in each mutant. Based on this assumption, it was decided to create a triple mutant for the proximal part of C-terminal domain. This was done by designing a primer containing a double mutation for S149A and S151A, and performing site-directed mutagenesis on the template already carrying the S171A mutation. Information about primers and reaction conditions is given in tables 6, 15 and 16 and section 2.2.13. When sequenced, quite remarkably, some of the samples contained the desired mutation, but the original mutation (S171A) seemed to have reverted (Figure 23). No samples contained all three mutations.

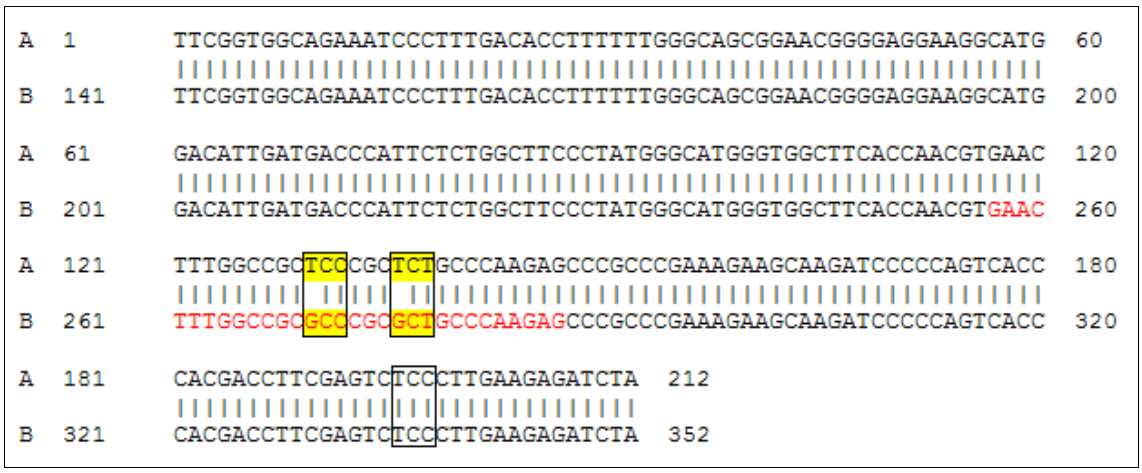

Figure 23: Result of site directed mutagenesis performed on DNAJB1 S171A with the S149A_S151A primers. The Incorporated forward primer is shown in red. Nucleotide triplets causing the change from amino acid Serine to Alanine are highlighted in yellow. The reverted mutation, S171A, is circled in black.

Based on this result, a new strategy for construction of the triple mutant was devised. The recombinant DNA carrying the double mutation (see Figure 23) was used as template for site-directed mutagenesis by the S171A primer, and, as seen in Figure 24, this time the mutagenesis was successful.

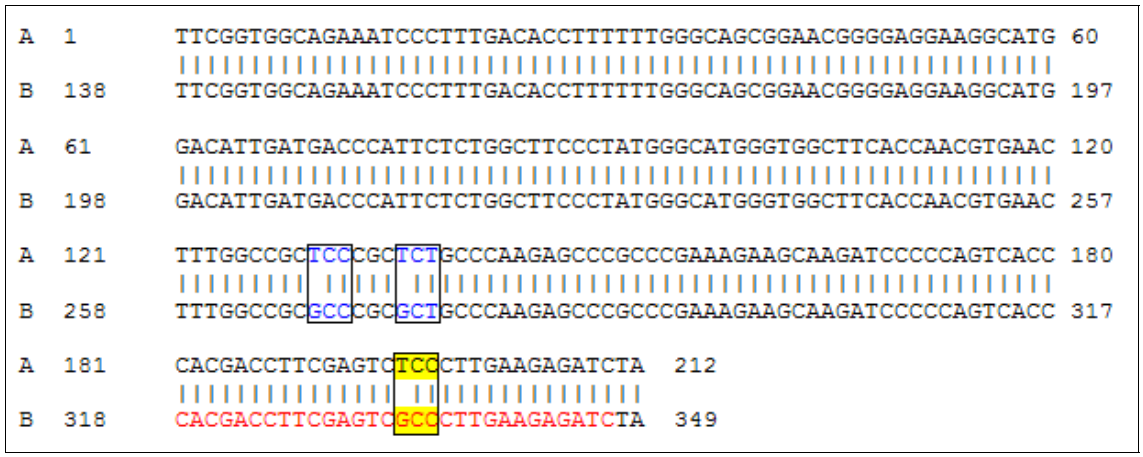

Figure 24: Result of site-directed mutagenesis performed on DNAJB1 S149A_S151A with the S171A primers. The incorporated forward primer is shown in red. The nucleotide triplet causing the change from amino acid Serine to Alanine is highligthed in yellow. The pre-existing mutations, S149A and S151A are shown i blue fonts.

After the search for possible phosphoacceptor sites within the J-domain and the proximal part of C-terminal had been initiated, the first IVK assay including all domains was repeated (Figure 25). In addition to phosphorylation of J-domain and proximal part of C-terminal, phosphorylation of G/F-rich domain was observed. A band also appeared in the distal part of C-terminal (aa 239-341), but this band was of a size too small to correspond to this domain. It might be Thrombin, which was used for protein purification, and has a molecular mass of approximately 36 kDa, but the band seems to be too small, and if it was indeed Thrombin, the band should be present in all samples.

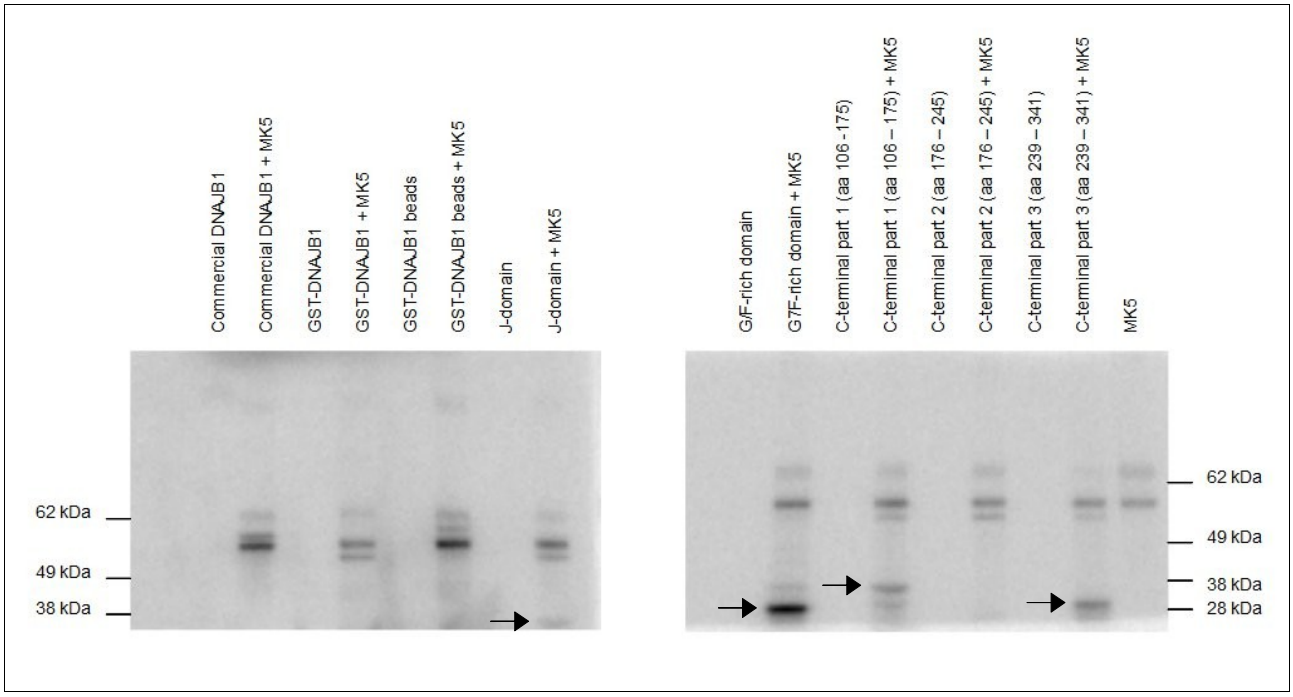

Figure 25: In vitro kinase assay performed on full length DNAJB1 + its individual domains in the presence of active MK5. Concentration of G/F-rich domain is increased while the rest of the procedure is identical to the one seen in in Figure 20.

Before the new mutants were included in an in vitro kinase assay, it was discovered that the pDEST™15 vector did in fact not contain a Thrombin cleavage-site, like previously assumed. GST-fusion protein purification of proteins expressed from the pDEST™15 vector had so far been executed according to the protocol for Thrombin elution. Without a Thrombin cleavage site present, the low protein yield from previous purification-attempts could easily be explained. As a consequence of this discovery, the full length protein, all domains and all mutants were purified once more, this time by the protocol for Glutathione elution. The results are given in Figure 26 and 27.

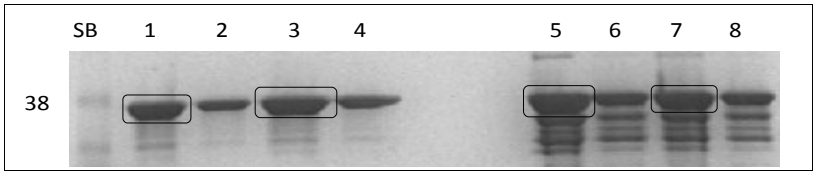

Figure 26: GST-fusion protein purification using Glutathione as eluting agent. 1: Y6A first eluate, 2: Y6A second eluate, 3: S16A first eluate, 4: S16A second eluate, 5: S149A_S151A first eluate, 6: S149A_S151A second eluate, 7: S149A_S151A_S171A first eluate, 8: S149A_S151A_S171A second eluate. SB: SeeBlue® protein standard.

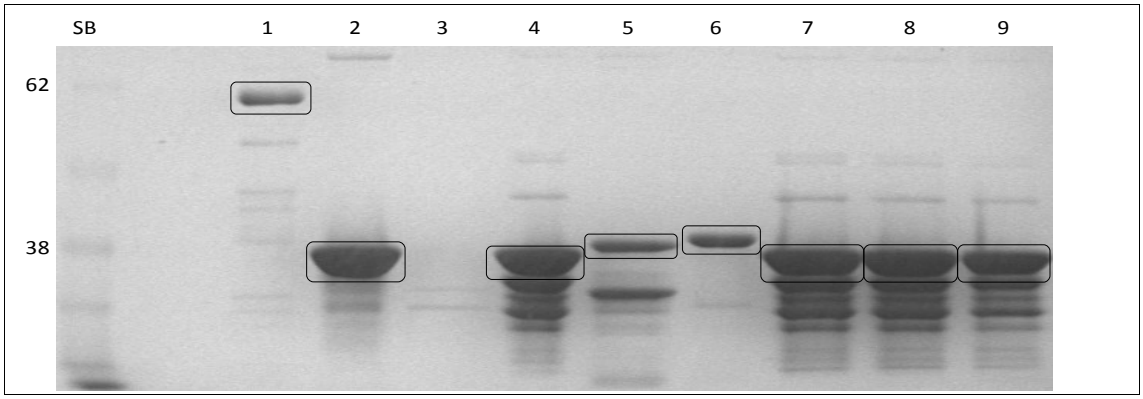

Figure 27: GST-fusion protein purification using Glutathione as eluting agent. 1: DNAJB1, 2: J-domain, 3: G/F-rich domain, 4: Proximal part of C-terminal (aa 106 - 175), 5: Central part of C-terminal (aa 176 - 245), 6: Distal part of C-terminal (aa 239- 341), 7: S149A, 8: S151A, 9: S171A. SB: SeeBlue® protein standard.

From figure 26 and 27 it is apparent that the yield of protein from the GST-fusion protein purification is quite variable. The yield of full length DNAJB1, the G/F-rich domain, the central part of C-terminal and the distal part of C-terminal is considerably lower than for the other domains and the mutants. The sample containing the G/F rich domain even seems completely devoid of protein. We also see that even though the desired proteins are enriched, most of the samples also contain contaminants, some more than others.

In vitro kinase assay was performed on full length protein, all domains and all mutants, including the two J-domain mutants (Y6A and S16A).

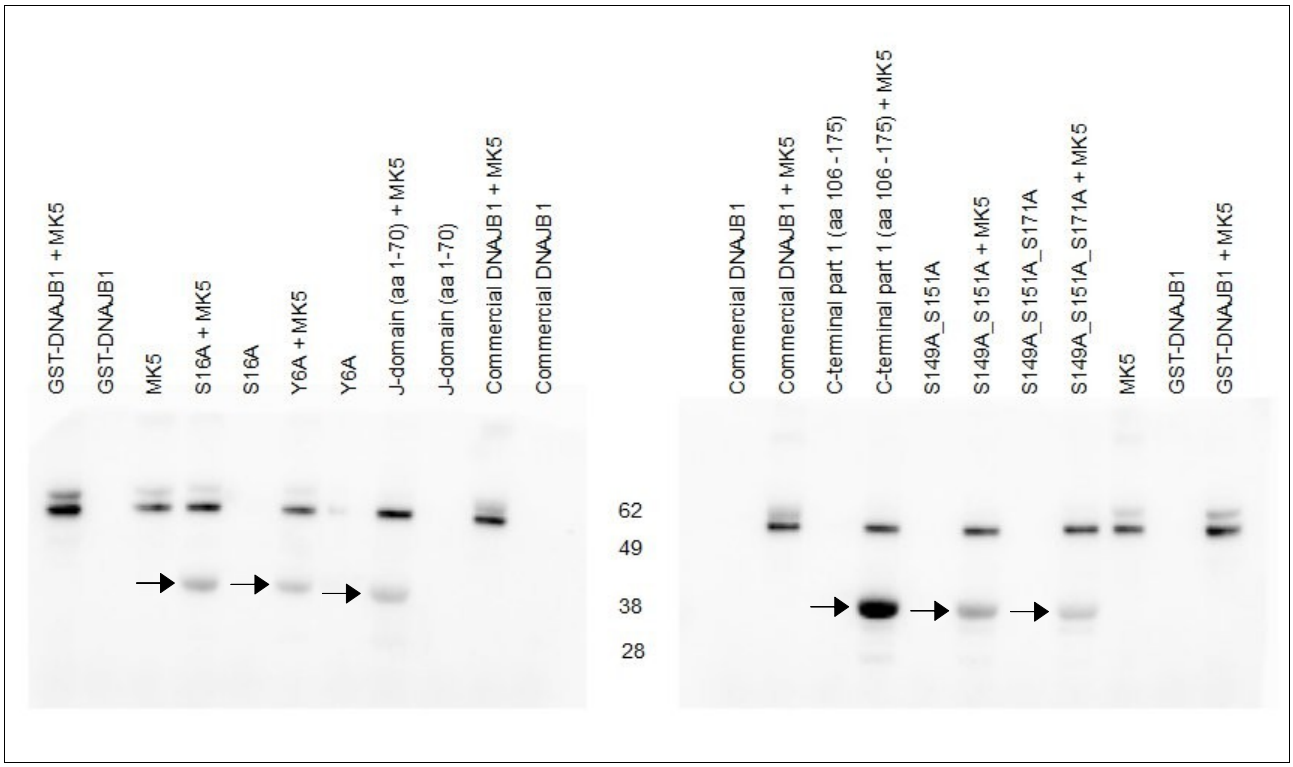

Figure 28: In vitro kinase assay performed on full length DNAJB1 protein, J-domain, proximal part of C-terminal and mutants Y6A, S16A, S149A_S151A and S149A_S151A_S171A in the presence of active MK5. Relevant phosphorylation is indicated by arrows.

The results from the IVK on full length protein and individual domains are not shown due to technical difficulties. However, it seemed that the J-domain, the proximal part of C-terminal and the G/F-rich domain were not the only domains of DNAJB1 to be phosphorylated by MK5 *in vitro.* Both the central and the distal part of C-terminal were also phosphorylated in this assay. This is in accordance with the results of the phosphorylation site prediction (see Figure 21) From the figure it is apparent that several putative phosphorylation sites are present in the two other domains.

It also seems that both Serine 149, Serine 151 and Serine 171 are phosphorylated by MK5 *in vitro* (Figure 28). Because of the fact that phosphorylation is not completely abolished in the triple mutant, it is plausible to assume there might be additional phosphoacceptor sites within the proximal part of the C-terminal region, although this is not reported by the phosphorylation site prediction algorithm that was used. Phosphorylation of J-domain carrying the Y6A mutation seems to be slightly weaker than for the wild-type J-domain, whilst the S16A mutation does not seem to influence phosphorylation of this domain. Taken together, these results indicate that in addition to Tyrosine 6, Serine 149, Serine 151, and Serine 171, DNAJB1 possesses additional MK5 phosphoacceptor sites, at least *in vitro*.

4.4 DNAJB1 inhibits MK5 activity

DNAJB1 has previously been shown to inhibit the transcriptional activity of HSF1 in COS-7 cells [23]. These cells express SV40 large T-antigen, a protein that similar to DNAJB1, contains a J-domain [41]. We wanted to repeat this experiment in HEK293 cells as these cells do not express viral proteins with a J-domain. To achieve this, Luciferase assays including GAL4-HSF1 and DNAJB1 or empty control vector were conducted. In both transfections, the reporter plasmid GAL4-E1b-Luc was also included.

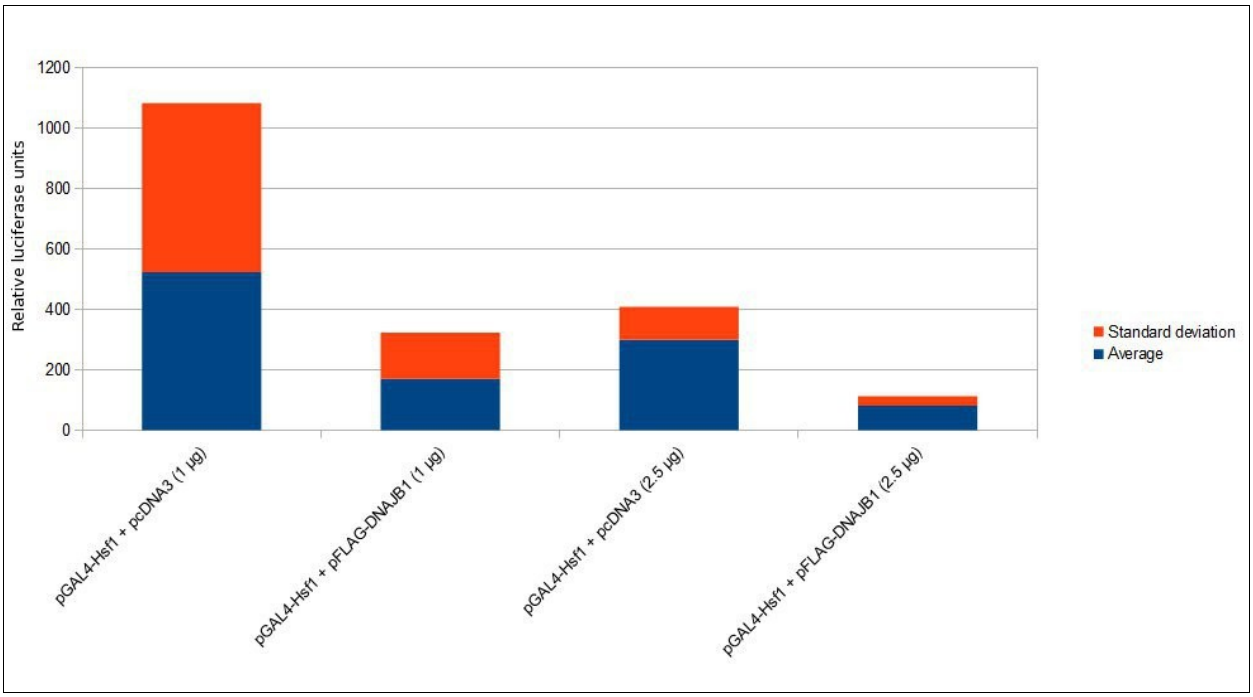

Figure 29: Luciferase assay of HEK293 cells transfected with pGAL4-HSF1 and pcDNA3 or pGAL4-HSF1 and pFLAG-DNAJB1, 1 µg and 2.5 µg respectively. Three parallels were made for each transfection. An unpaired t-test showed that the difference between the first two data-sets was not significant (p= 0.3479). For the second data-set, the difference was significant (p= 0.0289).

From figure 29 we can see that the trend seems to be that DNAJB1 downregulates HSF1-mediated transcription. This was expected based on the earlier findings of Shi et al. [23]. The significance of the difference between cells transfected with DNAJB1 and cells transfected with empty control vector is different for cells treated with 1 µg DNA and 2.5 µg DNA. This is most likely due to the high standard deviation observed in the former data-set.

We also wanted to see if MK5 had any impact on the expression or transcriptional activity of HSF1. Thereto, Luciferase assays including GAL4-HSF1 and MK5 or empty control vector were conducted. In both transfections, the reporter plasmid GAL4-E1b-Luc was also included.

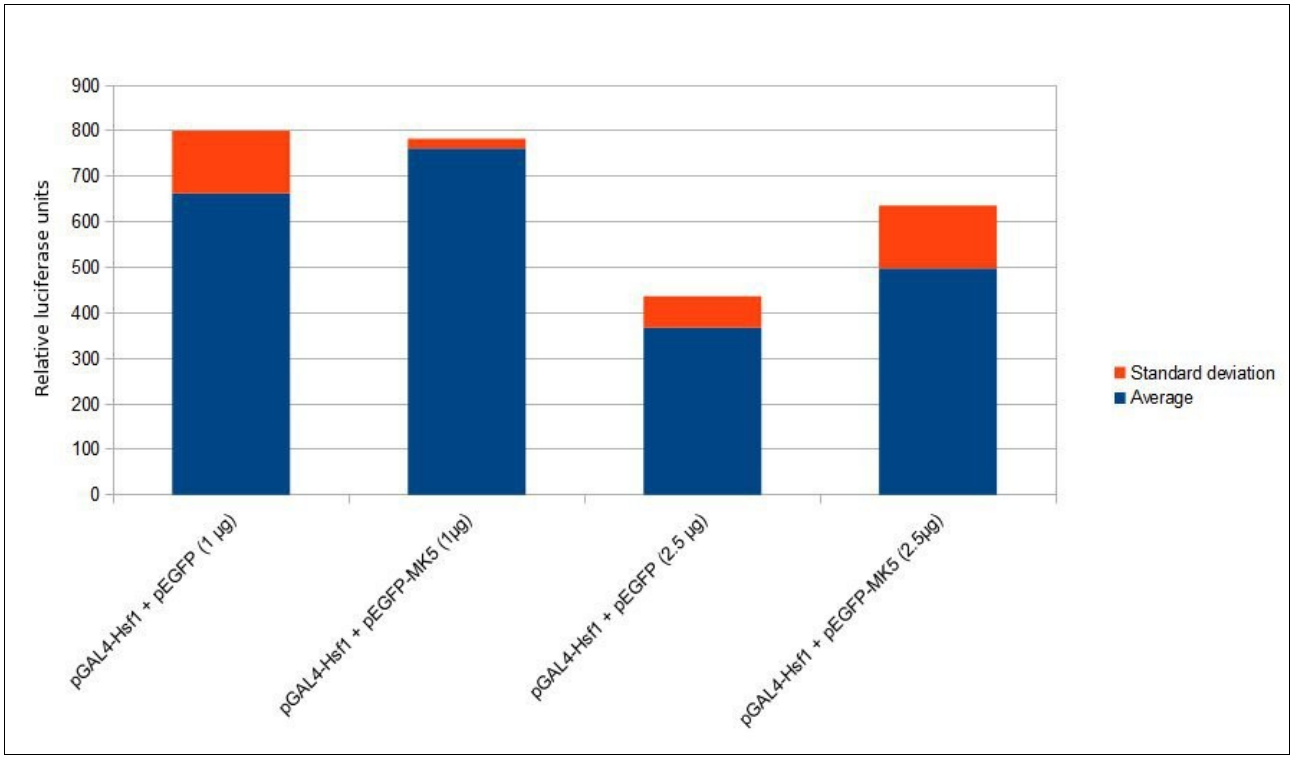

Figure 30: Luciferase assay of HEK293 cells transfected with pGAL4-HSF1 and pEGFP or pGAL4-HSF1 and pEGFP-MK5, 1 µg and 2.5 µg respectively. Three parallels were made for each transfection. An unpaired t-test showed that the difference between the data-sets was not significant (p= 0.2851 and 0.2813 respectively).

From Figure 30 it seems that MK5 has a slightly stimulating effect on HSF1, but the difference between cells transfected with MK5 and empty vector is too small to be significant. Therefore, the effect of MK5 on HSF1 remains inconclusive.

Since the main focus in this study is on the interaction between MK5 and DNAJB1, we wanted to investigate whether DNAJB1 had a regulatory effect on MK5. HEK293 cells were co-transfected with pDest3xFLAG-DNAJB1 + pM-MK5 and pDest3xFLAG (empty vector)+pM-MK5. In both transfections, the reporter plasmid GAL4-E1b-Luc was also included. The pM-MK5 plasmid encodes a fusion protein containing the DNA binding domain of GAL4 and MK5. This fusion protein will therefore bind to the GAL4 binding sites of the GAL4-E1b-LUC reporter plasmid and affect transcription of the Luciferase gene from the E1b promoter.

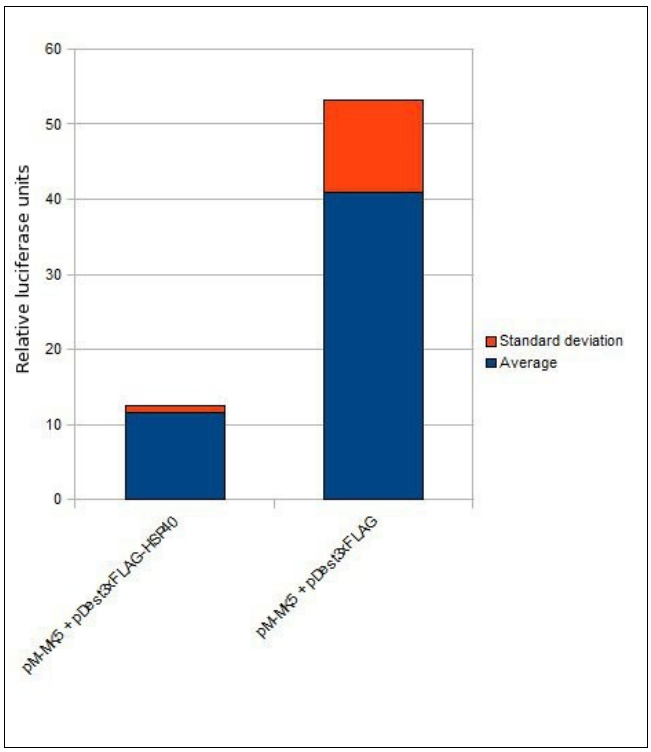

Figure 31: Luciferase assay of HEK293 cells transfected with either pM-MK5 + pDest 3 xFLAG-HSP40 or pM-MK5 + pDest3xFLAG. Three parallels were made for each transfection. An unpaired t-test showed that the difference between the data-sets was significant (p = 0.0149)

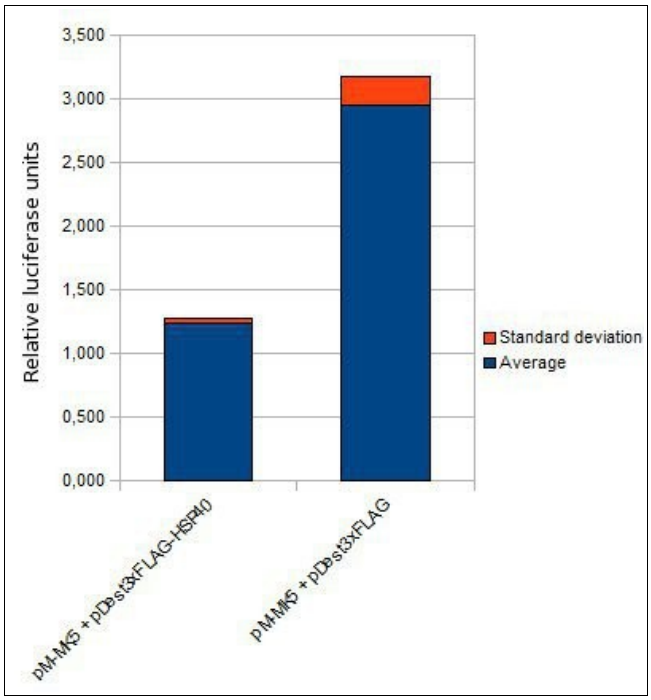

Figure 32: Luciferase assay of HEK293 cells transfected with either pM-MK5 + pDest 3 xFLAG-HSP40 or pM-MK5 + pDest3xFLAG. Three parallels were made for each transfection. An unpaired t-test showed that the difference between the data-sets was significant (p= 0.0002)

From Figure 31 and 32 it appears that DNAJB1 does indeed inhibit/downregulate MK5 in some manner, but what property remains unknown.

4.5 DNAJB1 seems to be involved in β-tubulin rearrangement through the cAMP/PKA pathway.

It has earlier been shown that MK5 is involved in F-actin rearrangement through HSP27 [15], and quite recently it was demonstrated that DNAJB6 large splice variant, a close relative of DNAJB1, can lead to morphological changes in cells through inhibition of Wnt/β-catenin signaling, thereby restricting malignant behavior [42]. On the basis of this, we decided to investigate whether DNAJB1 could be involved in rearrangement of any other structural proteins.

DNAJB1 was knocked down in PC12 cells by 300nM siRNA (Figure 33)

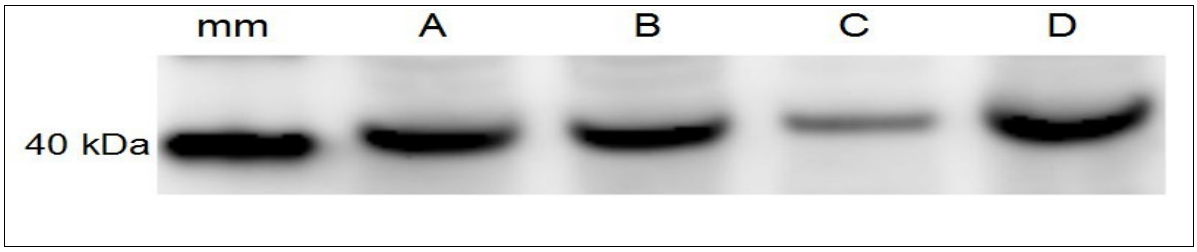

Figure 33: Western blot of PC12 cells using anti HSP40 antibody. Lane A: transfected with 50 nM siRNA directed against DNAJB1. Lane B: transfected with 100 nM siRNA directed against DNAJB1. Lane C: transfected with 300 nM siRNA directed against DNAJB1. Lane D: untransfected cells. mm: MagicMark™ protein standard. The cells were harvested 48 hours post-transfection.

From Figure 33 we see that transfection with 300 nM siRNA directed against DNAJB1 leads to drastically reduced levels of DNAJB1 in PC12 cells, although expression is not completely abolished.

New cells were transfected with siRNA and stained for β-tubulin (see table 4 and section 3.2.12).

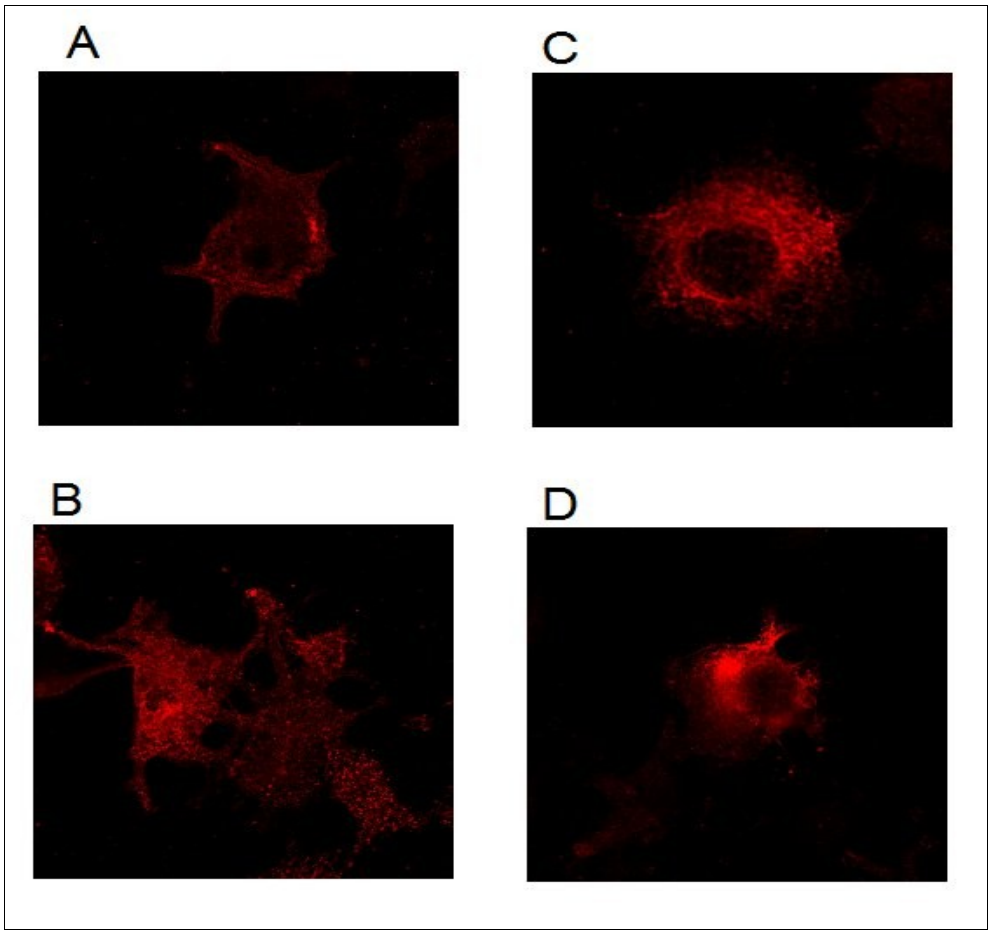

Figure 34: PC12 cells stained for β-tubulin isotype III. A: Mock nucleofector transfection, untreated. B: Mock Nucleofector transfection, treated with Forskolin for 30 minutes. C: Transfected with 300 nM siRNA directed against DNAJB1, untreated. D: Transfected with 300 nM siRNA directed against DNAJB1, treated with forskolin for 30 minutes.

As is not necessarily apparent from Figure 34, the overall impression was that β-tubulin rearrangement, as observed in mock-transfected cells after forskolin treatment, was not present in cells where DNAJB1 was knocked down by siRNA.

5 Discussion

In this study we have shown that DNAJB1 is a novel substrate for MK5. Both proteins co-localize and interact with each other in the cell, at least when ectopically expressed. Additionally, MK5 can phosphorylate DNAJB1 at several sites *in vitro*. Studies aimed at elucidating the functional importance of this interaction were initiated.

Co-localization studies revealed co-localization of ectopically expressed DNAJB1 and MK5, mainly within the nucleus. Previous studies have shown that in unstressed cells, DNAJB1 is localized faintly throughout the cell, and that upon heat-shock it accumulates in nuclei and nucleoli [43]. Ectopically expressed MK5 has been shown to mainly localize to the nucleus. From figure 9 and 12 it seems that DNAJB1 also localizes mainly to the nucleus in cells that are not co-transfected with MK5. This suggests that nuclear localization of DNAJB1 is not dependent upon co-expression of MK5, but could be due to a state of stress in the cell induced by transfection or simply the fact that the protein is over-expressed. Several attempts at immunofluorescence staining of the endogenous proteins were made, but none were unequivocally conclusive, most likely due to poor antibody quality.

Co-immunoprecipitation did not give any unambiguous answers to the question of interaction between MK5 and DNAJB1. Co-ip is a widely used method that allows the detection of protein-protein complexes in cells. However, one limitation is that often the two proteins of interest are ectopically over-expressed, which may lead to non-physiological concentrations and misplacing of the proteins in the cell. Therefore, if possible, co-immunoprecipitation of the endogenous proteins should be performed. Both approaches were performed on MK5 and DNAJB1, and interaction was only reported in co-ip where the proteins were ectopically over-expressed, and not in the endogenous precipitate.

Another drawback of the method is that it does not guarantee that the two proteins interact directly. Interaction can be through a third, or possibly even more proteins as part of a complex. To solve this problem, a GST pull-down can be performed. This is an in vitro method, but it shows only direct interaction between two proteins.

A third limitation is of technical nature. The method requires antibodies of good quality. Poor antibodies may fail to pull-down protein complexes in cells or may bind unspecifically, leading to complications in the interpretation of the co-ip.

The interaction observed in the first co-ip, performed with GFP-tagged MK5 (Figure 15) proved difficult to reproduce with HA-tagged MK5 (Figure 16 and 17). Uncertainty concerning the reactivity of DNAJB1 towards GFP coupled with this problem of reproducibility favors the conclusion that DNAJB1 and MK5 do

not interact with one another. However, the results of the FRET-study point in the opposite direction. According to these findings, MK5 and DNAJB1 reside in a proximity to each other corresponding to a direct interaction. Again, in these studies both proteins are ectopically over-expressed, so the interaction observed may be of an artificial nature. To confidently state that MK5 and DNAJB1 interact with one another, directly or through additional proteins as part of a complex, further studies are needed, such as GST-pulldown and repeated endogenous co-ip.

Assessing the in vitro kinase assays, one could argue that the observed phosphorylation could actually be phosphorylation of the GST moiety of the fusion proteins, and indeed, GST alone should have been included as a control. However, previous results have shown that MK5 does not phosphorylate GST [results not shown], and so we feel confident that the phosphorylation observed is indeed that of DNAJB1. Moreover, GST fusion proteins with different parts of the C-terminal domain did not become phosphorylated *in vitro* (Figures 20, 22 and 25), indicating that GST is not phosphorylated by MK5.

Initially, the results of the in vitro kinase assay on individual DNAJB1 domains indicated phosphorylation of only J-domain and the first part of the C-terminal domain. It was based on these results that candidate phosphoacceptor sites were determined (see Figure 20 and 21). When the assay was repeated, this time with a more concentrated sample of the G/F-rich domain, additional phosphorylation of this domain was observed. Then, when the confusion with the GST fusion protein purification was discovered, and elution with Thrombin was exchanged for Glutathione, the IVK was repeated yet again, this time with higher protein concentrations than before. It turned out that the other two domains (the central and distal part of C-terminal domain) were also phosphorylated [results not shown]. This corresponded well to the results given by the phosphorylation site prediction algorithm, which also reported putative phosphoacceptor sites for all domains.

Based on the results of the IVK on mutants in which phosphoacceptor sites had been rendered unphosphorylatable by site directed mutagenesis, it seems that all three putative phosphoacceptor sites in the first part of C-terminal are phosphorylated by MK5 *in vitro*. Phosphorylation of the proximal part of C-terminal appeared to be weaker in each single mutant (S149A, S151A and S171A), weaker still in the double mutant (S149A_S151A), and almost abolished in the triple mutant (S149A_S151A_S171A), indicating that all three sites are phosphorylated by MK5 (see Figure 22 and Figure 28). The weak residual phosphorylation in the triple mutant may be due to additional phosphoacceptor sites, although no such sites were predicted by the algorithm. The S16A mutation within the J-domain did not seem to have an effect on phosphorylation, while the Y6A mutation seemed to slightly reduce it. This indicates that Y6A might be a phosphoacceptor site, while S16A is not.

As seen in Figure 21 and appendix E, there are many putative phosphorylation sites in DNAJB1, and most of them have not been analyzed by in vitro kinase assays. Particularly Serine residues 186 and 196 within the central part of C-terminal domain and Serine 261 and Threonine 329 within the distal part of C-terminal appear to be good candidates, but Serine 252 and 330 also hold promise. It may turn out that several of these phosphosites are indeed phosphorylated by MK5 in vitro, but which sites, if any, are phosphorylated *in vivo* may be a completely different matter. To determine which sites are phosphorylated *in vivo,* detection by phosphospecific antibodies on cell lysates or mass spectrometry (MS) can be used.

Somewhat problematic with some of the figures (25 and 28), is the fact that phosphorylation of full length protein appears much weaker than phosphorylation of the individual domains. This could be due to differences in protein concentrations between the samples, which is not unlikely as protein concentration of GST-fusion proteins were not measured, only evaluated quantitatively by Coomassie staining. It could also be a consequence of conformational differences between the individual domains and the full length protein, rendering some phosphorylation sites more available than others.

Another problem is the presence of an additional band in MK5, which is of approximately the same size as GST-tagged DNAJB1. This complicates the interpretation of the results. Also, some samples show faint bands directly below the MK5 autophosphorylation band, and this could be contaminants present in the protein samples (see Figure 19 and 25).

Finally, WB with anti MK5 should have been performed to confirm the presence, and equal loading of MK5 in all samples.

Based on the result of the Luciferase assays it seems that DNAJB1 also represses HSF1 in HEK293 cells (Figure 29), and that it downregulates MK5 somehow (Figure 31 and 32), but it is difficult to say in which way. DNAJB1 could somehow repress the transcriptional activity of MK5 or interfere with the ability of MK5 to act as a trans-activator. To obtain this kind of information, further experiments are needed. Additionally, reciprocal experiments should have been performed, in which the effect of MK5 on DNAJB1 was investigated. Because of time limitations this was not done, but it remains a possible experiment for future studies.

It also seems that MK5 stimulates the transcriptional activity of HSF1 (Figure 30), but the difference between control cells and cells transfected with MK5 was too small to be significant, and therefore, further studies are needed to elucidate the effect of MK5 on HSF1. Since DNAJB1 inhibits HSF1, the effect of MK5 on HSP40 target genes could be monitored by real-time PCR or northern blot. One candidate HSP40 target gene is BAG3, which is regulated by HSF1 [44].

As previously mentioned, the impression when investigating cells under the

microscope was that rearrangement of β-tubulin in mock-transfected cells upon Forskolin treatment was not observed in cells where DNAJB1 had been knocked down by siRNA. In mock-transfected cells, the fine filaments observed in untreated cells seemed to aggregate upon Forskolin treatment. This did not seem to be the case with DNAJB1 knock down cells. Unfortunately, few pictures were taken (Figure 34), and by the time new ones were supposed to be shot, the samples had been contaminated by bacteria. Because of time limitations the experiment was not repeated. Repetitions of the experiment need to be done in order to confirm this tendency. In these repeated experiments, a control should be included in the WB of siRNA transfected cells to ensure even loading, so as to make sure that the observed reduced expression level of DNAJB1 is not a product of uneven loading of the gel. Additionally, cells in which DNAJB1 has been knocked down by siRNA should be monitored for amount of β-tubulin to investigate whether or not DNAJB1 has an effect on the expression levels of β-tubulin in the cell.

Staining for F-actin was also performed, but the procedure was unsuccessful, and due to time-limitations, the experiment was not repeated. This is however a possible future experiment.

5.1 Conclusions and future perspectives

In this study we have shown that ectopically co-expressed MK5 and DNAJB1 mainly localize to the nucleus. This could be a result of non-physiological conditions produced by ectopic over-expression, and to obtain more confident results, immunofluorescence staining of endogenous proteins should be performed.

We also obtained confounding evidence of the physical interaction between MK5 and DNAJB1. To confirm or dismiss such interaction, further studies are needed, such as GST-pulldown to check for direct interaction between MK5 and DNAJB1 and co-immunoprecipitation of the endogenous proteins.

Further we showed that MK5 phosphorylates DNAJB1 *in vitro* and that Tyrosine residue 6 and Serine residues 149, 151 and 171 are *in vitro* phosphorylation sites for MK5. Additionally our results indicate that there are other putative phosphorylation sites present within DNAJB1. To investigate the potential of these possible phosphoacceptor sites, additional site directed mutagenesis should be performed on these sites, followed by in vitro kinase assays. Additionally, all *in vitro* phosphorylation sites should be investigated for their *in vivo* phosphorylation potential by phosphospecific antibodies or MS analysis. Additional studies are also required to elaborate the functional implication of MK5-mediated phosphorylation of HSP40.

Luciferase studies indicated that DNAJB1 somehow downregulates the activity of MK5. Further studies are needed to elucidate in which way this downregulation is mediated. Additionally, reciprocal Luciferase assay of

DNAJB1 and MK5 should be performed to investigate the effect of MK5 on the activity of DNAJB1.

Aberrant HSP40 expression has been associated with malignant diseases and neurodegenerative diseases such as Huntington and ataxia [22]. Whether phosphorylation of DNAJB1 by MK5 has an effect on DNAJB1 in these processes remains unknown, but if so, it would make MK5 an attractive target for therapy.

6 References

1. David Secko, *The Science Creative Quarterly - Conversing at the cellular level: An introduction to signal transduction*, http://www.scq.ubc.ca/conversing-at-the-cellular-level-an-introduction-to-signal-transduction/

2. Sergiy Kostenko, *MAPKAP kinase 5 Its role in PKA-inuced F-actin rearrangement, regulation of subcellular localization by PKA, and identification of specific inhibitors*, 2009, Phd. dissertation, University of Tromsø: 13-16

3. Nancy Gerits, *Transcriptional regulation and functions of the mitogen-activated protein kinase MK5*, 2007, Phd. dissertation, University of Tromsø: 17, 18, 30, 34

4. Marie Cargnello, Philippe P. Roux, *Activation and Function of the MAPKs and Their Substrates, yhe MAPK-Activated Protein Kinases*. Microbiology and Molecular Biology Reviews, 2011. **75**(1): 50-83

5. Sergiy Kostenko, Gianina Dumitriu, Kari Jenssen Lægreid, Ugo Moens, *Physiological roles of the MAP kinase-activated protein kinase MK5/PRAK*. World Journal of Biological Chemistry, Acceptance pending 2011.

6. Philippe P. Roux, John Blenis, *ERK and p38 MAPK-Activated Protein Kinases: a Family of Protein Kinases with Diverse Biological Functions*. Microbiology and Molecular Biology Reviews, 2004. **68**(2): 320-344

7. Ni H, Wang XS, Diener K, Yao Z, *A novel mitogen-activated protein kinase (MAPK)-activated protein kinase, is a substrate of the extracellular-regulated kinase (ERK) and p38 kinase*. Biochem Biophys Ras Commun, 1998. **243**(2): 492-496

8. New L, Jiang Y, Zhao M, Liu K, Zhu W, Flood LJ, Kato Y, Parry GC, Han J, *PRAK, a novel protein kinase regulated by the p38 MAP kinase*. Embo J, 1998. **17**(12): 3372-3384

9. Gaestel M, *Molecular chaperones in signal transduction*. Handb Exp Pharmacol, 2006. **172**: 93-109

10. Alexey Shiryaev, *MAPK-activated protein kinase 5 (MK5)- The mechanisms of regulation and functions*, 2010, Phd. dissertation, University of Tromsø, Norwegian Cancer Society

11. Gaestel M., *MAPKAP kinases - MKs - two's a company, three's a crowd*. Nat Rev Mol Cell Biol, 2006. **7**(2): 120-130

12. Q. Li, D. Zhang, Y. Wang, T. Lin, Y. Wang, H. Zhou, Z. Ye, F. Zhang, SC. Lin, J. Han, *Determinants that control the distinct subcellular localization of p38a-PRAK and p38B-PRAK complexes*. J. Biol Chem, 2008. **283**(16): 11014-11023

13. Sergiy Kostenko, Alexey Shiryaev, Nancy Gerits, Gianina Dumitriu, Helle Klenow, Mona Johannesen, Ugo Moens, *Serine residue 115 of MAPK-activated protein kinase MK5 is crucial for its nuclear export by PKA, but not by p38MAPK, ERK3 and ERK4*. Cell Mol life Sci, 2011. **68**(5): 847-862

14. Nancy gerits, Theresa Mikalsen, sergiy Kostenko, Alexey Shiryaev, Mona Johannesen, Ugo Moens, *Modulation of F-actin Rearrangement by the Cyclic AMP/cAMP-dependent Protein Kinase (PKA) Pathway Is Mediated by MAPK-activated Protein Kinase 5 and Requires PKA-induced Nuclear Export of MK5*. The Journal of Biological Chemistry, 2007. **282**(51): 37232-37243.

15. Sergiy Kostenko, Mona Johannesen, Ugo Moens, *PKA-induced F-actin rearrangement requires phosphorylation of Hsp27 by the MAPKAP kinase MK5*. Cellular Signaling, 2009. **21**(5): 712-718

16. Theresia R. Kress, Ian G. Cannell, Arjan B. Brenkman, Birgit Samans, Matthias Gaestel, Paul Roepman, Boudewijn M. Burgering, Martin Bushell, Andreas Rosenwald, Martin Eilers, *The MK5/PRAK Kinase and Myc Form a Negative Feedback Loop that is Disrupted during Colorectal Tumorigenesis*. Molecular Cell, 2011. **41**(4): 445- 457

17. Peiqing Sun, Naoto Yoshizuka, Liguo New, Bettina A. Moser, Yilei Li, Rong Liao, Changchuan Xie, Jianming Chen, Qingong Deng, Maria Yamout, Meng-Qiu Dong, Costas G. Frangou, John R. Yates, III, Peter E. Wright, Jiahuai Han, *PRAK is essential for ras-Induced Senescence and Tumor Suppression*. Cell, 2007. **128**(2): 295-308

18. Michel J. Vos, Jurre Hagman, Serena Carra, Harm H. Kampinga, *Structural and Functional Diversities between Members of the Human HSPB, HSPH, HSPA and DNAJ Chaperone Families*. Biochemistry, 2008. **47**(27): 7001-7011

19. Aparna Mitra, Lalita A. Shevde, Rajeev S. Samant, *Multi-faceted role of HSP40 in cancer*. Clinical & Experimental Metastasis, 2009. **26**(6): 559-567

20. X.-B. Qiu, Y.-M. Shao, S. Miao, L. Wang, *The diversity of the DnaJ/Hsp40 family, the crucial partners for Hsp70 chaperones*. Cell. Mol. Life. Sci., 2006. **63**(22): 2560-2570

21. Jingzhi Li, Xinguo Qian, Bingdong Sha, *Heat shock protein 40: Structural studies and their functional implications*. Protein & Peptide Letters, 2009. **16**(6): 606-612

22. M. P. Zijlstra, M. A. Rujano, M. A. Van Waarde, E. Vis, E. R. Brunt, H. H. Kampinga, *Levels of DNAJB family members (HSP40) correlate with disease onset in patients with spinocerebellar ataxia type 3*. European Journal of Neuroscience, 2010. **32**(5): 760-770

23. Yanhong Shi, Dick D. Mosser, Richard I. Morimoto, *Molecular chaperones as HSF1-specific transcriptional repressors*. Genes and development, 1998. **12**(5): 654-666

24. Roger Davis, Seth A, Gonzalez, FA, Gupta S, Raden DL, Davis RJ., *Signal transduction within the nucleus by mitogen-activated protein kinase.* Biol Chem, 1992. **267**(34): 24796-24804

25. Yves Le Drean, Nathalie Mincheneau, Pascale Le Goff, Denis Michel, *Potentiation of Glucocorticoid Receptor Transcriptional Activity by Sumoylation*. Endocrinology, 2002. **143**(9): 3482-3489

26. Machery Nagel, *NucleoBond® Xtra Midi / Maxi*, http://www.mn-net.com/tabid/1479/default.aspx

27. Bitesizebio, *Quick reference: Determining DNA Concentration & Purity*, http://bitesizebio.com/articles/dna-concentration-purity/

28. Frederick M. Ausubel, Roger Brent, Robert E. Kingston, David D. Moore, J. G. Seidman, John A. Smith, Kevin Struhl, *Current protocols in molecular biology*, Vol. 1, 1995: John Wiley Sons, Inc. ISBN 0-471-50338-X: Chapter 3

29. Invitrogen, *Gateway Cloning*, http://www.invitrogen.com/site/us/en/home/Products-and-Services/Applications/Cloning/Gateway-Cloning.html

30. Kevin G. McCracken, *Dye-Terminator Cycle-Sequencing*, http://mercury.bio.uaf.edu/~kevin_mccracken/genetics/labs/lab5/lab-5.pdf

31. Alan R. Hibbs, *Confocal Microscopy for Biologists*, 2004: Springer. ISBN 0-306-48468-4: 254

32. Lee Yuan Kun, *Microbial Biotechnology- Principles and Applications*, 1 ed., 2006: World Scientific Publishing Co. ISBN 981-256-676-7: 444-445

33. Frederic M. Ausubel, Roger Brent, Robert E. Kingston, David M. More, J. G. Seidmann, John A. Smith, Kevin Struhl, *Current protocols in molecular biology*, Vol. 2, 2003: John Wiley & Sons, Inc. ISBN 0-471-50338-X: Chapter 9.0.1

34. Joseph Sambrook, David W. Russel, *Molecular Cloning - A laboratory manual*, vol. 3, 3 ed. , 2001: Cold Spring Harbor Laboratory Press. ISBN 0-87969-577-3: Chapter 16.2

35. Ivan Sadowski, Mark Ptashne, *A vector for expressing GAL4(1-147) fusions in mammalian cells*. Nucleic Acids Research, 1989. **17**(18): 7539

36. Frederick M. Ausubel, Roger Brent, Robert E. Kingston, David D. Moore, J. G. Seidman, John A. Smith, Kevin Struhl, *Current protocols in molecular biology*, Vol. 4, 2001: John Wiley & Sons, Inc. ISBN 0-471-50338-X: Chapter 20.5.1

37. Wikipedia, *Radiography*, http://en.wikipedia.org/wiki/Computed_radiography

38. J. sambrook, E. F. Fritsch, *Molecular Cloning - A laboratory maual*, Vol. 2, 2 ed. , 1989: Cold Spring Harbor Laboratory Press. ISBN 0-87969-309-6: Chapter 15.51

39. Invitrogen, *Gateway pDEST15 Vector*, http://products.invitrogen.com/ivgn/product/11802014

40. CBS, Technical University of Denmark, *NetPhos 2.0 Server*, http://www.cbs.dtu.dk/contact/

41. Srinivasan A, McClellan AJ, Vartikar J, Marks I, Cantalupo P, Li Y, Whyte P, Rundell K, Brodsky JL, Pipas JM., *The amino-terminal transforming region of simian virus 40 large T and small t antigens functions as a J domain*. Moll Cell Biol., 1997. **17**(8): 4761-4773

42. Aparna Mitra, Mitchell E. Menezes, Lalita A. Shevde, Rajeev S. Samant, *DNAJB6 Induces Degradation of B-catenin and Causes Partial Reversal of Mesenchymal Phenotype*. Journal of Biological Chemistry, 2010. **285**(32): 24686-94

43. Hattori H, Liu YC, Tohnai I, Ueda M, Kaneda T, Kobayashi T, Tanabe K, Ohtsuka K., *Intracellular localization and partial amino acid sequence of a stress-inducible 40-kDa protein in HeLa cells.* Cell Struct Funct., 1992. **17**(1): 77-86.

44. Franceschelli S, Rosati A, Lerose R, De Nicola S, Turco MC, Pascale M., *BAG3 gene expression is regulated by heat shock factor 1.* J cell Physiol., 2008. **215**(3): 575-577

Appendix A

Primers used to separate DNAJB1 into its individual domains [Kostenko unpublished results].

Nucleotide sequence of DNAJB1:

ATGGGTAAAGACTACTACCAGACGTTGGGCCTGGCCCGCGGCGCGTCGGACGAGGAGATCAAGCGG
GCCTACCGCCGCCAGGCGCTGCGCTACCACCCGGACAAGAACAAGGAGCCCGGCGCCGAGGAGAAG
TTCAAGGAGATCGCTGAGGCCTACGACGTGCTCAGCGACCCGCGCAAGCGCGAGATCTTCGACCGC
TACGGGGAGGAAGGCCTAAAGGGGAGTGGCCCCAGTGGCGGTAGCGGCGGTGGTGCCAATGGTACC
TCTTTCAGCTACACATTCCATGGAGACCCTCATGCCATGTTTGCTGAGTTCTTCGGTGGCAGAAAT
CCCTTTGACACCTTTTTTGGGCAGCGGAACGGGGAGGAAGGCATGGACATTGATGACCCATTCTCT
GGCTTCCCTATGGGCATGGGTGGCTTCACCAACGTGAACTTTGGCCGCTCCCGCTCTGCCCAAGAG
CCCGCCCGAAAGAAGCAAGATCCCCCAGTCACCCACGACCTTCGAGTCTCCCTTGAAGAG**ATC**TAC
AGCGGCTGTACCAAGAAGATGAAAATCTCCCACAAGCGGCTAAACCCCGACGGAAAGAGCATTCGA
AACGAAGACAAAATATTGACCATCGAAGTGAAGAAGGGGTGGAAAGAAGGAACCAAAATCACTTTC
CCCAAGGAAGGAGACCAGACCTCCAACAACATTCCAGCTGATATCGTCTTTGTTTTAAAGGACAAG
CCCCAC**AAT**ATCTTTAAGAGAGATGGCTCTGATGTCATTTATCCTGCCAGGATCAGCCTCCGGGAG
GCTCTGTGTGGCTGCACAGTGAACGTCCCCACTCTGGACGGCAGGACGATACCCGTCGTATTCAAA
GATGTTATCAGGCCTGGCATGCGGCGAAAAGTTCCTGGAGAAGGCCTCCCCCTCCCCAAAACACCC
GAGAAACGTGGGGACCTCATTATTGAGTTTGAAGTGATCTTCCCCGAAAGGATTCCCCAGACATCA
AGAACCGTACTTGAGCAGGTTCTTCCAATA**TAG**

J domain (70 aminoacids), **Glycine/Phenylalanine-rich region** (35 aminoacids), **C-terminal region**

ENTR1A
F 5'GCAGTCGACACC**ATG**GGTAAAG SalI

CTACGGGGAGGAA**TAA**GCGGCCGCATA
R 5'TATGCGGCCGC**TTA**TTCCTCCCCGTAG NotI

ENTR3C
F 5' AATGGATCCGGCCTAAAGGGGAG BamHI

CATGTTTGCTGAGTTC**TAA**CTCGAGACC
R 3' GGTCTCGAG**TTA**GAACTCAGCAAACATG XhoI

ENTR3C
F 5' AATGGATCCTTCGGTGGCAGAAATC BamHI

CTCCCTTGAAGAGATC**TAA**CTCGAGACC
R 3' GGTCTCGAG**TTA**GATCTCTTCAAGGGAG XhoI

F 5' AATGGATCCTACAGCGGCTGTAC BamHI

CAAGCCCCACAATTAACTCGAGACC
R 3′ GGTCTCGAGTTAATTGTGGGGCTTG XhoI

F 5′ GCCGGATCCATCTTTAAGAGAGATG BamHI

CAGGTTCTTCCAATATAGCTCGAGACC
R 3′ GGTCTCGAGCTATATTGGAAGAACCTG XhoI

Appendix B

Single mutations in putative phosphorylation sites in the J-domain and the proximal part of C-terminal (aa 106–175) were created by site-directed mutagenesis mediated by oligonucleotides. The oligonucleotides/primers used to introduce the mutations were as follows:

Primer	Sequence
Y6A F	5' AATTCAGTCGACACCATGGGTAAAGACTAC**GC**CCAGACGTTG
Y6A R	5' CAACGTCTGG**GC**GTAGTCTTTACCCATGGTGTCGACTGAATT
S16A F	5' GTTGGGCCTGGCCCGCGGCGCG**G**CGGACGAGGAGATCAAG
S16A R	5' CTTGATCTCCTCGTCCG**C**CGCGCCGCGGGCCAGGCCCAAC
S149A F	5' CTTCACCAACGTGAACTTTGGCCGC**G**CCCGC
S149A R	5' GCGGG**C**GCGGCCAAAGTTCACGTTGGTGAAG
S151A F	5' CTCCCGC**G**CTGCCCAAGAGCCCGCCCGAAAGAAGC
S151A R	5' GCTTCTTTCGGGCGGGCTCTTGGGCAG**C**GCGGGAG
S171A F	5' CACGACCTTCGAGTC**G**CCCTTGAAGAGATC
S171A R	5' GATCTCTTCAAGGG**C**GACTCGAAGGTCGTG

The rest of the procedure is identical to the protocol given in section 2.2.13.

The mutations appear as follows in the sequence of DNAJB1:

[Kostenko, unpublished results]

Appendix C

pENTR3C-CREB was constructed from pcDNA3-CREB and pENTR3C by digestion of restriction endonucleases.

Several different incubation times and nucleases were tested, and buffers changed accordingly. The successful restriction cutting was accomplished by the following set-up:

Reagent	Sample 1	Sample 2
10 x TA buffer	2 µl	2 µl
pcDNA3-CREB	1 µg	
pENTR3C		0.5 µg
KpnI	1 µl	1 µl
NotI	0.5 µl	0.5 µl
BSA	0.7 µl	0.7 µl
ddH_2O	To 20 µl	To 20 µl

The samples were incubated at 37 °C o.n.

The rest of the procedure was identical to the description in section 3.2.14

Appendix D

pENTR1A-HSF1 was constructed from pEGFP-N1-HSF1 and pENTR1A by digestion of restriction endonucleases.

Reagent	Sample 1	Sample 2
Neb buffer 2	2 µl	
Neb buffer 3		2 µl
pEGFP-N1-HSF1	1 µg	
pENTR1A		1 µg
EcorI	1 µl	1 µl
SalI		1 µl
XhoI	1 µl	
ddH_2O	To 20 µl	To 20 µl

The samples were incubated at 37 °C for 2 hours

The rest of the procedure was identical to the description in section 3.2.14

Appendix E

Predicted phosphorylation sites in DNAJB1 by NetPhos 2.0

Serine predictions

Name	Pos	Context	Score	Pred
Sequence	16	ARGASDEEI	0.996	*S*
Sequence	56	YDVLSDPRK	0.593	*S*
Sequence	75	GLKGSGPSG	0.031	.
Sequence	78	GSGPSGGSG	0.817	*S*
Sequence	81	PSGGSGGGA	0.143	.
Sequence	89	ANGTSFSYT	0.119	.
Sequence	91	GTSFSYTFH	0.089	.
Sequence	132	DDPFSGFPM	0.385	.
Sequence	149	NFGRSRSAQ	0.888	*S*
Sequence	151	GRSRSAQEP	0.985	*S*
Sequence	171	DLRVSLEEI	0.995	*S*
Sequence	177	EEIYSGCTK	0.010	.
Sequence	186	KMKISHKRL	0.971	*S*
Sequence	196	PDGKSIRNE	0.972	*S*
Sequence	228	GDQTSNNIP	0.009	.
Sequence	252	KRDGSDVIY	0.838	*S*
Sequence	261	PARISLREA	0.994	*S*
Sequence	330	IPQTSRTVL	0.889	*S*

Threonine predictions

Name	Pos	Context	Score	Pred
Sequence	8	DYYQTLGLA	0.607	*T*
Sequence	88	GANGTSFSY	0.164	.
Sequence	93	SFSYTFHGD	0.040	.
Sequence	114	NPFDTFFGQ	0.334	.
Sequence	142	MGGFTNVNF	0.056	.
Sequence	165	DPPVTHDLR	0.368	.
Sequence	180	YSGCTKKMK	0.739	*T*
Sequence	205	DKILTIEVK	0.655	*T*
Sequence	216	WKEGTKITF	0.355	.
Sequence	219	GTKITFPKE	0.041	.
Sequence	227	EGDQTSNNI	0.190	.
Sequence	270	LCGCTVNVP	0.018	.
Sequence	275	VNVPTLDGR	0.129	.
Sequence	280	LDGRTIPVV	0.036	.
Sequence	307	PLPKTPEKR	0.686	*T*
Sequence	329	RIPQTSRTV	0.962	*T*
Sequence	332	QTSRTVLEQ	0.029	.

Tyrosine predictions

Name	Pos	Context	Score	Pred
Sequence	5	MGKDYYQTL	0.118	.
Sequence	6	GKDYYQTLG	0.947	*Y*
Sequence	24	IKRAYRRQA	0.033	.
Sequence	31	QALRYHPDK	0.029	.
Sequence	52	IAEAYDVLS	0.220	.
Sequence	67	IFDRYGEEG	0.386	.
Sequence	92	TSFSYTFHG	0.604	*Y*
Sequence	176	LEEIYSGCT	0.543	*Y*
Sequence	256	SDVIYPARI	0.141	.